



Facultad de Ciencias

Departamento de Química Orgánica



**Design, Synthesis and Biological  
Evaluation of Novel 4(1*H*)-Pyridones  
as Antimalarial Inhibitors of *Plasmodium  
falciparum* Cytochrome *bc1***

**MEMORIA PARA OPTAR AL GRADO DE DOCTOR**

**PRESENTADA POR:**

Margarita Puente Felipe

Bajo la supervisión de la Doctora:

Pilar Manzano Chinchón

**MADRID, 2018**

### **Research Involving Animals**

“All animal studies were ethically reviewed and carried out in accordance with European Directive 2010/63/EU and the GSK Policy on the Care, Welfare and Treatment of Animals.”

## Abstract

Malaria remains one of the most widespread infectious diseases of our time. Resistance to all current chemotherapeutics used in the treatment of this illness has been observed. Therefore, there is an urgent requirement for the development of novel agents to combat this disease, particularly against those strains which have developed resistance to previously used therapies.

The mitochondrial respiratory chain of *P. falciparum* makes an attractive target for chemotherapy, being both chemically and clinically validated by atovaquone. Furthermore, the parasitic respiratory chain differs from the analogous mammalian system, suggesting that parasite specific agents should be achievable. 4(1*H*)-Pyridones have been developed at GlaxoSmithKline as selective inhibitors of *Plasmodium* mitochondrial function by blocking the electron transport chain at the cytochrome *bc1* level. However, the most potent 4-pyridones are lipophilic molecules with poor solubility in aqueous media and low oral bioavailability.

This thesis describes efforts to identify novel derivatives with improved physicochemical and solubility properties whilst maintaining, if not improving the antimalarial potencies and safety margins shown by the parent 4(1*H*)-pyridones.

The synthesis of a phosphate prodrug has validated the strategy as a successful approach to overcoming limited oral bioavailability and poor solubility of classical 4(1*H*)-pyridones. Furthermore, this prodrug was associated with improved linearity in dose-escalation studies, allowing the progression of the family to further development stages.

In addition, a series of cyclic 4(1*H*)-pyridones has been studied and validated, constituting a promising family of antimalarial compounds that maintain excellent *in vitro* activity and *in vivo* efficacy in both *P. yoelii* model and *P. falciparum* humanized mouse model. Pharmacological and molecular modeling data presented in this thesis suggest a slightly different active site binding pose is being adopted by this novel family of tricyclic 4(1*H*)-pyridone derivatives, offering the opportunity to overcome safety issues found in the classical 4(1*H*)-pyridones.

## Abbreviations

<b>Ac</b>	Acyl
<b>ACT</b>	Artemisinin combination therapy
<b>ADME</b>	Absorption, distribution, metabolism and excretion
<b>AUC</b>	Area under the curve
<b>BCS</b>	Biopharmaceutical Classification System
<b>Bn</b>	Benzyl
<b>bs</b>	Broad singlet
<b>CDCl<sub>3</sub></b>	Deuterated chloroform
<b>CHIlogD</b>	Chromatographic hydrophobicity index distribution coefficient
<b>CLND</b>	Chemiluminescent nitrogen detection
<b>clogP</b>	Calculated logP (partition coefficient)
<b>C<sub>max</sub></b>	Maximum concentration
<b>CoQ</b>	Ubiquinone
<b>d</b>	Doublet
<b>DCE</b>	Dichloroethane
<b>DCM</b>	Dichloromethane
<b>DHFR</b>	Dihydrofolate reductase
<b>DHODH</b>	Dihydroorotate dehydrogenase
<b>DIPEA</b>	<i>N,N</i> -Diisopropylethylamine
<b>DMF</b>	<i>N,N</i> -Dimethylformamide
<b>DMSO</b>	Dimethyl sulfoxide
<b>DPPA</b>	Diphenyl phosphoryl azide
<b><i>E. coli</i></b>	<i>Escherichia coli</i>
<b>EC<sub>50</sub></b>	Half maximal effective concentration
<b>Et</b>	Ethyl
<b>EtOAc</b>	Ethyl acetate

<b>EtOH</b>	Ethanol
<b>eq.</b>	Equivalent
<b>F</b>	Oral bioavailability
<b>FaSSIF</b>	Fasted state simulated intestinal fluid
<b>FeSSIF</b>	Feed state simulated intestinal fluid
<b>g</b>	Grams
<b>GI</b>	Gastrointestinal
<b>GSK</b>	GlaxoSmithKline
<b>HMQC</b>	Heteronuclear multiple quantum coherence
<b>HPLC</b>	High pressure liquid chromatography
<b>HTS</b>	High throughput screening
<b>IBN</b>	Intravenous
<b>IC<sub>50</sub></b>	Half maximal inhibitory concentration
<b>iv</b>	Intravenous
<b>K<sub>i</sub></b>	Inhibition constant
<b>LCMS</b>	Liquid chromatography mass spectrometry
<b>LE</b>	Ligand Efficiency
<b>m</b>	Multiplet
<b>Me</b>	Methyl
<b>mCPBA</b>	<i>m</i> -Chloroperbenzoic acid
<b>mtETC</b>	Mitochondrial Electron Transport Chain
<b>mg</b>	Milligrams
<b>MHz</b>	Megahertz
<b>mL</b>	Millilitres
<b>min</b>	Minutes
<b>MOA</b>	Mode of action
<b>mol</b>	Mole
<b>mmol</b>	Millimole

<b>MS</b>	Mass spectrometry
<b>N/A</b>	Not available
<b>NBS</b>	<i>N</i> -Bromosuccinimide
<b>NMP</b>	<i>N</i> -Methylpyrrolidone
<b>NMR</b>	Nuclear magnetic resonance
<b><i>P. berghei</i></b>	<i>Plasmodium berghei</i>
<b>Pd/C</b>	Palladium on carbon
<b>Pd(PPh<sub>3</sub>)<sub>4</sub></b>	Tetrakis(triphenylphosphine)palladium(0)
<b><i>P. falciparum</i></b>	<i>Plasmodium falciparum</i>
<b><i>PfCyt bc<sub>1</sub></i></b>	<i>Plasmodium falciparum</i> cytochrome <i>bc<sub>1</sub></i>
<b><i>PfCRT</i></b>	<i>Plasmodium falciparum</i> chloroquine resistance transporter
<b><i>PfDHODH</i></b>	<i>Plasmodium falciparum</i> dihydroorotate dehydrogenase
<b>Ph</b>	Phenyl
<b>PK</b>	Pharmacokinetics
<b>pK<sub>a</sub></b>	Acid dissociation constant
<b>po</b>	<i>per os</i> (Latin; by mouth); oral
<b>ppm</b>	Parts per million
<b><i>P. vivax</i></b>	<i>Plasmodium vivax</i>
<b>q</b>	Quartet
<b>R&amp;D</b>	Research and development
<b>rt</b>	Room temperature
<b>s</b>	Singlet
<b>SAR</b>	Structure-activity relationship
<b>t</b>	Triplet
<b>t<sub>½</sub></b>	Half-life
<b>TBME</b>	<i>tert</i> -Butyl methyl ether
<b>tBu</b>	<i>tert</i> -Butyl
<b>TCCA</b>	Trichloroisocyanuric acid

<b>TEMPO</b>	2,2,6,6-Tetramethylpiperidin-1-yl)oxyl
<b>TFA</b>	Trifluoroacetic acid
<b>THF</b>	Tetrahydrofuran
<b>TLC</b>	Thin layer chromatography
<b>TMHD</b>	2,2,6,6-tetramethyl-3,5-heptadione
<b>TMS</b>	Tetramethylsilane
<b>μl</b>	Microlitres
<b>μM</b>	Micromolar
<b>UPLC</b>	Ultra-performance liquid chromatography
<b>UV</b>	Ultraviolet
<b>V<sub>ss</sub></b>	Volume of distribution
<b>WHO</b>	World health organisation

## Amino acids and their three letter and one letter codes

Alanine	Ala	A
Arginine	Arg	R
Asparagine	Asn	N
Aspartic Acid	Asp	D
Cysteine	Cys	C
Glutamic Acid	Glu	E
Glutamine	Gln	Q
Glycine	Gly	G
Histidine	His	H
Iso-leucine	Ile	I
Leucine	Leu	L
Lysine	Lys	K
Methionine	Met	M
Phenylalanine	Phe	F
Proline	Pro	P
Serine	Ser	S
Threonine	Thr	T
Tryptophan	Trp	W
Tyrosine	Tyr	Y
Valine	Val	V



# Table of Contents

<b>Abstract .....</b>	<b>i</b>
<b>Abbreviations.....</b>	<b>iii</b>
<b>Amino acids and their three letter and one letter codes.....</b>	<b>vii</b>
<b>1 INTRODUCTION.....</b>	<b>1</b>
1.1 MALARIA OVERVIEW .....	1
1.2 MALARIA CHEMOTHERAPY .....	4
1.2.1 Antimalarial aminoquinolines .....	4
1.2.2 Arylamino alcohols .....	7
1.2.3 Antifolates .....	9
1.2.4 Endoperoxides .....	11
1.2.5 2-Hydroxynaphthoquinone .....	13
1.2.6 Antibiotics.....	14
1.3 NOVEL ANTIMALARIALS IDENTIFIED VIA HIGH-THROUGHPUT SCREENING.....	16
1.3.1 Future in Malaria .....	20
1.4 MITOCHONDRIAL ELECTRON TRANSPORT CHAIN AS ANTIMALARIAL TARGET....	22
1.4.1 Complex III – Cytochrome bc <sub>1</sub> .....	23
1.5 4(1H)-pyridones as potential antimalarials.....	25
<b>2 OBJECTIVES.....</b>	<b>33</b>
<b>3 RESULTS AND DISSCUSIONS .....</b>	<b>37</b>
3.1 4(1H)-PYRIDONE DERIVATIVES AT POSITION 2.....	39
3.1.1 Synthesis of the hydroxy methyl 4(1H)-pyridones at position 2.....	39
3.1.2 Synthesis of ionizable 4(1H)-pyridones at position 2.....	41

3.1.3	Synthesis of the 2-carbaldehyde oxime of GW844520.....	42
3.1.4	Biological activity and analysis results.....	43
3.1.5	Molecular modelling.....	47
3.1.6	Conclusions.....	51
3.2	THE PRODRUG APPROACH.....	52
3.2.1	Previous work.....	52
3.2.2	The Prodrug Theory.....	53
3.2.3	Prodrug Classification.....	55
3.2.4	Prodrug rational for GSK932121 and GSK1146191.....	56
3.2.5	Prodrugs for hydroxyl functionalities.....	58
3.2.6	Synthesis of GSK932121 Prodrugs.....	62
3.2.7	Synthesis of GSK1146191 Prodrugs.....	66
3.2.8	Biological activity and analysis results.....	68
3.2.9	Conclusions.....	79
3.3	AZAFLUORENONES.....	81
3.3.1	Previous work.....	82
3.3.2	Chemical synthesis of the 1-azafluorenone series.....	83
3.3.3	Biological analysis of the 1-azafluorenone series.....	85
3.3.4	Chemical synthesis of the 1-azafluorenone scaffold.....	88
3.3.5	Mechanistic study for the synthesis of the 1-azafluorenone scaffold.....	90
3.3.6	Synthesis of a suitable intermediate for SAR studies.....	93
3.3.7	Conclusions.....	93
3.4	TRICYCLIC BENZOTHIENOPYRIDINONES.....	95
3.4.1	“Confidential Section”.....	95

<b>4 CONCLUSIONS.....</b>	<b>97</b>
4.1 Conclusiones .....	99
<b>5 EXPERIMENTAL SECTION .....</b>	<b>105</b>
5.1 Instrumentation .....	107
5.2 General methods and experimental data .....	108
5.3 Assay details.....	132
<b>6 REFERENCES.....</b>	<b>137</b>

Additional data is attached in the CD:

**APPENDIX I: Structural elucidation for key compounds.**

    APPENDIX I-A: Structural elucidation compound **15**

    APPENDIX I-B: Structural elucidation compound **19**

    APPENDIX I-C: Structural elucidation compounds **26**

**APPENDIX II: Spectroscopic data collection NMR, MS and HPLC**

    APPENDIX II-A: Compounds decrypted in section 3.1

    APPENDIX II-B: Compounds decrypted in section 3.2

    APPENDIX II-C: Compounds decrypted in section 3.3

---

# **1 INTRODUCTION**

---

## 1.1 MALARIA OVERVIEW

Malaria remains one of the most widespread infectious diseases of our time. It is an endemic disease in many tropical and subtropical regions and shows a major prevalence in Sub-Saharan Africa. The World Health Organization (WHO) has estimated that 216 million people were infected with malaria across the globe in 2016, leading to nearly 445,000 deaths, the vast majority being women and children under the age of five (Figure 1.1).<sup>1</sup>

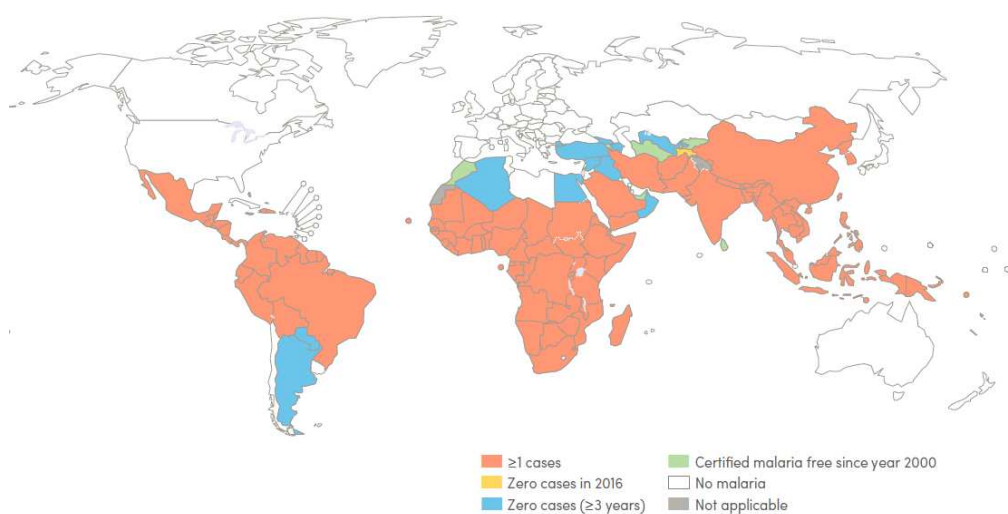


**Figure 1.1** Countries with ongoing transmission of malaria, 2016.<sup>1</sup>

This disease is caused by protozoan parasites of the genus *Plasmodium*, which are transmitted to people during the blood meal of a female *Anopheles* mosquito, destroying red blood cells and leading to fever, severe anemia, cerebral malaria and, if untreated, death. There are five species of the parasite known to infect humans: *Plasmodium malariae*, *Plasmodium ovale*, *Plasmodium knowlesi*, *Plasmodium vivax*, and *Plasmodium falciparum*, the last two being responsible for the highest morbidity and mortality, respectively.<sup>2</sup>

The *Plasmodium falciparum* life cycle starts when the mosquito bites a human and sporozoites are injected into the bloodstream (Figure 1.2). In several minutes the sporozoites arrive at the liver cells where they find the requisite machinery to develop into schizonts that will reproduce asexually into merozoites. In the case of *P.vivax* and

## Introduction

*P. ovale*, the parasite can remain dormant in the hepatocytes (the parasite stage known as hypnozoites) for months or several years and eventually causing clinical symptoms in the absence of a new mosquito bite.

After the liver cells rupture, mature merozoites are released into the bloodstream invading erythrocytes where parasites continue their cycle, known as the asexual stage that lasts 43-48h. With the rupture of the erythrocyte, the parasite's waste and cell debris are released into the blood stream causing the clinical symptoms of malaria: chill, headache, abdominal and back pain, nausea, and sometimes vomiting. Thus, the early stages of malaria often resemble the onset of an influenza infection. *P. falciparum* malaria infection can progress within a few days from uncomplicated to severe malaria with a fatal outcome in 10–40% of all cases of severe malaria. Observed complications include: coma (cerebral malaria), respiratory distress, renal failure, hypoglycemia, circulatory collapse, acidosis, and coagulation failure.<sup>3,4</sup>

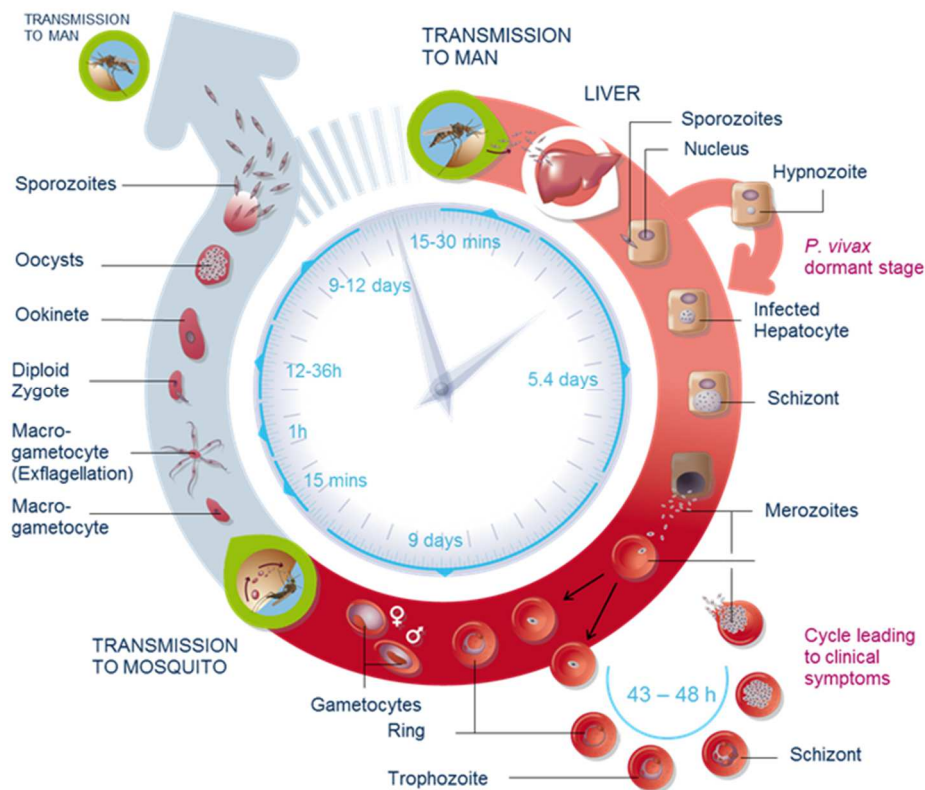


**Figure 1.2** Life cycle of Plasmodium.<sup>5</sup>

A small percentage of merozoites differentiate into male and female gametocytes which are taken up by the mosquito in her blood meal, starting the sexual-stage of the parasite and causing the transmission of the disease. The details of the mechanism are still unknown. Once in the mosquito, male and female gametocytes form diploid zygotes and then ookinetes that stay in the midgut of the insect to develop oocysts which, by meiotic division, will form the sporozoites. Sporozoites migrate to the salivary glands of the female *Anopheles* mosquito ready to continue the cycle of transmission back to man.<sup>5</sup>

Traditionally, antimalarial agents are classified by the stages of the malaria life cycle that are targeted by the drug: **Blood schizonticides**, focus on the erythrocytic stages of *Plasmodium falciparum* to cure the infection. **Tissue schizonticides**, act on hepatic schizonts, and thus prevent the invasion of erythrocytes. **Hypnozoitocides**, kill the dormant stages of *P. vivax* and *P. ovale*. **Gametocytocides**, destroy the intraerythrocytic sexual forms of the parasites and acts as transmission blocking agents to prevent transmission from human to mosquito.<sup>6</sup>

The interruption of malaria transmission worldwide is one of the greatest challenges for international health and developing communities.<sup>7</sup> The fight against malaria is multifaceted and, as with other mosquito-borne diseases, different strategies for malaria vector control have been pursued. Programmes for the distribution of insecticide treated nets and indoor residual spraying campaigns have led to a significant reduction in the number of disease cases. Inevitably, the major malaria vectors have developed resistance to these insecticides and the resistance alleles are spreading at an exceptionally rapid rate throughout Africa.<sup>8</sup>

While malaria vaccines complete their clinical development,<sup>9</sup> chemotherapy is the cornerstone of malaria control. However, multidrug resistant *Plasmodium falciparum* strains<sup>10,11</sup> have spread globally and only a limited number of efficacious drugs are currently available.<sup>12</sup> Critically, there is evidence of emerging resistance to the artemisinins,<sup>13</sup> which are the main component of the current gold standard

combinations for the treatment of malaria,<sup>14</sup> known as ACTs (artemisinin combination therapies) (Figure 1.3).

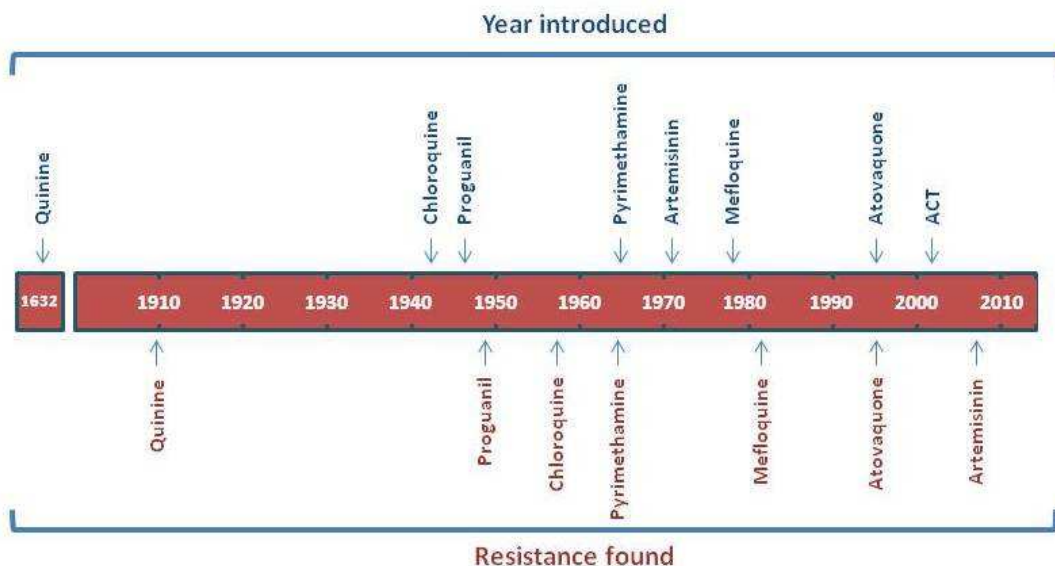


**Figure 1.3** Year of introduction of new antimalarial therapies versus the emergence of clinical resistance.<sup>15</sup>

## 1.2 MALARIA CHEMOTHERAPY

### 1.2.1 Antimalarial aminoquinolines

#### QUININE

Quinine (Figure 1.4) is a natural alkaloid extracted from the bark of the cinchona (quina–quina) tree and presents antipyretic, antimalarial, analgesic, and anti-inflammatory properties.<sup>16</sup> Historically, it was the first antimalarial to be used and it was the reference therapeutic agent until the 1940s.

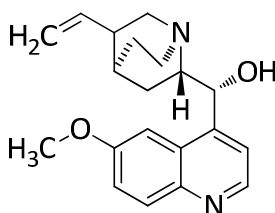


**Figure 1.4** Quinine



Quinine has a low therapeutic index and presents important adverse effects such as vertigo, nausea and vomiting, abdominal pain, diarrhea, marked auditory loss, visual symptoms, including loss of vision, tinnitus, slight impairment of hearing, and headache. However, the limited availability of ACT's (artemisinin combination therapies) and the increasing resistance to other classical antimalarials have increased its use in recent times. Therefore, studies evaluating the role of quinine in the management of malaria have been reviewed.<sup>17</sup>

The antimalarial mode of action of quinine has not yet been fully resolved, but the most widely accepted hypothesis is based on the closest related quinoline drug: chloroquine (Figure 1.5). Quinine shows rapid schizonticidal action against *intra*-erythrocytic malaria parasites. It is also gametocytocidal for *P. vivax* and *P. malariae*, but not for *P. falciparum*.<sup>16</sup>

### CHLOROQUINE

Chloroquine (CQ) (Figure 1.5) was achieved with the introduction of a diethylaminoisopentylamino side chain into position 4 of a 7-chloroquinoline, yielding a compound named resochin by the German inventors (later known as chloroquine) and has been the most successful single drug for the treatment and prophylaxis of malaria. This 4-aminoquinoline compound was first synthesized in 1934 by Bayer laboratories in Elberfeld, Germany,<sup>18</sup> although, it was during World War II when its therapeutic value was observed.<sup>19</sup> Chloroquine is a safe and affordable drug and was successfully used for many years as the primary chemotherapeutic agent for the treatment and prevention of malaria caused by different *Plasmodium* species. However, resistant strains began to emerge in the 1960s.

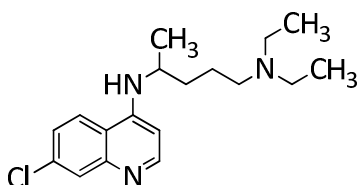


**Figure 1.5** Chloroquine

The mechanism of action of chloroquine is still unknown and a number of theories have been proposed. However, there is common agreement that CQ interferes with the parasite's ability to digest hemoglobin. CQ efficacy is thought to be dependent on the acid–base properties of this molecule, which allow it to accumulate to high levels as a di-protonated form in the acidic digestive vacuole; the pH of the vacuole is around 5.4 which means that CQ is more than 99.99% protonated, given the pK<sub>a</sub> of the molecule. Once there, CQ is thought to interact with the toxic heme species produced during haemoglobin degradation, which leads to disruption of the detoxification process that sequesters the reactive iron complexes into haemozoin crystals,<sup>6</sup> leading to inhibition of parasite growth. The exact killing mechanism is not well understood but peroxidation of parasite lipid membranes, damage of DNA and oxidation of proteins are implicated in parasite death.<sup>20</sup>

### *PRIMAQUINE, TAFENOQUINE, AMODIAQUINE*

The quinoline scaffold has inspired the development of other synthetic antimalarial analogues to chloroquine such as primaquine (PQ) (Figure 1.6), the main representative of the class of 8-aminoquinoline derivatives that show a better tolerability and are the only drug approved to prevent the relapse of the dormant hypnozoites. The standard primaquine therapy is 15 mg daily for 14 days; however available evidence refutes primaquine's reputation for being toxic and poorly tolerated.<sup>21</sup>

Tafenoquine (TQ) (Figure 1.6) was developed by GlaxoSmithKline (GSK), in collaboration with the Medicines for Malaria Venture (MMV), for the treatment and relapse-prevention (radical cure) of *P. vivax* malaria.<sup>22</sup> TQ was submitted for FDA approval at the end of 2017 after showing a good efficacy and tolerability profile in a recent phase 2 base dose ranging study<sup>23</sup> as well as positive results in Phase III.<sup>24</sup> TQ was finally approved by the US FDA in July 2018 becoming the first drug in 60 years to treat relapsed malaria.<sup>25</sup>

Amodiaquine (ADQ) and Piperaquine (PPQ) (Figure 1.6) belong to a second-generation of chloroquine analogues that have shown efficacy against chloroquine resistant strains.

However, clinical use has been limited due its association with hepatotoxicity and granulocytosis.<sup>6</sup>

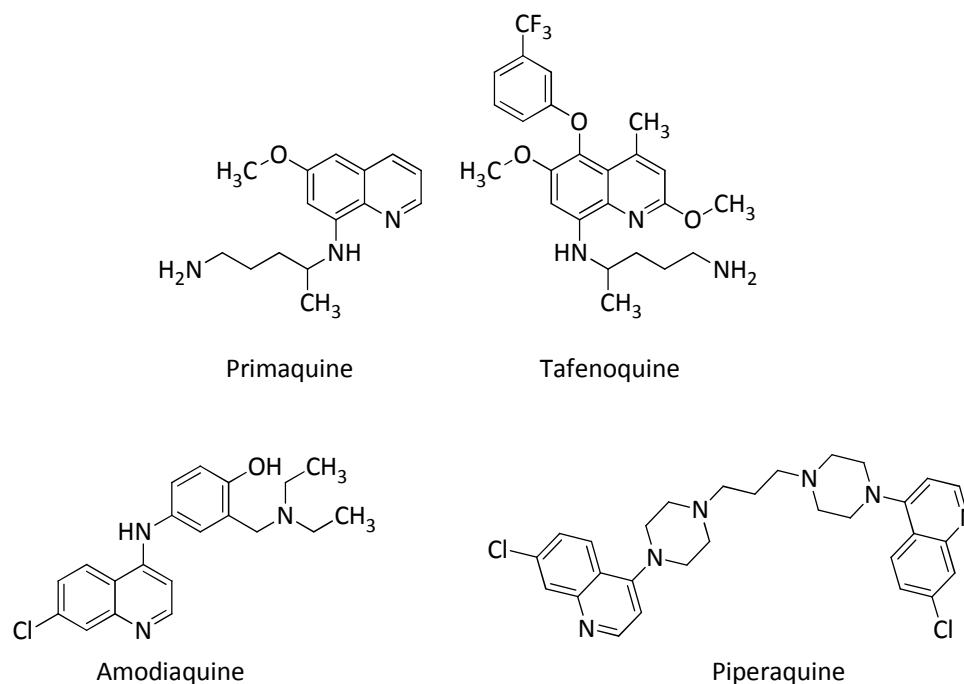


**Figure 1.6** Antimalarial Aminoquinolines

### 1.2.2 Arylamino alcohols

#### *MEFLOQUINE, HALOFANTRINE AND LUMEFANTRINE*

Mefloquine<sup>26</sup> (Figure 1.7) was developed from analogues of the most representative aminoalcohol, Quinine, and initially synthesized during World War II.<sup>27</sup> Due to the emerging resistance to chloroquine, in 1963 the Walter Reed Army Institute of Research (WRAIR) conducted an extensive screening campaign with the intention of finding a replacement for chloroquine and this 4-quinolinemethanol structurally related to quinine was selected from nearly 300 quinoline methanol derivatives. *Mefloquine* was marketed in 1985 as Lariam<sup>®</sup> and is perhaps the most studied of all antimalarial agents.<sup>28</sup> Mefloquine is orally active and effective against the intra-erythrocytic stages of the plasmodium life-cycle. It has no effect on mature gametocytes. Although mefloquine does cause recognizable changes in pre-erythrocytic forms, the effects are insufficient to prevent further development of the tissue parasite, thus, mefloquine cannot be used

as prophylactic agent. It is a relatively slow-acting drug with greatest activity against the more mature blood stages.

Halofantrine was also developed by the WRAIR from a series of phenanthrene methanols and was launched onto the market in 1988 as Halfan<sup>®</sup>. Halofantrine is associated with a high risk of cardiac arrhythmias, therefore, it has been withdrawn from the market in several countries.

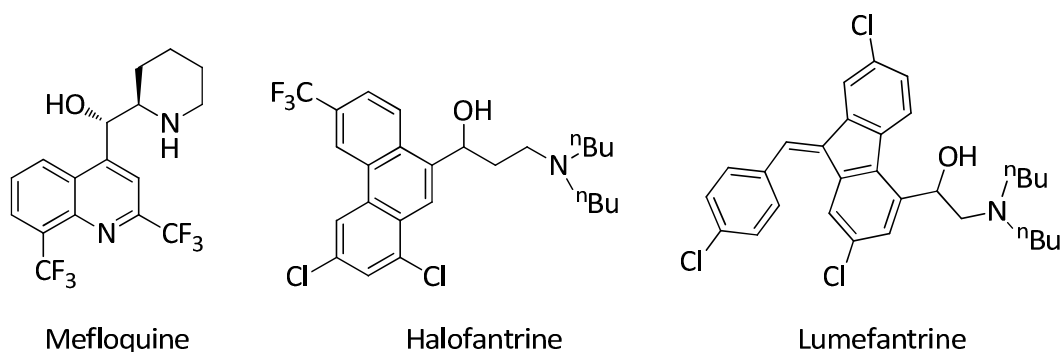


Figure 1.7 Arylamino alcohols

A third representative of this chemical series, Lumefantrine, displays lower antimalarial activity than halofantrine but it does not present the dangerous cardiac side effects. Lumefantrine displays *in vitro* synergism with artemether (described in section 1.2.4) so currently it is the preferred partner to combine with artemether for first-line acute therapies. This combination, marketed as Coartem<sup>®</sup>, constitutes 75% of the current ACTs (artemisinin combination therapies) used in the clinic and provides a rapid relief of symptoms due to the fast killing mode of action of the artemisinin and prevents recrudescence due to the long half-life (4 days) presented for lumefantrine.<sup>29</sup>

The mechanism of action of Mefloquine and other arylamino alcohols remains unclear and it is most likely different from the mechanism of 4-aminoquinolines. Due to their historical contest, these compounds were marketed without phase III trials and some years later, in the early 1980s, randomized controlled trials were carried out in healthy populations, confirming these aminoalcohols as a potential source of psychological illnesses.<sup>6</sup>

### 1.2.3 Antifolates

Whereas humans depend on dietary intake of pre-formed dihydrofolic acid as an essential nutrient, which is then reduced to tetrahydrofolic acid, pathogenic microorganisms including *Plasmodia* can synthesize dihydrofolic acid from simple precursors (Figure 1.8). Furthermore, *P. falciparum* is able to use exogenous dihydrofolic acid via a salvage pathway.<sup>30</sup>

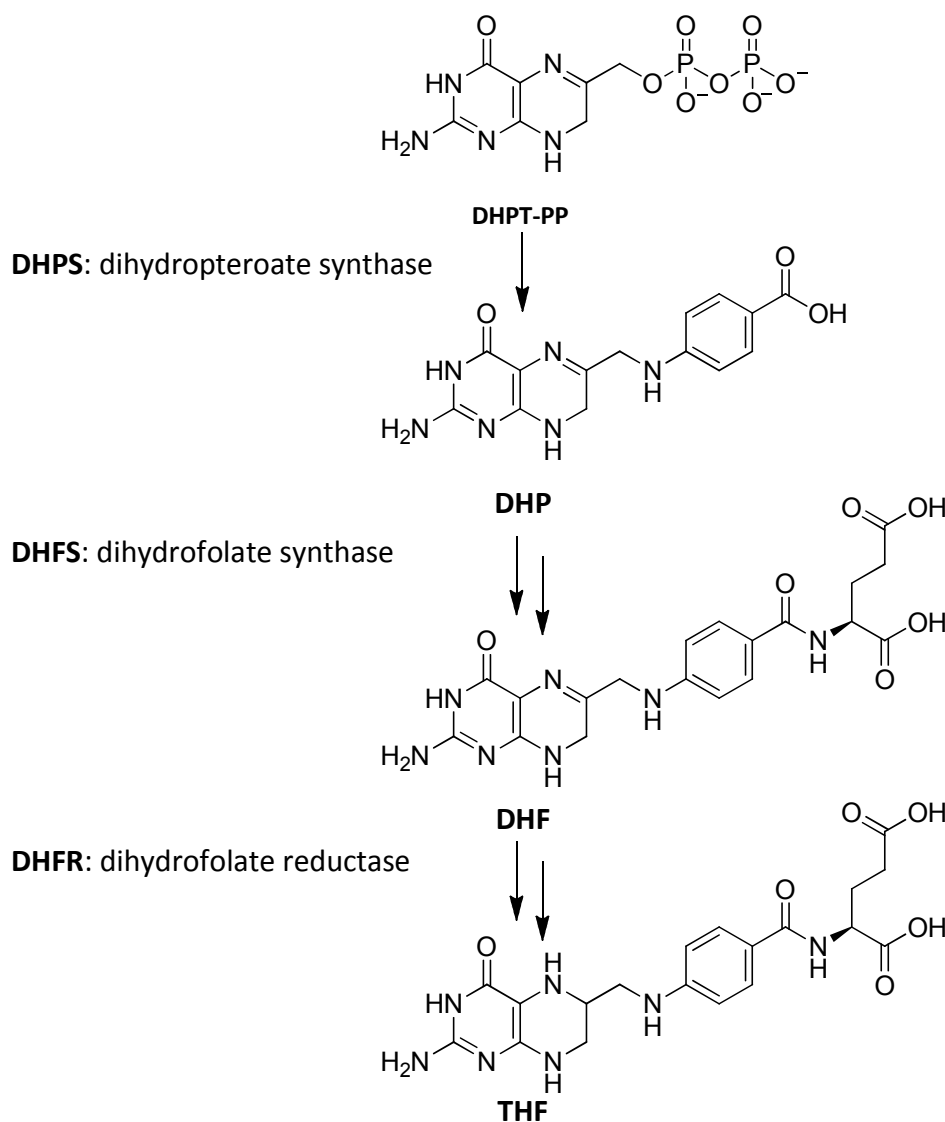


**Figure 1.8** The folate pathway (simplified) showing the targets of the antifolates. DHPT-PP, 6-hydroxymethyl-7,8-dihydropterin pyrophosphate; DHPS, dihydropteroate synthase; DHP, 7,8-dihydropteroate; DHFS, dihydrofolate synthase; DHF, 7,8-dihydrofolate; DHFR, dihydrofolate reductase; THF, tetrahydrofolate.

A number of agents have been discovered that affect antimalarial activity through inhibition of the parasite dihydrofolate pathways.<sup>31-34</sup> These agents are divided into two types: inhibitors of dihydrofolate reductase (DHFR) and those that inhibit dihydropteroate synthase (DHPS), both key enzymes of the folate biosynthetic pathway.<sup>6</sup> DHPS is completely absent in humans while bacterial and protozoal DHFR are sufficiently different from their human counterpart to allow the development of selective inhibitors.

### SULFONAMIDES

Sulfonamides and sulfones (Figure 1.9) are selectively toxic to malaria parasites because they inhibit the plasmodial enzyme, dihydropteroate synthase (DHPS). The first antifolate to be used against malaria was the well-known DHPS inhibitor *Sulfachrysoidine*. It was developed in 1932 by Domack as an antibacterial agent (Prontosil<sup>®</sup>). Later it was found that Sulfanilamide arising from the reductive cleavage of the azo substructure is the active component. In 1937, *Sulfachrysoidine* was successfully used in a trial against malaria, but interest in sulfonamides diminished because of the continuing effectiveness of quinine and the development of other synthetic antimalarials.<sup>6</sup>

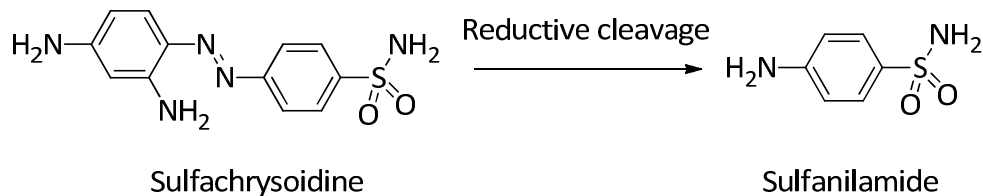
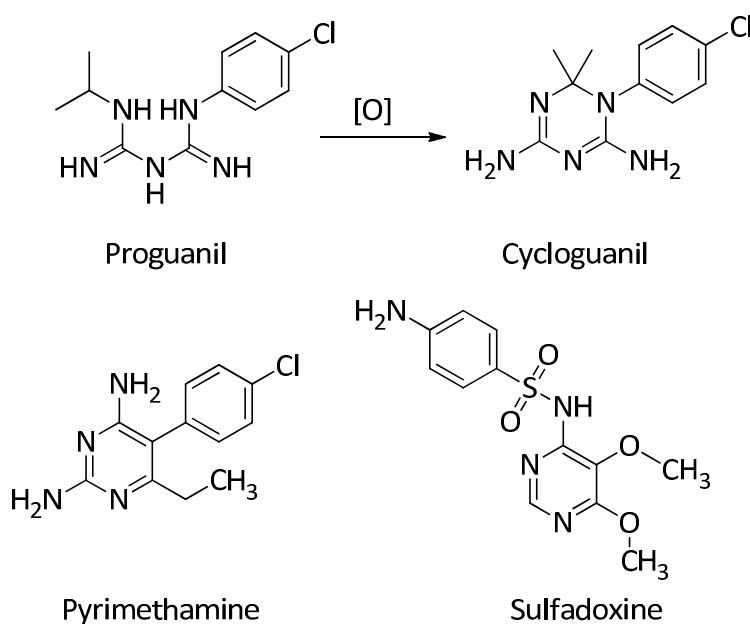


Figure 1.9 Dihydropteroate synthase inhibitors

### PYRIMETHAMINE & PROGUANIL

Pyrimethamine (Figure 1.10) is the most important representative of the well-known antimalarial chemical class of diamine-pyrimidines that are antifolates. Another is Proguanil, the prodrug that yields the active metabolite *Cycloguanil* through oxidative ring closure. Both interfere with tetrahydrofolic acid synthesis from folic acid by inhibiting the enzyme dihydrofolate reductase (DHFR) and were introduced in close succession in the late 1940s and early 1950s respectively, for the therapy and

prophylaxis of malaria.<sup>35, 30</sup> Pyrimethamine is commercialized in combination with the sulfonamide antibiotic sulfadoxine, as the antimalarial drug Fansidar®. The actions of the two drugs have been shown to be synergistic<sup>36,37</sup> and have been used both in a prophylactic regimen as well as for treatment. However, due to observed side effects, this combination is only recommended in severe malaria cases or as a means of prevention in areas where other drugs may not work.



**Figure 1.10** Dihydrofolate reductase inhibitors

#### 1.2.4 Endoperoxides

##### ARTEMISININS

Extracts from the weed *Artemisia annua* have been used in Chinese herbal medicine for the treatment of fever and malaria for more than 2000 years.<sup>38,39</sup> In 1971, Chinese chemists isolated the active ingredient, Artemisinin (Figure 1.11), a sesquiterpene lactone with an endoperoxide functionality that is critical for its antimalarial activity.<sup>40,41,</sup>

Artemisinin has limited availability from the plant, relatively low potency, poor oral activity, poor oil and water solubility, and a short half-life. All these have resulted in a continuing search for improved compounds. In an initial phase of medicinal chemistry, semisynthetic derivatives of artemisinin were prepared. The reduction of the lactone of artemisinin led to the hemiacetal containing compound dihydroartemisinin and

alkylation yielded artemether. A modification of dihydroartemisinin was artesunate, a water-soluble drug in which the hemiacetal OH group was acylated with succinic acid (Figure 1.11).

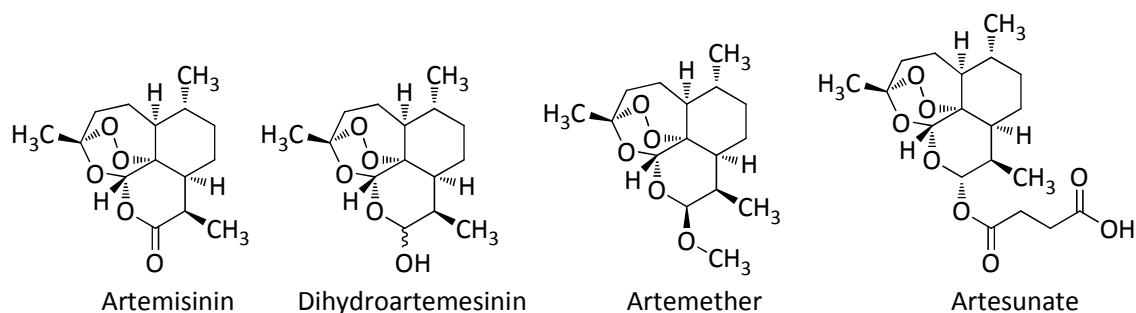


**Figure 1.11** Artemisinin and “first-generation semisynthetic artemisinins”

Artemisinin (ART) and its derivatives display an acceptable safety profile, produce the fastest clinical responses of all currently available treatments and deliver symptomatic relief that is unmatched by other antimalarials. Several proposals have been published regarding the mechanism of action of ART, but the exact mechanism is still unknown. However, several lines of evidence indicate that artemisinins exert their antimalarial action by radical formation that depends on their endoperoxide bridge.<sup>42,43</sup>

Currently the ACTs (artemisinin combination therapies), which include artemisinin or any of its derivatives, are the preferred treatment for acute infection of *P. falciparum*. Amongst of the ART derivatives, Artemether is the most widely prescribed and it is typically used in combination with lumefantrine, marketed as Coartem®, which also has a pediatric formulation.<sup>44</sup>

### SYNTHETIC ENDOPEROXIDES

The search for more metabolically stable peroxide motifs resulted in a second generation of antimalarials, synthetic endoperoxides.<sup>45–52</sup> Despite the high activity reported in some cases, complicated synthesis that often resulted in racemic products and poor pharmacokinetic properties hinder the progression of these compounds to preclinical studies. Only OZ-277, with an adamantane residue on one side and a cyclohexane group on the other, showed the critical balance between stability and reactivity (Figure 1.12). The addition of an aminoacyl residue provided the correct



polarity and solubility, resulting in the desired pharmacological properties. OZ-277 has demonstrated clinical efficacy as a single drug and it has been tested in combination safety studies with piperazine (Figure 1.6).<sup>53-55</sup> Combination of OZ-277 and piperazine received approval in India in 2012 under the name Synriam<sup>®</sup>, however, it has lower oral exposure in patients than expected and this was hypothesized to be due to instability in infected blood, due to interaction with ferrous iron. Derivative OZ-439, which demonstrated a longer PK half-life and improved infected blood stability, has progressed through Phase I trials and demonstrated a good safety profile up to 1600 mg. Combination efficacy clinical trials with piperazine are currently on going.<sup>56</sup> The clinical half-life of OZ-439 is 25-30 hours; hence, Phase II studies will explore the potential of this product to deliver a single-dose cure.<sup>57,58</sup>

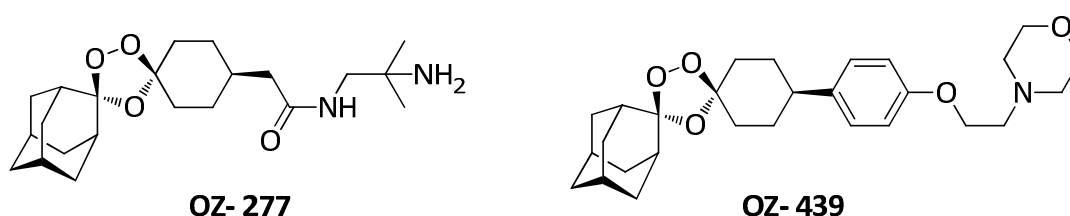


**Figure 1.12** The most advanced synthetic peroxides

### 1.2.5 2-Hydroxynaphthoquinone

#### *ATOVAQUONE*

Compounds with the quinone substructure have distinct biological activities and their antiplasmodial activity has been known since the 1940s. However, it was only after the occurrence of chloroquine resistance that the interest in hydroxynaphtho quinones resurged. Atovaquone (Figure 1.13)<sup>59,60</sup> has a 2-hydroxynaphthoquinone substructure with a cyclohexyl residue in the side chain and displays broad-spectrum antiprotozoal activity and a potent antiplasmodial activity. However, due to the rapid development of resistance, its use as a single agent is inappropriate for the therapy and prophylaxis of malaria.<sup>61</sup> Fortunately, a strong synergism with proguanil was observed when it was tested *in vivo* with Atovaquone and through this synergism the selection for resistant strains during therapy was diminished. Although the mechanism of such interaction is still unknown, since the mid 1990s the combination of Atovaquone and proguanil (Figure

1.13) has been used under the brand name Malarone® (GSK) for the prophylaxis and therapy of uncomplicated malaria.<sup>62–64</sup>

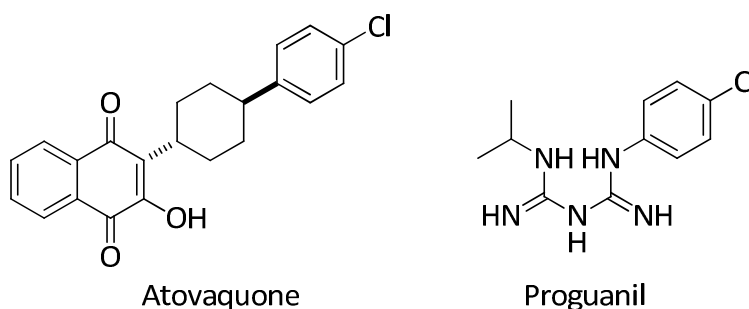


**Figure 1.13** Atovaquone and Proguanil synergic combination

Atovaquone binds to the Q<sub>o</sub> site of the cytochrome *bc*<sub>1</sub> complex,<sup>65</sup> which is a key mitochondrial enzyme that catalyses transfer of electrons to maintain the membrane potential of mitochondria. Inhibition of the cytochrome *bc*<sub>1</sub> complex leads to a rapid collapse of the mitochondrial membrane potential,<sup>66</sup> which causes a complete shutdown of mitochondrial metabolism and ultimately, death of the parasite. (More details in section 1.3)

Currently, atovaquone is the only drug in clinical use targeting the *Plasmodium falciparum* *bc*<sub>1</sub> complex. However, cases of clinical resistance to Malarone have been described.<sup>67,68</sup> Parasite isolates from clinical treatment failures frequently carry a Tyr268 mutation in cytochrome *bc*<sub>1</sub> complex, implicating this modification as the main reason for the observed resistance. This mechanistic link is also observed *in vitro* where it is suggested that mutations around the Q<sub>o</sub> site are responsible for producing resistance to atovaquone without affecting fitness of the parasite. Considering these facts, the main focus for the development of new antimalarials targeting cytochrome *bc*<sub>1</sub> should be to ensure activity against existing atovaquone-resistant strains while maintaining a low propensity for resistance selection. There are relatively few reports on naphthoquinone derivatives with activity against *P. falciparum* in the recent literature.

### 1.2.6 Antibiotics

Several antibacterial agents display considerable activity against the eukaryotic malaria parasites, and antibiotics are known to specifically target prokaryotic structures.

This activity can be explained by the presence of two organelles, the mitochondrion and the apicoplast, both with their own DNA and bacteria-like machinery for replication, transcription and translation. Apart from tetracyclines, which are thought to act mainly against the mitochondrion,<sup>69</sup> all other antibiotics seem to target the apicoplast<sup>70</sup> (Figure 1.14).

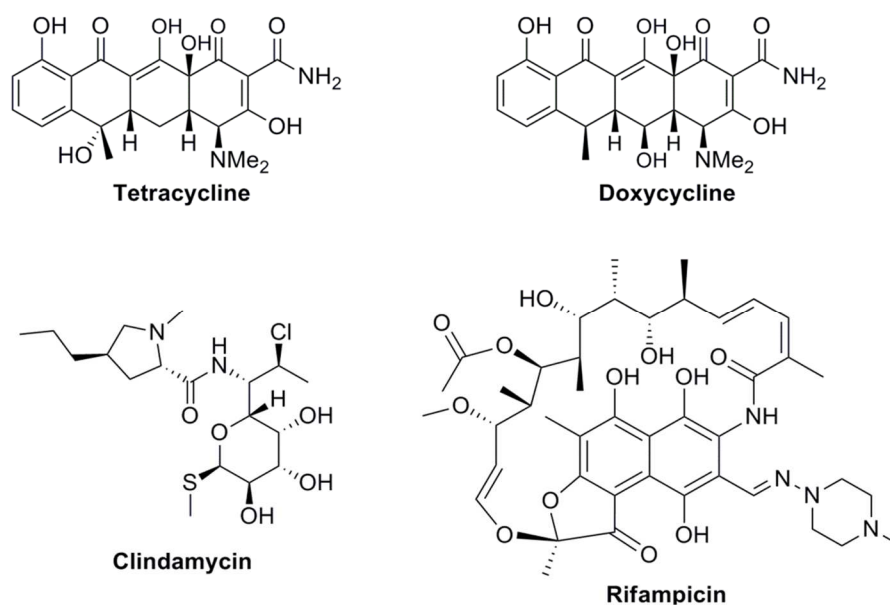


**Figure 1.14** Antibiotics (tetracyclines, doxycycline, clindamycin and rifampicin) that inhibit protein biosynthesis of the parasite

The antibiotic-mediated inhibition displays a delayed kill effect and it is not fully understood. Also fever and parasite clearance times are significantly longer than they are with classical antimalarials (approximately 4 *versus* 2 days) when antibiotics are administered as single agents. This delayed mode of action may be fatal in non-immune patients. Antibiotics are used only in combination with a faster-acting drug for the therapy of acute malaria.<sup>71</sup> However, antibiotics, especially doxycycline, can be used prophylactically as single agents, although they are not registered as antimalarial drugs.

### 1.3 NOVEL ANTIMALARIALS IDENTIFIED VIA HIGH-THROUGHPUT SCREENING

During the past few decades, target-based high-throughput screening has been the main approach to the discovery of new antimalarial agents. A potent and selective triazolopyrimidine-based inhibitor of the *P. falciparum* enzyme dihydroorotate dehydrogenase (*Pf*DHODH) was recently identified *via* a high-throughput enzyme screen (DSM1, Figure 1.15).<sup>72</sup> This was an interesting molecule, but with non-optimal pharmacokinetics. The three-dimensional structure of the enzyme-inhibitor complex was resolved and the subsequent lead optimization programme led to the identification of the preclinical candidate; DSM265, which is now in Phase IIa trials for the treatment of *P. falciparum* and *P. vivax*.<sup>73</sup>

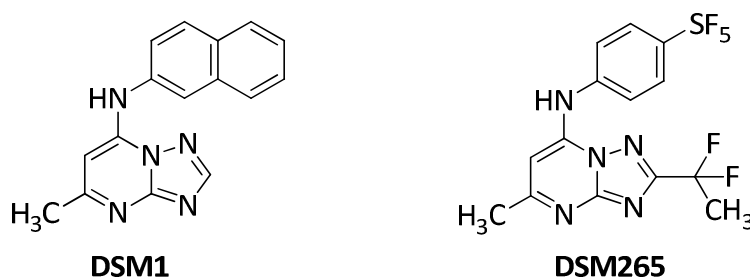


**Figure 1.15** Development of DSM265

DSM265 is a unique example, so far. In general, the target-based screening reveals small molecules with potent activity against an enzyme but that are still unable to clear an infection, either because the target is not really essential to the microbe's viability in the host or because the compound is unable to inhibit the target in the *in vivo* environment.<sup>74</sup> An alternative approach has been the whole-cell screening, also known as phenotypic screening. It is a cell-based screen performed directly against living organisms in which small molecules are tested against all targets in a physiologically relevant context. The disadvantage is that once a compound with potent cellular activity is discovered, lead optimization is hindered by not knowing which protein target the compound interact with.

The development of automated HTS (high-throughput screening) has made it possible to screen large compound libraries looking for chemical 'starting points' with promising

antimalarial activity.<sup>75–79</sup> In 2010, a GSK group, along with St. Jude Children’s Research Hospital and Novartis, reported extensive results from whole-cell high-throughput screens. Structures, molecular descriptors and relevant biological data for thousands of potent *P. falciparum* growth inhibitors were deposited in public databases.<sup>80</sup>

GSK performed an extensive profiling and prioritization exercise which was published as the TCAMS, the Tres Cantos Antimalarial Set of compounds.<sup>77</sup> The TCAMS comprises 13,533 individual compounds derived from the screening of the GSK corporate compound collection (more than 2 million compounds), with most active compounds having submicromolar IC<sub>50</sub> values against the *in vitro* growth of *P. falciparum*. This set contains many different chemical scaffolds although their antimalarial mechanism of action is unknown for the majority of them. *In silico* filtering and developability profiling of the TCAMS allowed the identification of promising new antimalarial chemotypes such as cyclopropyl carboxamides (TCMDC-125454),<sup>81</sup> indolines (TCMDC-139046),<sup>82</sup> aminoalcohols (TCMDC-138152)<sup>83</sup> and aminooxadiazoles (TCMDC-134278)<sup>84</sup> (Figure 1.16).

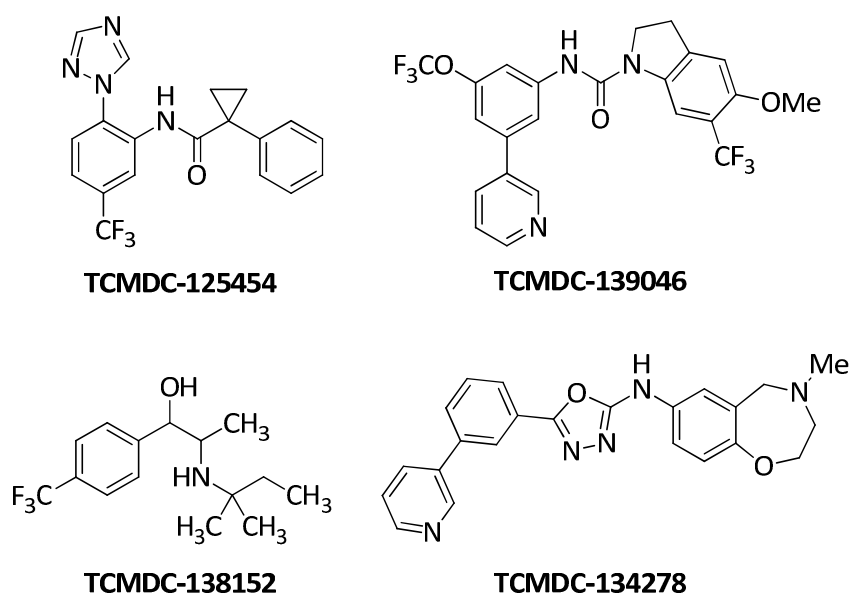


**Figure 1.16** Promising antimalarial chemotypes from the TCAMS

Another promising chemotype identified were the quinazolinones, represented by TCMDC-125133 (Figure 1.17), a particularly interesting compound due to its fast killing mode of action and transmission blocking potential. An efficient medicinal chemistry

effort led to GSK607, a potent antimalarial compound against both asexual and sexual stages of the parasite and with an improved pharmacokinetic profile.<sup>85</sup> Efforts to identify the mode of action for the series were also made, and the *Pf*ATP4 pathway (implicated in regulation of *P. falciparum* sodium homeostasis) was identified as the potential target. *P. falciparum* maintains a low cytosolic Na<sup>+</sup> concentration and the plasma membrane P-type cation translocating ATPase '*Pf*ATP4' has been implicated as playing a key role in this process.<sup>86</sup>

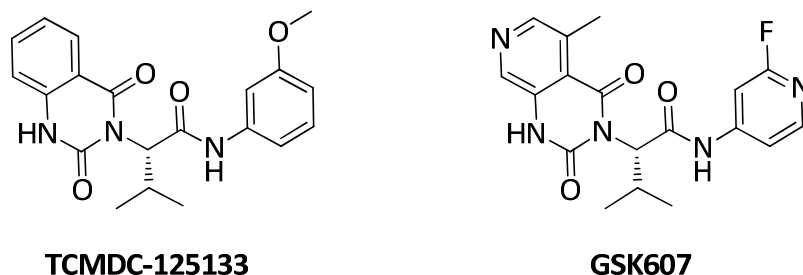


Figure 1.17 Development of GSK607

Phenotypic screening<sup>75,87</sup> of a library of about 12,000 pure natural products and related compounds at Novartis resulted in the identification of 275 primary hits with submicromolar activity against *P. falciparum*. Compounds that showed cross-resistance were discarded and examination of their physiochemical and pharmacokinetic properties led to the selection of a spiroindolone racemate (Figure 1.18) as a lead for optimisation,<sup>88</sup> which concluded with the discovery of NITD609, the first compound to be developed using whole-cell screening of a library of natural products.<sup>89</sup>

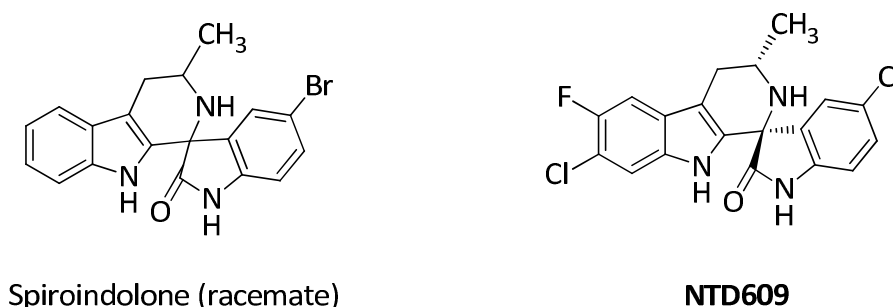
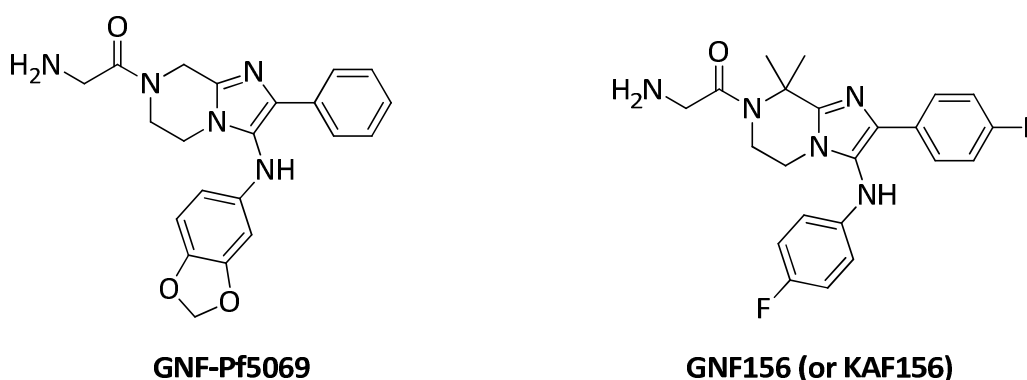


Figure 1.18 Development of NITD609

NITD609 has passed proof-of-concept and has been shown to clear parasites in patients infected with either *P. vivax* or *P. falciparum*.<sup>90</sup> NITD609 successfully completed

phase Ia and Ib trials in 2013 and has just completed phase II clinical trials.<sup>91,92</sup> The mode of action (MoA) has been identified through generation resistant strains and, as in the case of the quinazolidinediones GSK607, it inhibits the *Pf*ATP4 pathway.

A second high-throughput screening campaign was carried out at Novartis,<sup>93,75</sup> leading to the identification of GNF-Pf5069 and the *Imidazolopiperazines* series (Figure 1.19).<sup>94</sup> Poor plasma exposure from the oral route was identified as the main liability and a medicinal chemistry campaign lead to the optimized compound GNF156,<sup>95</sup> which demonstrated a good overall profile with transmission blocking potential. The compound was well tolerated in preclinical safety studies, and has now safely completed phase I studies. Currently GNF156 (also known as KAF156) is in phase II clinical trials.<sup>96</sup> The exact mechanism by which GNF156 exerts its antimalarial activity is unknown, but parasite resistance to GNF156 is associated with the accumulation of mutations in the *Plasmodium falciparum* cyclic amine resistance locus (*Pf*CARL).<sup>97, 98</sup>



**Figure 1.19** Development of KAF156

Another interesting approach is the use of target-focus libraries of compounds which are designed to interact with an individual protein target or, frequently, a family of related targets (such as kinases, voltage-gated ion channels, serine/cysteine proteases).<sup>99</sup> *3,5-Diaryl-2-aminopyridines* (Figure 1.20) were identified from phenotypic whole cell high-throughput screening of a commercially available SoftFocus kinase library and carried out by the University of Cape Town.<sup>100</sup> Synthesis and structure-activity studies identified MMV390048, as a novel antimalarial compound active against the blood stages and able to treat uncomplicated malaria in a single dose, instead of the current three days treatments. This aminopyridine was chosen as a clinical candidate

and progressed to phase I studies.<sup>101</sup> The mechanism of action has clearly been identified using a proteomic approach showing affinity against *P. falciparum* PI4 kinase evidence to conclude that the target of this class of compounds in *P. falciparum* is PfPI4K.<sup>102</sup>

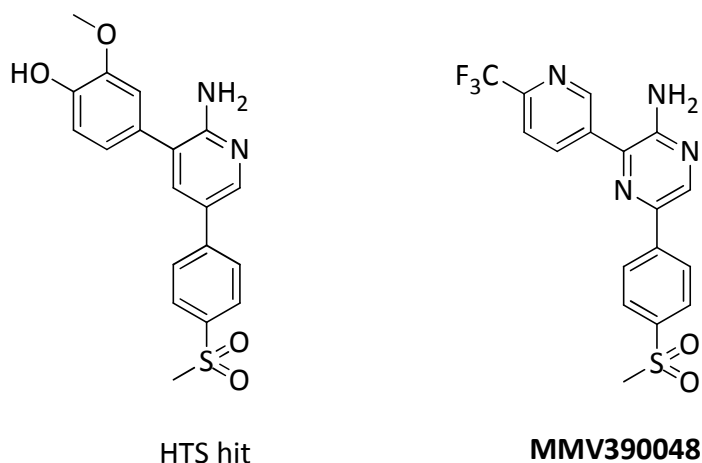


**Figure 1.20** Development of MMV390048

In summary, HTS has become the major tool to find hit compounds to be further developed into drugs, however fundamental research will always be required to elucidate the biological foundation for their mechanism of actions.

### 1.3.1 Future in Malaria

Although malaria has been known for centuries, not many antimalarial chemotypes have been developed. Historically, one of the main reasons for early attrition in target-based programs was the lack of correlation with whole cell activity. However, over the past decade, substantial progress has been made toward the identification of new chemical entities. Programs focusing on the rational design of antimalarials and the development of high-throughput phenotypic screenings as a strategy for unbiased early lead discovery, have delivered compounds into the clinic.<sup>103</sup>

With the aim of malaria eradication, the first *Global Malaria Action Plan (GMAP)* was launched by the *Roll Back Malaria Partnership (RBM)*. RBM is a global platform for coordinated action against malaria which mobilizes for action and resources and forges consensus among partners.<sup>104</sup> GMAP became a valuable advocacy tool that provided the malaria community with a roadmap for progress, and an evidence-based strategy for



delivering effective prevention and treatment.<sup>105</sup> Built on the success of the first GMAP-*for a malaria free world 2008-2015*, a new plan, *Action and Investment to defeat Malaria 2016–2030 (AIM)*, has been developed, serving as both a clarion call and a guide for collective action for all those engaged in the fight against malaria.<sup>106</sup>

However, sustained investment over the next decade in discovery and development of new molecules is essential to enable the long-term delivery of the medicines needed to combat malaria. The development of an effective oral drug is an objective with appreciable challenges and hallmarks of an ideal antimalarial drug have recently been reviewed.<sup>107–109</sup> Any emerging entity must satisfy a range of factors relating to: efficacy, oral bioavailability, a strong safety profile, a new and rapid mode of action and activity against all the resistant strains isolated in the clinic. In addition, an ideal antimalarial should be delivered at an overall cost per treatment of less than 1\$, in order to provide access to the populations hardest hit by the disease. Moreover, with the eradication of the disease in mind, it is highly desirable to develop a drug which can act against hepatic and/or sexual forms, as well as mosquito stages. Any of these characteristics would add extra value to the new drug.<sup>28</sup>

Despite the reported malarone treatment failures due to resistance, the clinical success of atovaquone has validated Cytochrome *bc<sub>1</sub>* as an interesting target for therapeutic exploitation. The combination atovaquone/proguanil (known as Malarone<sup>®</sup>) is currently used for treatment of multidrug-resistant malaria and also for prophylaxis in areas with chloroquine resistance. It is the only drug in clinical use targeting the *Plasmodium falciparum bc<sub>1</sub>* complex.

Considering these facts, the development of new antimalarial drugs targeting the Mitochondrial Electron Transport Chain (mtETC), concretely the cytochrome *bc<sub>1</sub>* complex, should be to ensure activity against existing atovaquone resistant strains while maintaining a low propensity for resistance.

#### 1.4 MITOCHONDRIAL ELECTRON TRANSPORT CHAIN AS ANTIMALARIAL TARGET

In contrast to other eukaryotic cells, malaria parasites obtain almost all their ATP via anaerobic glycolysis.<sup>110,111</sup> Additionally, the sequence of the *Plasmodium* genome has revealed that genes encoding enzymes from the pyrimidine biosynthetic pathway have been conserved, whereas those involved in the pyrimidines salvage have not.<sup>112</sup> Therefore, malaria parasites rely completely on *de novo* pyrimidine biosynthesis essential for the formation of nucleic acids, glycoproteins and phospholipids.

The mtETC is responsible for maintaining an electrochemical gradient across the mitochondrial membrane, as well as a constant pool of ubiquinone for pyrimidine biosynthesis.<sup>113,114</sup> The mtETC differs from the analogous mammalian system in a number of ways<sup>115</sup> and the shutdown of this electron gradient completely arrests crucial metabolic pathways within the microorganism. All this makes the respiratory chain of *P. falciparum* an attractive target for chemotherapy.

The electron transport chain (ETC) of intraerythrocytic malaria parasites is believed to contain five dehydrogenases (Figure 1.21)<sup>116</sup> : 1) NADH:ubiquinone oxidoreductase (*Pf*NDH2) catalyses the electron transfer from NADH to ubiquinone (CoQ) in a pingpong mechanism, to maintain a constant pool of oxidized NADH (NAD<sup>+</sup>) for reductive metabolic pathways such as glycolysis or the tricarboxylic acid cycle;<sup>117</sup> 2) Succinate:ubiquinone oxidoreductase (Complex II or SDH), on the other hand, feeds electrons to the mtETC, and subsequently to complex III;<sup>118</sup> 3) Glycerol-3-phosphate dehydrogenase; 4) the malate quinone oxidoreductase (MQO); 5) dihydroorotate dehydrogenase (*Pf*DHODH) is the final enzyme in the *de novo* biosynthesis of pyrimidines and catalyses the oxidation of dihydroorotate to orotate at the outer side of the inner membrane. The pair of electrons abstracted from dihydroorotate in this oxidation is transferred through flavin mononucleotide cofactor to ubiquinone, itself having been generated at the *bc*<sub>1</sub> complex.<sup>119,120</sup> Moreover, it is thought that the main metabolic function of the mtETC is to regenerate the ubiquinone necessary for the final step of pyrimidine biosynthesis.<sup>114</sup>

The dehydrogenase activity serves, at least in part, to provide electrons to the downstream complexes, namely ubiquinol:cytochrome c oxidoreductase (Complex III or cytochrome *bc*<sub>1</sub>) and cytochrome c oxidase (Complex IV) with ubiquinone (coenzyme Q) and cytochrome c functioning as electron carriers between the complexes. The ATP synthase (Complex V) is not reported to generate ATP (unlike its mammalian counterpart), but is nevertheless proposed as an essential component, possibly acting as a proton leak for the ETC.

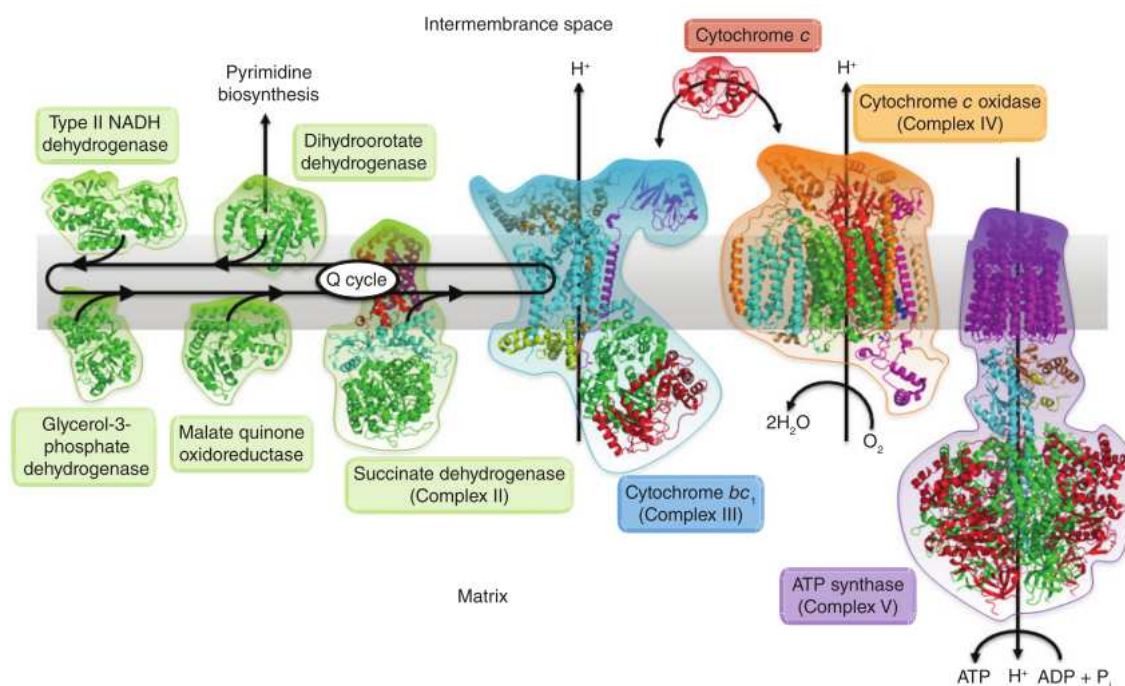


**Figure 1.21** Mitochondrial electron transfer chain enzymes<sup>121</sup>

### 1.4.1 Complex III – Cytochrome *bc*<sub>1</sub>

Cytochrome *bc*<sub>1</sub> represents the only enzyme complex common to almost all respiratory electron transfer chains from Archaea and Bacteria to Eukarya, and its structure has been extensively studied.<sup>122,123</sup> Cytochrome *bc*<sub>1</sub> complex is a homodimeric, multi-subunit membrane protein complex (Figure 1.22-a). It consists of 11 different polypeptides, three of which display catalytic functions: cytochrome *b*, cytochrome *c*<sub>1</sub> and the Rieske protein (or iron-sulfur protein, ISP, due to the iron-sulfur cluster present in it).<sup>124</sup> ISP is highly mobile and evidence suggests that this feature is crucial for the activity of the complex.<sup>125–128</sup> The function of the remaining subunits is not fully

understood but they are likely to contribute to complex stability and the assembly process.

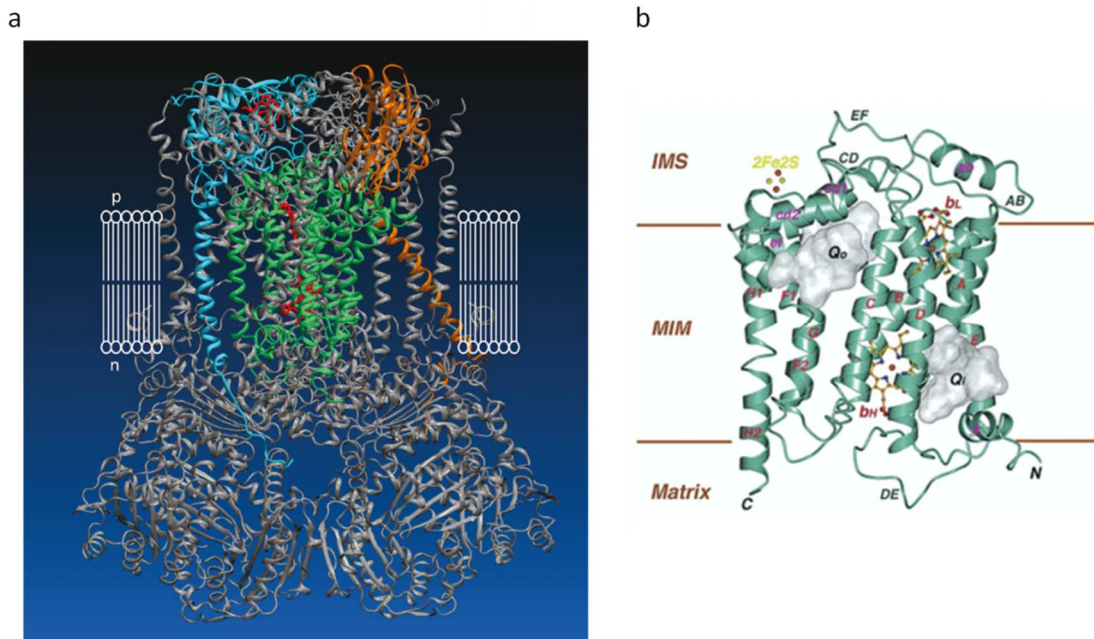


**Figure 1.22** (a) Structure of the cytochrome  $bc_1$  complex: cytochrome  $b$ , cytochrome  $c_1$  and the Rieske protein are represented in green, cyan and orange, respectively. (b) Cytochrome  $b$  subunit of  $bc_1$  complex. (MIM) Mitochondrial inner membrane, (IMS) Intermembrane space.<sup>129</sup>

Cytochrome  $bc_1$ , (or complex III), is the central component of the mitochondrial electron-transfer chain which is responsible for the electron flow from ubiquinol to cytochrome  $c$ . This *Plasmodium* cytochrome  $bc_1$  complex has ubiquinol cytochrome  $c$  oxidoreductase enzymatic activity, which reoxidizes the Coenzyme Q following its reduction by the dehydrogenases present in parasite mitochondria (Figure 1.23). Consequently, inhibition of cytochrome  $bc_1$  impairs pyrimidine biosynthesis, leading to parasite death.

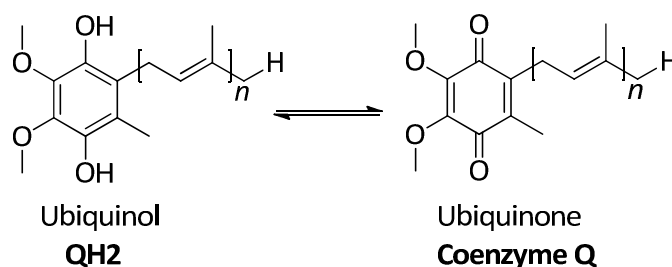


**Figure 1.23** Ubiquinol-Ubiquinone redox reaction

The  $bc_1$  complex contains two distinct quinone-binding sites, the quinol oxidation site  $Q_o$  (or center P) located at the electropositive side and the quinone binding site  $Q_i$  (or center N) at the electronegative side. These binding sites are located at opposite sides of the membrane and are linked by a transmembrane electron-transfer pathway (Figure 1.22-b). Ubiquinol is oxidized to ubiquinone in the oxidative ( $Q_o$ ) site, with two protons released into the intermembrane space, while ubiquinone binds to the reductive ( $Q_i$ ) site, where it is reduced to ubiquinol and takes two protons from the matrix (Mitchell, 1976). This process allows proton translocation from the matrix space to the intermembrane space, thus increasing the electrochemical gradient across the membrane.

### 1.5 4(1H)-pyridones as potential antimalarials

In studies carried out under the aegis of the Walter Reed Army Institute of Research in the late 1960s, clopidol (Figure 1.24) was shown to have activity against *Plasmodium*, including chloroquine-resistant strains, in a number of animal models.<sup>130</sup> Clinical trials in man confirmed activity against chloroquine-resistant *P. falciparum*, although this was not sufficient to warrant further development. Attempts at the time to improve activity through a range of simple derivatives were not successful. Evidence subsequently emerged indicating the mode of action of clopidol involved inhibition of mitochondrial respiration.<sup>131</sup> Furthermore, clopidol was shown to potentiate the antimalarial activity of hydroxynaphthoquinones, *in vitro* and *in vivo*, and retained activity against an atovaquone resistant strain.<sup>132,133</sup> This raised the prospect that clopidol was acting by a novel mechanism, and its simple structure clearly offered some scope for manipulation to improve antimalarial activity.

With the aim of finding novel and affordable antimalarials drugs and to develop compounds to overcome the issues found with atovaquone, scientists at the Wellcome Laboratories and more recently at GlaxoSmithKline's Diseases of the Developing World Centre at Tres Cantos (Madrid, Spain) developed a medicinal chemistry program based on 4(1H)-pyridones which are related to the anticoccidial drug clopidol (Figure 1.24).

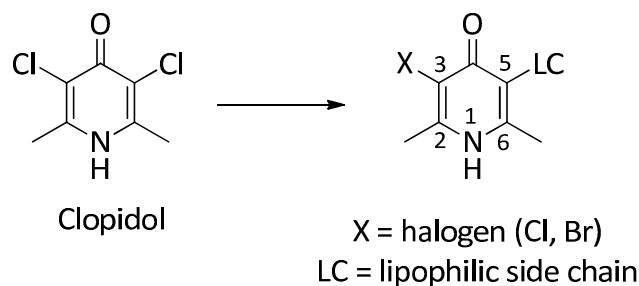


**Figure 1.24** Antimalarial 4(1*H*)-pyridones

Initially the medicinal chemistry strategy was focused on position 5 of the 4(1*H*)-pyridone core by replacing one of the chlorine atoms present at clodolol with different lipophilic moieties (Figure 1.25).<sup>134</sup> It was noteworthy that the introduction of different side chains bearing aromatic rings produced a significant increase in the *in vitro* activity. Introduction of lipophilic groups at the phenyl ring 3 led to compounds with antimalarial activity *in vitro* in the low nanomolar range against the *P. falciparum* sensitive 3D7A strain, however a loss of antimalarial activity was observed when the flexibility of the lipophilic chain was increased by introducing a methylene. The relative position of the substituents at the phenyl ring 2 was also studied and the potency displayed by the compound substituted at the *para* position was retained in the *meta* isomer, but not in the *ortho* analogue.

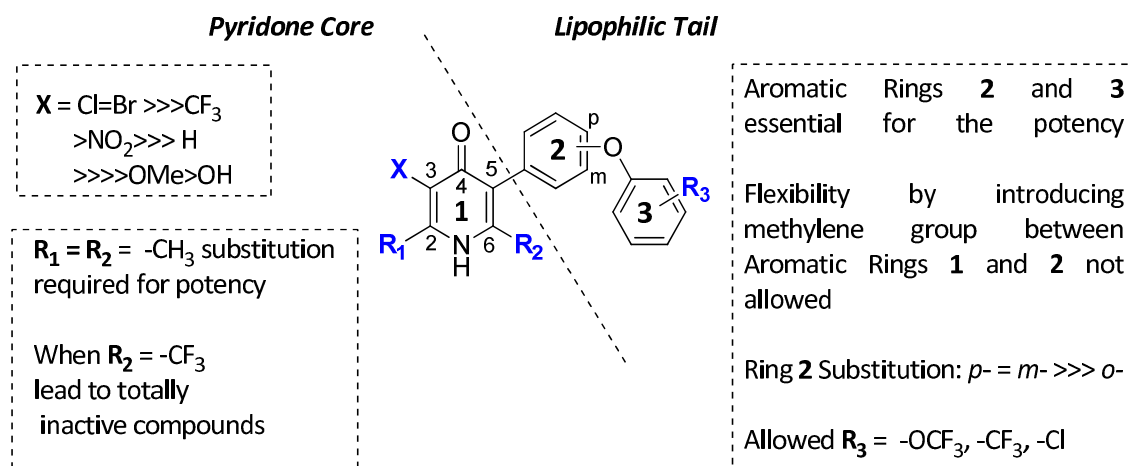


**Figure 1.25** Antimalarial SAR summary for 4(1*H*)-pyridones

Regarding the pyridone ring, in general, replacement of the halogen atom at position 3 (X = Cl, Br) by hydrogen led to less potent compounds. Other electron-withdrawing groups such as -CF<sub>3</sub> or -NO<sub>2</sub> were tolerated, providing the same range of antimalarial activity however, electron-donating substituent (X = OH, OMe) or phenyl resulted in a drop of in activity. Removal of either the 2- or 6- methyl groups resulted in a significant drop in the *in vitro* activity, which was exacerbated by the electron-withdrawing CF<sub>3</sub>.

This MedChem program developed at GSK Tres Cantos identified compounds GW308678 and GW844520 as the most promising 5-phenyloxy-phenyl derivatives and were progressed for further biological studies (Figure 1.26, Table 1.1).

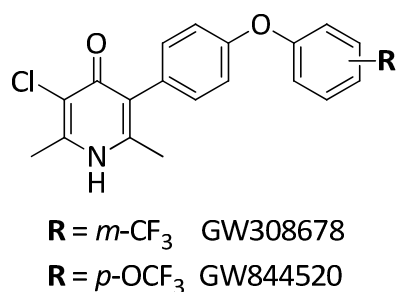


**Figure 1.26** 5-Phenyloxy-phenyl lead compounds

Both compounds were potent inhibitors of the plasmodial ubiquinol: cytochrome c oxidoreductase (Cyt *bc*<sub>1</sub>) with potencies in the low nanomolar range (IC<sub>50</sub> = 0.002 μM), similar to the whole-cell *in vitro* activities observed against *P. falciparum* cultures (IC<sub>50</sub> = 0.005 μM). They also showed potent activity against atovaquone-resistant strain FCR3A (IC<sub>50</sub> = 0.001 & 0.002 μM, respectively) indicating that, despite the similar mechanism of action, the binding modes of the antimalarial 4(1*H*)-pyridones and atovaquone to the active site of the plasmodial cytochrome *bc*<sub>1</sub> might be different. Selectivity against human cells was also analyzed. The IC<sub>50</sub> for human Cyt *bc*<sub>1</sub> was 150–250-fold higher than the IC<sub>50</sub> for *Plasmodium* Cyt *bc*<sub>1</sub>, while in the whole cell assays selectivity was >500–1000-fold higher. Cytotoxicity assays were hampered by the poor solubility of the samples in the media used for IC<sub>50</sub> determination in the HepG2 cell line. Finally, GW308678 and GW844520 displayed high efficacy when tested in the *P. yoelii* murine model (ED<sub>90</sub> = 0.16 & 0.4 mg/kg, respectively).

**Table 1.1** Biological profile of GW308678 & GW844520

Compound	<i>In vitro</i> IC <sub>50</sub> (uM)							<i>In vivo</i> (mg/kg) <sup>a</sup>	
	Target Cyt bc1			Whole cell				<i>P. yoelii</i> CD1 mice	
	<i>P.falciparum</i>	Human (HEK293)	SI.	<i>P.falciparum</i>		Human HepG2	SI.	ED <sub>50</sub>	ED <sub>90</sub>
			3D7A	FCR3A					
GW308678	0.002	0.5	250	0.005	0.001	>2.5	>500	0.13	0.16
GW844520	0.002	0.3	150	0.005	0.002	>5	>1000	0.2	0.4

(a) Seven doses po over 4 days. SI.: Selectivity Index= HepG2 IC<sub>50</sub>/Pf IC<sub>50</sub>

Analysis of the physicochemical properties allowed us to determine the ADME profile (Absorption, Distribution, Metabolism and Excretion) for the 5-(4-phenoxyphenyl)-4(1*H*)-pyridones (summarized in Table 1.2). GW308678 and GW844520 showed relatively high lipophilicity (ChromlogD<sub>7.4</sub>= 4.99 & 5.12, respectively),<sup>135</sup> good permeability values (Papp MDCK = 434 & 357 nm/s, respectively), high protein plasma binding (PPB > 99%) and poor solubility in aqueous media over a wide range of pH values (<0.1 µg/mL, pH = 2–12) as well as in biorelevant simulated fluids FaSSIF (fasted state /small intestine) and FeSSIF (fed state /small intestine).<sup>136</sup>

**Table 1.2** Physicochemical properties of GW308678 & GW844520

Compound	Solubility (µg/mL)			Chrom_logD			Papp MDCK (nm/s)	Protein binding (%)
	pH 2-12	FeSSIF	FaSSIF	pH=2	pH=7.4	pH=10.5		
GW308678	<0.1	4.8	0.9	4.89	4.99	5.04	434	99.6
GW844520	<0.1	3	0.9	5.25	5.12	4.95	357	>99.8

On the basis of its promising anti-malarial profile and safety margin and in order to have a prediction of the pharmacokinetic behavior in humans, compound GW844520 was progressed to pharmacokinetic studies in four different animal species: mouse, rat, monkey and dog (Table 1.3). GW844520 showed low blood clearance across all the preclinical species (ranging from 0.5 to 5% of liver blood flow), a steady-state volume of distribution in the range of 2 to 4 times totally body water and relatively long-half lives, close to 100 h in monkey. Oral bioavailability in all the species was excellent from solution formulations at low dose (F = 50-100 % at < 1 mg/kg), which was consistent with the high passive permeability across MDCK cell monolayers.<sup>137</sup>



**Table 1.3** GW844520 Pharmacokinetic studies after intravenous and oral administration to Mouse, Rat, Dog and Monkey

Species	i.v. PK <sup>a</sup>			p.o PK <sup>b</sup>		
	Cl (ml/min/kg)	V <sub>ss</sub> (L/kg)	T <sub>½</sub> (h)	AUC	T <sub>½</sub> (h)	F (%)
Mouse	0.74	1.6	25	8.54	23.6	72
Rat	2.3 ± 0.4	2.0 ± 0.8	7.9 ± 0.7	4.14 ± 0.96	7.1 ± 1.7	118
Dog	0.15 ± 0.04	2.4 ± 0.2	NE	22.8 ± 7.8	214 ± 30	51 ± 11
Monkey	0.35 ± 0.02	2.7 ± 0.1	89 ± 3	13.5 ± 0.6	88.4 ± 4.4	69 ± 6

(a) Dose = 0.25 mg/kg (b) Dose = 0.5 mg/kg (mouse, rat); Dose = 0.4 mg/kg (dog, monkey). NE : not estimated

However oral bioavailability dropped dramatically when the compound was administered in suspension at higher doses (F~20% at 10 mg/kg), presumably due to low solubility or dissolution rate limited oral absorption from the solid dosage form.<sup>138</sup>

The low oral bioavailability in preclinical species at higher doses was identified as the main issues for the progression of this compound into preclinical studies. GW844520 displayed nonlinear pharmacokinetics, resulting in an inability to raise systemic exposures above a certain limit.

No visible signs of toxicity in the repeated dose studies in both rat and dog were observed at the highest exposures. However, although no clinical findings were observed in the 14-day dog study, the progression of GW844520 was discontinued because of mild and reversible histopathological findings seen in skeletal and cardiac muscles.<sup>138</sup> These alterations were tentatively attributed to the accumulation of the drug into these tissues, probably as a result of its high lipophilicity and long half-life in the dog (T<sub>1/2</sub>= 214 h).

Within an attempt of improving the ADME profile of the chemical series, our group identified GSK932121 (Figure 1.27), the hydroxyl derivative of GW844520 at position 6, which retained the antimalarial potency and showed improved physicochemical properties.<sup>139</sup>

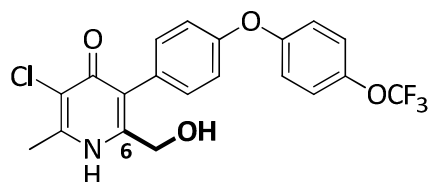


**Figure 1.27** GSK932121

Like GW844520, the hydroxymethyl derivative GSK932121 inhibited the plasmodial Cyt *bc1* in the low nanomolar range, similar to the whole cell *in vitro* activities seen against *P. falciparum* cultures, maintaining similar selectivity index over both. GSK932121 displayed an outstanding *in vivo* efficacy in *P. yoelii* murine malaria model (ED<sub>90</sub>= 0.6 mg/kg), similar to GW844520 (Table 1.4).

**Table 1.4** Biological profile of GSK932121 & GW844520 in mouse

Compound	<i>In vitro</i> IC <sub>50</sub> (uM)							<i>In vivo</i> (mg/kg)	
	Target Cyt <i>bc1</i>			Whole cell				<i>P. yoelii</i> CD1 mice	
	<i>P. falciparum</i>	Human (HEK293)	SI.	<i>P. falciparum</i>		Human HepG2	SI.	ED <sub>50</sub>	ED <sub>90</sub>
				3D7A	FCR3A				
GSK932121	0.007	0.4	57	0.006	0.006	10	>1666	0.3	0.6
GW844520	0.002	0.3	150	0.005	0.002	>5	>1000	0.2	0.4

However, the more polar compound GSK932121 showed better physicochemical properties than its predecessor GW844520 (Table 1.5). Although GSK932121 was slightly less lipophilic than GW844520, expressed in terms of ChromlogD, the hydroxymethyl group conferred a significant improvement in the solubility when it was measured in FeSSIF media. In comparison with GW844520, GSK932121 showed lower protein binding and higher permeability in the MDCK cell line.

**Table 1.5** Physicochemical properties of GSK932121 & GW844520

Compound	Solubility (µg/mL)			Chrom_logD			Papp MDCK (nm/s)	Protein binding (%)
	pH 2-12	FeSSIF	FaSSIF	pH=2	pH=7.4	pH=10.5		
GSK932121	<0.1	91.10	0.7	4.53	4.42	4.05	712	97
GW844520	<0.1	3.00	0.9	5.25	5.12	4.95	357	>99.8

The higher solubility of GSK932121 in FeSSIF, together with a lower protein binding, translated into a significant enhancement in oral bioavailability when it was

administered as suspension in 1% methylcellulose in mice (F 50% for GSK932121 vs F 20% for GW844520, dose = 10 mg/Kg) and particularly when it was administered in dogs (F 16% for GSK932121 vs F 4% for GW844520, dose = 2 mg/Kg) (Table 1.6). Pharmacokinetic studies also showed that GSK932121 seemed to be more sensitive to metabolic degradation, evidenced by the significant increase in clearance and reduction in half-life in both mice and dog. Superior oral bioavailability was demonstrated by GSK932121 however, a nonlinear pharmacokinetics was observed at high doses of the solid dosage form, resulting in an inability to raise systemic exposures above a certain limit.

**Table 1.6** Pharmacokinetic profile of GSK932121 & GW844520

Compound	CD1 mouse					Beagle dog				
	Vd (L/kg) <sup>a</sup>	CL (mL/min/kg) <sup>a</sup>	T <sub>1/2</sub> (h) <sup>a</sup>	C <sub>max</sub> (mg/mL) <sup>b</sup>	% F <sup>b</sup>	Vd (L/kg) <sup>c</sup>	CL (mL/min/kg) <sup>c</sup>	T <sub>1/2</sub> (h) <sup>c</sup>	C <sub>max</sub> (mg/mL) <sup>d</sup>	% F <sup>d</sup>
GSK932121	1	3	3.8	1.1	50	2.8	0.8	42	0.3	16
GW844520	1.2	0.6	24.1	0.9	20	2.9	0.2	143	0.03	4

<sup>a</sup> Solution in 1% DMSO/7.5% PEG/20% encapsin/saline pH= 6; intravenous (0.2 mg/kg)

<sup>b</sup> Oral gavage: suspension 1% methyl cellulose; per orem (10 mg/kg)

<sup>c</sup> Solution in 1% DMSO/7.5% PEG/20% encapsin/saline; intravenous (0.05 mg/kg)

<sup>d</sup> Oral gavage: suspension 1% methyl cellulose; per orem (2 mg/kg)

More recently studies carried out in our group, identified the ring-fused 4-pyridone (1-azafluorenone) shown in the figure 1.28. This compound was obtained as a side product in the last chlorination step of the scale-up synthesis of GW308678. After removal of GW308678 by a filtration process, a red solid was isolated after maintaining the mother liquors at 5 °C for several days. This red solid, azafluorenone, showed an outstanding *in vitro* antimalarial activity, IC<sub>50</sub> = 0.039 μM which encourage the group to further explore ring-fused 4-pyridones as antimalarial compounds.

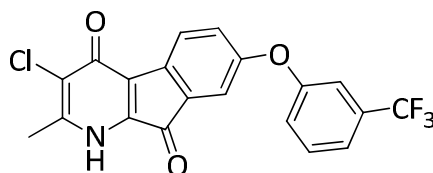


**Figure 1.28** 1-Azafluorenone

---

## **2 OBJECTIVES**

---

The 4(1*H*)-pyridones identified in our group represent a new family of compounds with outstanding antimalarial activity. Unfortunately, the low aqueous solubility showed with this family precluded dose escalation studies and therefore the progression of the family to further development stages.

The objective of this thesis was the identification of novel derivatives with improved physicochemical and solubility properties whilst maintaining, if not improving, the antimalarial potencies and safety margins shown by the parent 4(1*H*)-pyridones.

Whit this aim different approaches were followed.

1.- Synthesis of more polar 4(1*H*)-pyridones (Chapter 3.1). This chapter describes the synthesis of new analogues focus on improving the physicochemical profile by the introduction of polar groups at position 2 of the 4(1*H*)-pyridone (Figure 2.1):

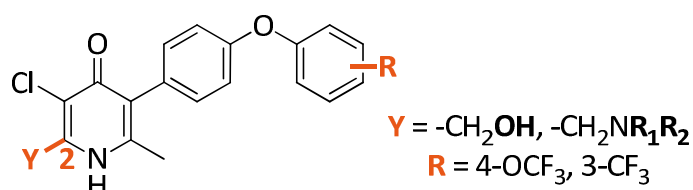


**Figure 2.1** Improved 4(1*H*)-pyridones

2.- Design and synthesis of 4(1*H*)-pyridones prodrugs (Chapter 3.2). This chapter describes the design, synthesis and biological evaluation of pro-drugs at different positions of the pyridone scaffold, being the ultimate aim the identification of a molecule with a profile suitable for progression into preclinical safety studies at high doses, and the implementation of a suitable synthetic route to provide material for these studies (Figure 2.2):

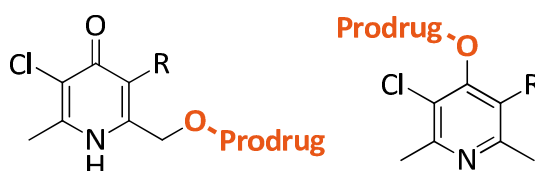


**Figure 2.2** Pro-drug strategy

3.- Synthesis of cyclic 4(1*H*)-pyridones (Chapter 3.3). This chapter describes the synthesis and structure-activity relationship (SAR) studies for the structurally related ring-fused 4-pyridone (1-azafluorenone). This novel tricyclic scaffold warranted further investigation of the series not only focus on the improvement of physicochemical properties but also to explore whether the mode of action is different in comparison with the classical 4(1*H*)-pyridones (Figure 2.3):

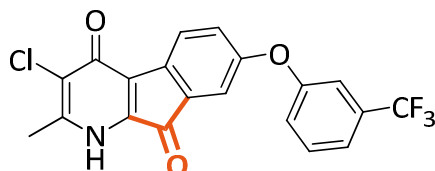


**Figure 2.3** Azafluorenones

4.- \*CONFIDENTIAL SECTION\*: Synthesis of more tractable cyclic 4(1*H*)-pyridones (Chapter 3.4). This chapter describes the synthesis and the structure-activity relationship (SAR) studies for a more tractable tricyclic scaffold, being the ultimate aim to identify a ring-fused 4-pyridone suitable not only to improve ADME profile also to overcome the safety issues found in the classical 4(1*H*)-pyridones.

---

## **3 RESULTS AND DISCUSSIONS**

---

### 3.1 4(1H)-PYRIDONE DERIVATIVES AT POSITION 2

Previous work carried out in our group led to the identification of the compound GSK932121, a potent antimalarial pyridone (Figure 1.27) with a hydroxy methyl group at position 6. This result encouraged us to explore the introduction of polar groups at the 4(1H)-pyridone core. As mentioned previously, introduction of ionizable tertiary amines, methoxy or polar hydroxyl groups at position 3 of the pyridone ring resulted in a significant or complete loss of the antimalarial activity.<sup>134</sup> However, 2 and 6 positions of the 4(1H)-pyridone ring had not been studied.

The medicinal chemistry herein described was focused on the synthesis of more soluble compounds and enhancing oral bioavailability by attaching polar hydrophilic groups such as CH<sub>2</sub>OH and ionizable moieties such as basic amines at the yet unexplored position 2 of the 4(1H)-pyridone ring (Figure 3.1).

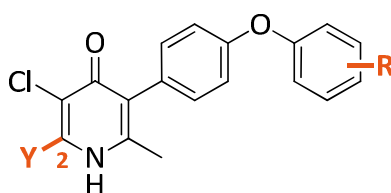


**Figure 3.1** 4(1H)-pyridones modified at position 2 <sup>139</sup>

#### 3.1.1 Synthesis of the hydroxy methyl 4(1H)-pyridones at position 2.

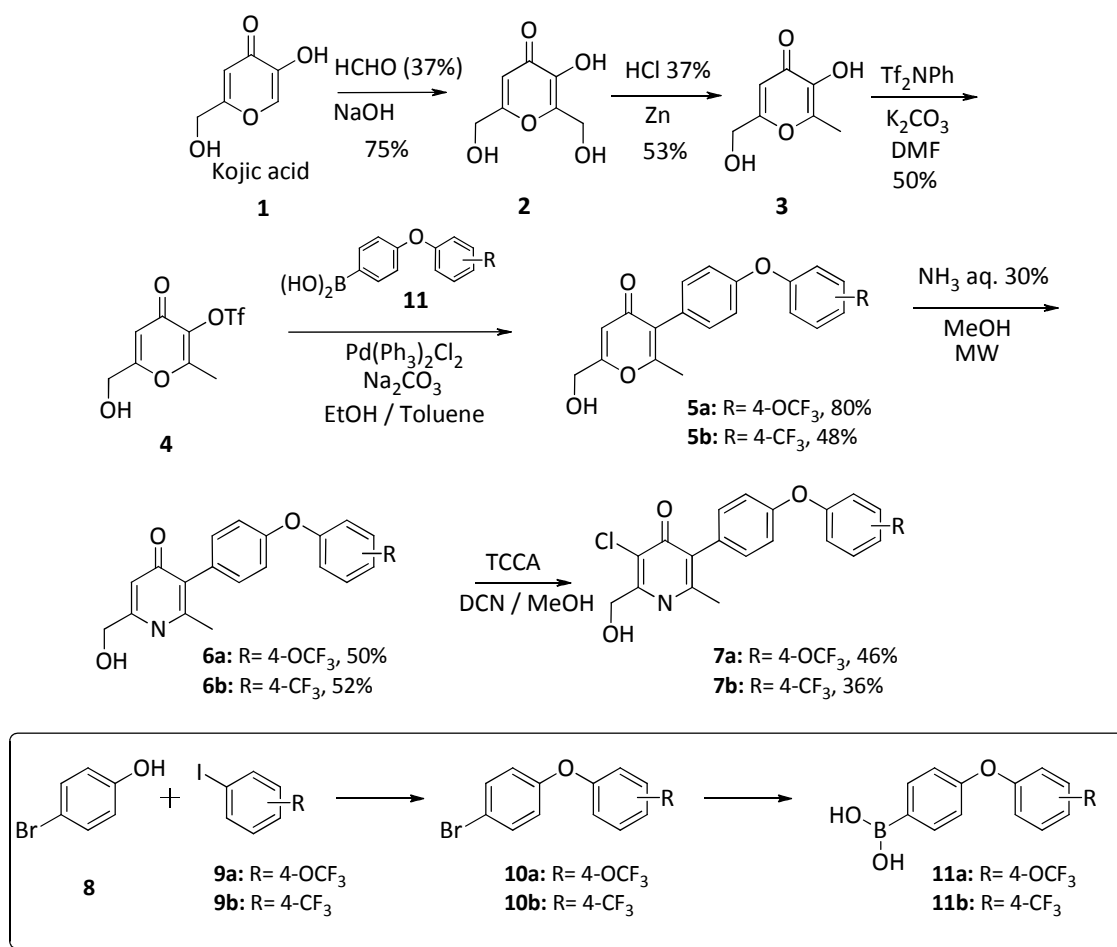
The synthesis of the corresponding hydroxymethyl derivatives of the lead compounds GW844520 and GW308678 at position 2 (**7a** and **7b**), were prepared according with the synthetic rout depicted in Scheme 3.1.

Reaction of Kojic acid **1** with formaldehyde in presence of a base (NaOH) led to 3-hydroxy-2,6-dihydroxy-methyl- $\gamma$ -pyrone **2** in 75% yield.<sup>140</sup> Selective reduction of the alcohol at position 2 of the pyridone scaffold was achieved by reaction of **2** with Zinc powder in the presence of HCl 37% to give **3** in 54% yield.<sup>141</sup> Regiospecific activation of the most reactive alcohol at position 3 with *N*-phenyl-trifluoromethanesulfonimide and potassium carbonate lead to **4** in 50% yield.<sup>142</sup>

The introduction of the key phenoxy phenyl lipophilic moiety was carried out by Suzuki coupling between triflate **4** and the appropriate boronic acid **11** to afford the pyrone **5**.



Bis(triphenylphosphine)palladium(II) chloride was used as catalyst and Suzuki reaction was performed in the presence of sodium carbonate at 80 °C. Desired pyrones were obtained after purification by column chromatography (80% and 48% yield, **5a** and **5b**, respectively). Boronic acids **11a** and **11b** were prepared in our group by Ullman coupling between the commercially available 4-bromophenol **8** and the iodophenyl compounds **9a** and **9b**. Further reaction of the bromo phenoxy phenyl derivatives **10a** and **10b** with triisopropylborate, followed by acid hydrolysis led to the desired boronic acids in excellent yields (80% and 70%, **11a** and **11b**, respectively).<sup>142</sup>



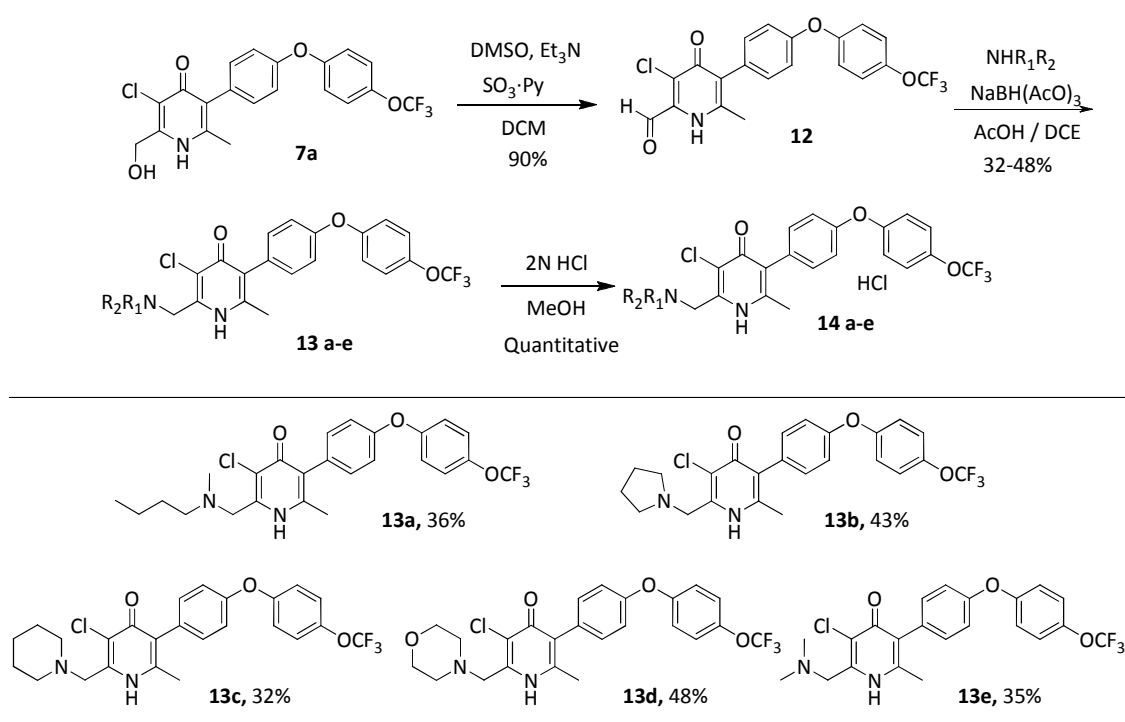
**Scheme 3.1.** Synthesis of 4(1H)-pyridones derivatives at position 2

The construction of the 4-pyridone scaffold involved ammonolysis<sup>134</sup> and further chlorination by reaction with trichloroisocyanuric acid.<sup>143</sup> Reaction of **5** in 30% aqueous ammonia under microwave conditions (140 °C for 30min) resulted in the desired pyridone **6a** (50% and 52% yield, **6a** and **6b**, respectively). In general, the use of trichloroisocyanuric acid (TCCA) was found to provide a suitable alternative to *N*-

chlorosuccinimide, used previously in the chlorination of pyridones derivatives, with advantages in shorter reaction times, lower reaction temperatures, cleaner reaction crudes and higher yields of final materials. In this case, reaction with TCCA was performed in a mixture DCM/MeOH (2:1) due to the low solubility of **6**. After 1h at 0 °C, compound **7** was obtained in moderate yield (46% and 36% yield, **7a** and **7b**, respectively).

### 3.1.2 Synthesis of ionizable 4(1H)-pyridones at position 2.

The introduction of ionizable moieties such as basic amines was explored in order to reduce the lipophilicity of the 5-(4-phenoxyphenyl)-4(1H)-pyridone derivatives but also with the aim of improving solubility and oral bioavailability by the corresponding salt formation (Scheme 3.2).



**Scheme 3.2** Synthesis of 4(1H)-pyridones derivatives with ionizable substitution at position 2.

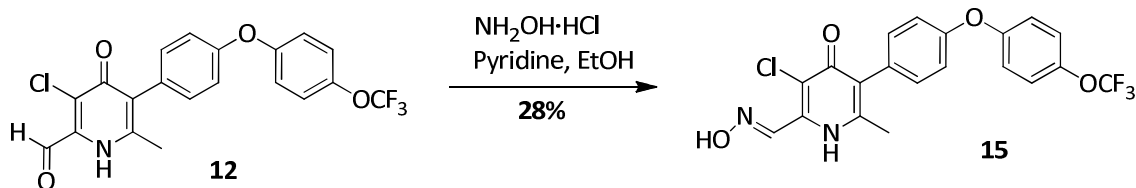
To carry out the synthesis of the different analogues at position 2 of the pyridone scaffold compound **7a** was used as starting point. Compound **7a** was oxidized to the corresponding aldehyde **12** in excellent yield (90%) using sulfur trioxide-pyridine complex as oxidizing agent in DCM at rt. Reductive amination to obtain different tertiary amines at position 2 of the pyridone was performed by reaction of **12** with the

corresponding amine. Sodium triacetoxyborohydride in DCE was used as reductant in the presence of AcOH. Amino derivatives **13a-e** were obtained in moderate yields (32-48%) and the corresponding salts were prepared by treatment with 2N HCl in MeOH. Further evaporation of the solvent led to the pure hydrochloride salts (**14a-e**) quantitatively.

### 3.1.3 Synthesis of the 2-carbaldehyde oxime of GW844520

Small oximes are highly polar moieties which could result in an improvement in the solubility, so we completed the study at the position 2 with the synthesis of the carbaldehyde oxime of GW844520.

The carbaldehyde oxime at position 2 was easily obtained by reflux of compound **12** with hydroxylamine hydrochloride and pyridine (Scheme 3.3). Crude reaction mixture was purified by precipitation and after several washes, compound **15** was isolated in 28% yield.



**Scheme 3.3** Synthesis of the *N*-Oxide of GW844520.

The structure of all the compounds synthesized in this section was determined by proton Nuclear Magnetic Resonance Spectroscopy ( $^1\text{H-NMR}$ ) and Liquid chromatography–mass spectrometry (LC/MS). Carbon Nuclear Magnetic Resonance Spectroscopy ( $^{13}\text{C-NMR}$ ) analysis was done for final compounds. Proton and carbon assignment for compound **15** has been done based on HMQC and HMBC spectra analysis (see Appendix I).

### 3.1.4 Biological activity and analysis results

Physicochemical data of the final compounds is summarized in Table 3.1. This analysis was done according with the GSK criteria.<sup>144</sup> Lipophilicity is expressed in terms of chromatographic log  $D^{145}$  which provides reliable hydrophobicity predictions. This parameter is calculated according the following equation,

$$\text{Chrom log } D_{\text{pH}} = \text{CHI}_{\text{pH}} \times 0.0857 - 2$$

where CHI (chromatographic hydrophobicity index) represents a measure of hydrophobicity which has been used alongside the octan-1-ol/water partition coefficients for several years. Chrom log D is measured at pH 2.0, pH 7.4 and pH 10.5 in order to analyze the acid/base character of compounds, being pH 7.4 value the most relevant as it represents the physiological pH. Solubility was assessed using a miniaturized shake flask method with ChemiLuminescent Nitrogen Detection (CLND).<sup>146</sup> Only the most potent compounds were progressed to solubility studies in biorelevant simulated fluids FaSSIF and FeSSIF.<sup>136</sup>

As shown in Table 3.1 hydroxylated derivatives **7a** and **7b** displayed partially better physicochemical properties than their corresponding predecessor GW844520 and GW308678. Lipophilicity at the physiological pH (pH = 7.4) was slightly lower in comparison to the rest of compounds in the table (Chrom log  $D_{\text{pH}7.4} = 4.54$  and  $4.32$ , for **7a** and **7b** respectively) and it was translated in an improvement of the solubility in both biorelevant simulated fluids, particularly in FeSSIF, leading to solubility values of  $28.62 \mu\text{g/mL}$  and  $11.92 \mu\text{g/mL}$  for **7a** and **7b**, respectively. However, comparison of **7a** with its corresponding analogue at position 6 (GSK932121), the presence of the polar hydroxymethyl group  $\text{CH}_2\text{OH}$  at position 2 did not showed the expected solubility enhancement.

For analogues **14a-e**, the only improvement in the lipophilicity was observed when Chrom logD was tested at pH = 2.0, as all the amino derivatives are protonated. The kinetic aqueous solubility for these amino derivatives (**14a-e**) was assessed using CLND assay, displaying all of them very low values ( $\text{CLND} \leq 3 \mu\text{g/ml}$ ). None of them induced the expected solubility improvement, only the introduction of the butyl(methyl)amino moiety (**14a**) led to a slight more soluble compound in comparison with its analogues

(CLND  $\leq$  1  $\mu\text{g/ml}$  for **14b**, **14c** and **14e**). The introduction of an oxygen atom as a morpholine (**14d**) afforded the less lipophilic compound of this amino series but it was not translated in aqueous solubility improvement (CLND = 3  $\mu\text{g/ml}$ ). Finally, Chrom LogD of the carbaldehyde oxime **15** was similar to the parent GW844520, and only a slightly improvement in solubility was observed.

**Table 3.1.** Physicochemical properties of the new pyridones **7a-15**.

Compound	Chrom LogD				Solubility ( $\mu\text{g/ml}$ )		
	th (pH 7.4)	pH 2.0	pH 7.4	pH 10.5	CLND	FaSSIF	FeSSIF
<b>7a</b>	5.25	4.63	4.54	4.23	-	5.43	28.62
<b>7b</b>	5.19	4.33	4.32	4.04	2	2.52	11.92
<b>14a</b>	6.78	1.12	7.82	7.98	3	-	-
<b>14b</b>	6.06	2.10	6.42	6.47	1	-	-
<b>14c</b>	6.53	2.20	7.34	7.47	1	-	-
<b>14d</b>	5.91	3.01	5.34	5.17	3	-	-
<b>14e</b>	5.84	1.89	5.62	5.50	0	-	-
<b>15</b>	5.02	5.13	5.03	3.71	-	1.51	7.49
<b>GSK932121</b>	4.5	4.53	4.42	4.05	1.00	<1	91.10
<b>GW844520</b>	6.67	5.25	5.12	4.95	22.00	<1	3.00
<b>GW308678</b>	7.37	4.89	4.99	5.04	14.00	<1	4.80

Antimalarial data for all the 4(1H)-pyridones derivatives at position 2 are summarized in Table 3.2. In order to assess the effects of these compounds on the malaria parasite metabolic activity, a modification of the [ $^3\text{H}$ ]-hypoxanthine uptake assay described by Desjardins et al.<sup>147</sup> was used. The activity value against *P. falciparum* along with cytotoxicity in hepatocytes human cell lines (HepG2) are provided as IC<sub>50</sub> and details related to the procedure of the IC<sub>50</sub> determination are described at the experimental section.

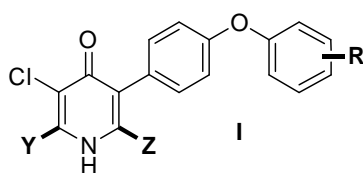
Ligand Efficiency (LE) metrics are also included. This parameter combines both “potency and lipophilicity” and attempts to provide a useful measure of the effective contribution of each atom in the activity of the compound.<sup>148</sup> It is in fact a simple average of atomic contribution and it works by taking the number of heavy (non-hydrogen) atoms as the size metric. The Ligand Efficiency parameter is measured according to the following equation,

$$LE = 1.37 \times pIC_{50} / n_{HA}$$

where the antimalarial potency is expressed as  $pIC_{50}$  and  $n_{HA}$  is the number of heavy atoms. This gives a simple number where higher is the better and determines how “efficient” a ligand is at binding. Optimizing ligand efficiency metrics has the potential to ameliorate the inflation of these properties, potency and lipophilicity, and to increase the quality of drug candidates.

In order to make the analysis of these results as efficient as possible, key analogues previously prepared in our group but not included in the work presented in this thesis, are included in the table and duly indicated (\*).

In comparison with the parent nonhydroxylated counterparts GW844520 and GW308678, the introduction of polar hydroxymethyl group  $CH_2OH$  at position 2 showed a significant reduction in the *in vitro* antimalarial activity in compounds **7a** and **7b** ( $IC_{50} = 0.30 \mu M$  and  $0.29 \mu M$ , respectively). But most interestingly, we observed that the polar hydroxymethyl group  $CH_2OH$  showed a very different behaviour when it was attached at different positions in the 4(1H)-pyridone core. Thus, when  $CH_2OH$  group was attached at position 6 retained the high level of antimalarial activity observed for GSK932121 ( $IC_{50} = 0.006 \mu M$ ), while induced a significant reduction in the *in vitro* antimalarial activity when located at position 2 (**7a** and **7b**). The introduction of ionizable tertiary amines at position 2 produced similar results to those observed at position 3, leading to inactive compounds (**14a-e**,  $IC_{50} > 0.5 \mu M$ ). This loss of the potency was also observed when the same ionizable tertiary amines were attached at position 6 (**14f-h\***,  $IC_{50} > 0.5 \mu M$ ).

**Table 3.2.** Biological results for compounds of general Formula I

Compound	Y	Z	R	IC <sub>50</sub> (μM)	HepG2 (μM)	LE
<b>7a</b>	CH <sub>2</sub> OH	CH <sub>3</sub>	4-OCF <sub>3</sub>	0.30	-	0.31
<b>7b</b>	CH <sub>2</sub> OH	CH <sub>3</sub>	4-CF <sub>3</sub>	0.29	-	0.32
<b>14a</b>		CH <sub>3</sub>	4-OCF <sub>3</sub>	> 0.5	-	< 0.25
<b>14b</b>		CH <sub>3</sub>	4-OCF <sub>3</sub>	> 0.5	-	< 0.25
<b>14c</b>		CH <sub>3</sub>	4-OCF <sub>3</sub>	> 0.5	-	< 0.25
<b>14d</b>		CH <sub>3</sub>	4-OCF <sub>3</sub>	> 0.5	-	< 0.25
<b>14e</b>		CH <sub>3</sub>	4-OCF <sub>3</sub>	> 0.5	-	< 0.27
<b>15</b>	HO-N=	CH <sub>3</sub>	4-OCF <sub>3</sub>	0.029	15	0.34
<b>14f*</b>	CH <sub>3</sub>		4-OCF <sub>3</sub>	> 0.5	-	< 0.25
<b>14g*</b>	CH <sub>3</sub>		4-OCF <sub>3</sub>	> 0.5	-	< 0.25
<b>14h*</b>	CH <sub>3</sub>		4-OCF <sub>3</sub>	> 0.5	-	< 0.25
<b>GW844520</b>	CH <sub>3</sub>	CH <sub>3</sub>	4-OCF <sub>3</sub>	0.005	> 61	0.40
<b>GW308678</b>	CH <sub>3</sub>	CH <sub>3</sub>	4-CF <sub>3</sub>	0.003	> 63	0.43
<b>GSK932121</b>	CH <sub>3</sub>	CH <sub>2</sub> OH	4-OCF <sub>3</sub>	0.006	10	0.39

(\*) Compound prepared in our group;<sup>139</sup> LE. Ligand Efficiency

The only derivative able to retain a good level of antimalarial activity was the carbaldehyde oxime **15** (IC<sub>50</sub> = 0.029 μM), indicating that a hydrogen bonding interaction

at this position 2 of the pyridone could play an important role in ligand–enzyme affinity. However, it was also translated in an increase in the toxicity in human cell lines (HepG2 = 15  $\mu$ M) in comparison with its predecessor GW844520 (HepG2 = > 61  $\mu$ M). The ligand efficiency for compounds **7a**, **7b** and **15** showed good values (LE = 0.31, 0.32 and 0.34, respectively) being the oxime **15** the most effective derivative at binding despite its high lipophilicity (Chrom log  $D_{pH7.4}$  = 5.03).

We conclude that regarding the PhysChem properties, compound **7a** displayed the most balance profile in comparison with **7b** and **15**, nevertheless **7a** was not enough potent for further progression. On the other hand, compound **15** was the most promising derivative regarding potency and LE, however low improvement of physicochemical profile and a higher cytotoxicity in HepG2 precluded the progression of this compound.

### 3.1.5 Molecular modelling

Recent studies have been published describing the cocrystallization of the cytochrome  $bc_1$  complex with the 4(1H)-pyridones GW844520 and GSK932121.<sup>149</sup> These studies reveal that 4(1H)-pyridones compounds do not bind the  $Q_o$  site but bind at the  $Q_i$  site. This discovery can explain the ability of this class of compounds to overcome parasite  $Q_o$ -based atovaquone resistance. The overall structure of  $bc_1$  is highly conserved between species and Complex III from numerous organisms has been crystallized with several ligands bound to the oxidation and reduction sites, providing further insight into the complex function. However, the  $Q_i$  site of cytochrome  $bc_1$  has been less explored in the search for antimalarial compounds and only the binding of a few compounds has been visualized directly.<sup>150–152</sup>

In this thesis, a theoretical model of the Cyt  $bc_1$   $Q_i$  active site was built using the public available X-ray structure of the Cyt  $bc_1$  from bovine heart bound to GSK932121 (4D6U).<sup>153</sup> The program MOE (2014) was used for homology protein modeling and molecular calculations. The experimental protein-ligand interactions between the  $Q_i$  site and GSK932121 are summarized in 3D and 2D illustrations where electrostatic and other physical properties are mapped in the binding pocket in order to explore the protein binding site (Figure 3.2).



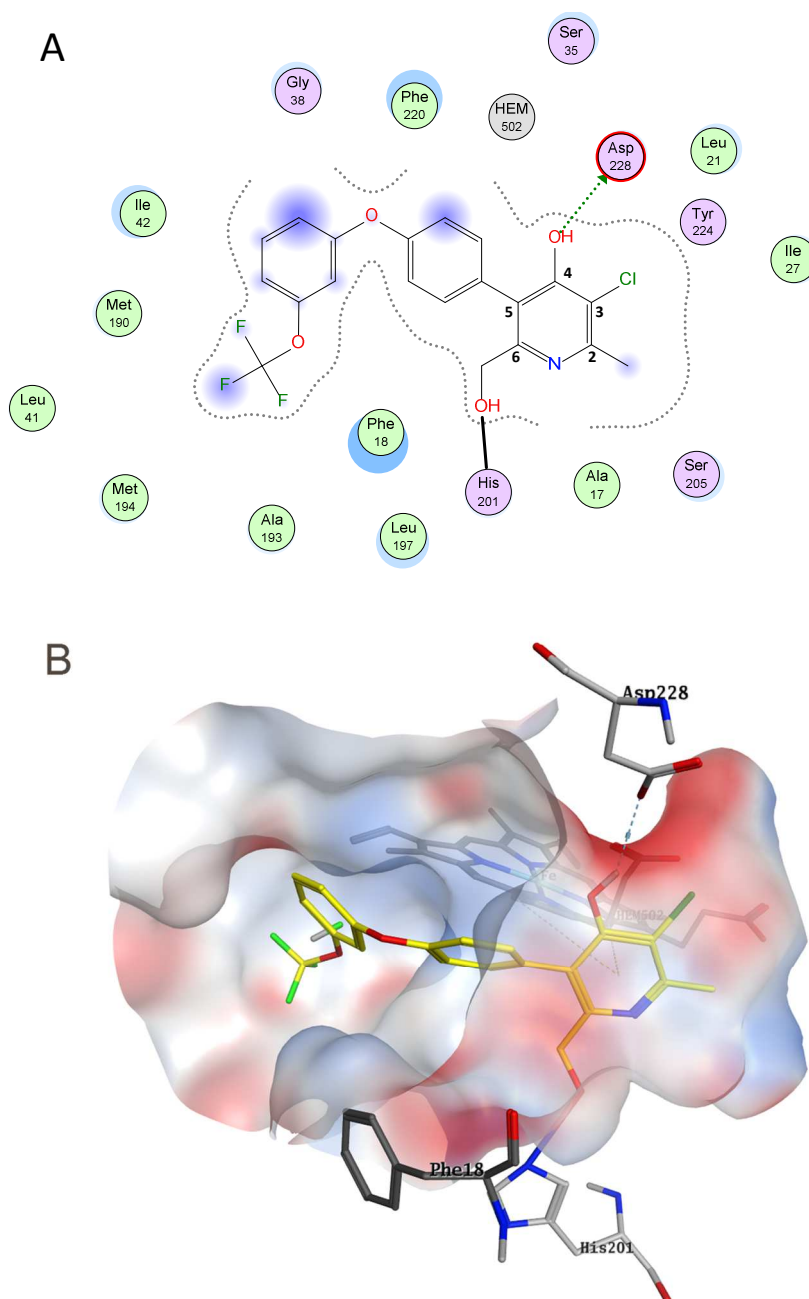


**Figure 3.2** (A) 2D pharmacophore binding interactions between the  $Q_i$  site and GSK932121; (B) 3D-experimental model of the Cyt  $bc_1$   $Q_i$  binding site occupied by GSK932121 using the crystal structures of the bovine Cytochrome b as templates. PDB access code:4D6U. The grey, red, and blue surface represent regions that can be occupied by ligand hydrophobic atoms, H-bond acceptors and H-bond donors respectively.

This model shows the hydrophobic nature of aminoacids surrounding the position 2 (grey surface) and the hydrogen bond interaction with His201 that allows the OH substitution at position 6. The carbonyl group interaction with Asp228 which is an important interaction common among many  $Q_i$  binding ligands is also observed. The tail

region appears more flexible and Phe18 and Phe220 can be seen forming stacking interactions with both phenyl rings of the tail.

When the most potent derivative obtained at position 2, compound **15** ( $IC_{50} = 0.029 \mu M$ ), was minimized in the  $Q_i$  active site, a hydrogen bond interaction was observed between the oxime and Ser205, which could justify the potency of this derivative (Figure 3.3 (A)). Comparison of the **15**'s docking pose with the GSK932121 X-ray crystal structure is represented in Figure 3.3 (B).

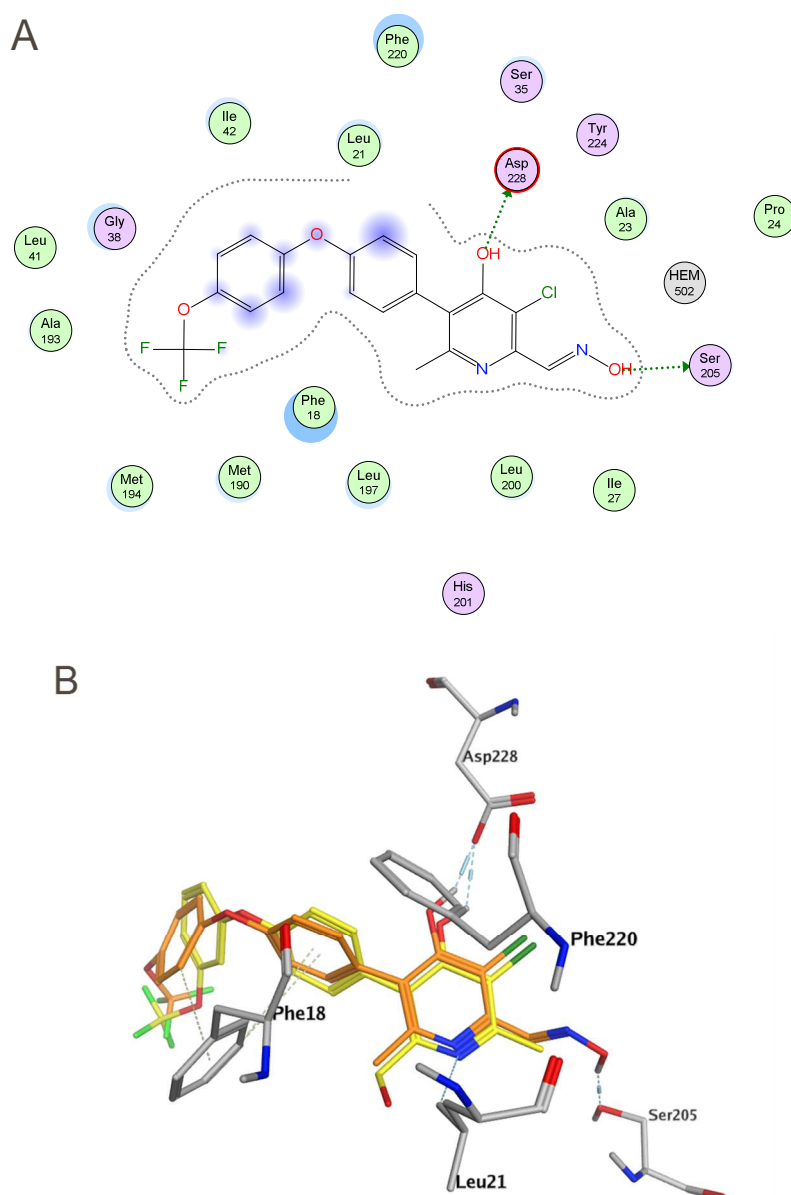


**Figure 3.3** (A) 2D pharmacophore binding interactions between the  $Q_i$  site and **15**. (B) 3D-theoretical comparison between the minimized binding pose of *N*-oxide derivative (**15**) (in orange) and GSK932121 (in yellow).

Concerning tertiary amines which showed not activity in the assay, steric constraints around position 2 might explain why compounds with larger substituents were not active. A 3D-theoretical model was built for the tertiary amine **13e** (Figure 3.4 (A)), thus confirming that to accommodate the substitution at position 2, a critical displacement of the 4(1H)-pyridone core in the active site occurs, leading to a totally inactive molecule. The same steric effect was observed in derivative **7b** (Figure 3.4 (B)), where a slight displacement in the active site was translated in a reduction in the antimalarial potency.

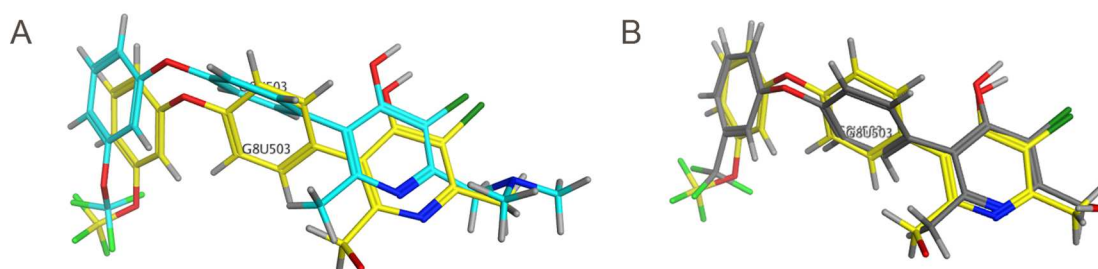


**Figure 3.4** 3D-theoretical comparison between GSK932121 (in yellow) and the putative binding pose of (A) tertiary amine **13e** (in blue) and hydroxylated **7b** (in grey).

Although bovine and human cytochrome *b* show ~80% conservation, the conservation between human and *P. falciparum* is only 40%. Surprisingly, the Q<sub>o</sub> site is the most conserved region, with 65% conservation. The N-terminal of the parasite cytochrome *b*, which constitutes half of the Q<sub>i</sub> site, is four residues shorter and has 39% conservation in comparison with mammalian homologues, leading to considerable differences in the Q<sub>i</sub> binding site, which may offer a way to rationally optimize lead compounds to give more selective inhibitors of the parasite enzyme. Ser205 has been shown to be involved in the binding of ubiquinone<sup>154</sup> and it is conserved between all of the sequences aligned as well as His201 and Asp228 (Figure 3.5), suggesting that these interactions between the ligand and the Q<sub>i</sub> binding site may be maintained across species, which might be translated in low selectivity margins.

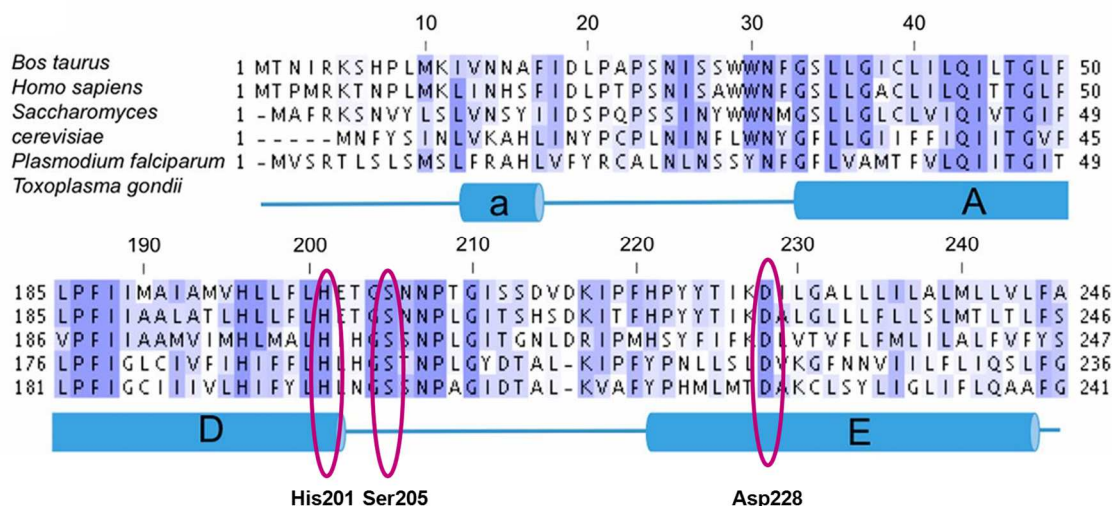


**Figure 3.5** Protein sequence alignment between bovine, human, *S. cerevisiae*, *P. falciparum*, and *T. gondii* showing conservation in the Q<sub>i</sub> binding site. Residues fully conserved between human and malaria are coloured in deep blue, partially conserved in light blue, and unconserved in white. Scale at the *Top* is numbered according to bovine sequence.<sup>149</sup>

### 3.1.6 Conclusions

The introduction of polar moieties (-CH<sub>2</sub>OH or =N-OH) at position 2 of the pyridone led to compounds with a slightly improvement in the physicochemical properties, but not good enough for any of them. On the other hand, ionizable tertiary amines did not provide any amelioration from the PhysChem point of view, leading to totally inactive compounds. Also, we have confirmed that compounds bearing the hydroxymethyl group at position 2 of the 4-pyridone ring are significantly less potent than the corresponding isomers at position 6.<sup>139</sup>

In general, data reported suggested that Physchem properties can be improved by performing certain chemical transformations at the 4-pyridone ring and it can be translated in an improvement in the pharmacokinetic profile of the 5-(4-phenoxyphenyl)-4(1H)-pyridones. However, those compounds modified at position 2 of the pyridone scaffold led to the significant or complete loss of the antimalarial activity. This result along with the poor physicochemical profile displayed by these analogues, discarded derivatives at position 2 of the pyridone as a possible candidate for a back-up strategy in order to obtain potent and more soluble antimalarial 4(1H)-pyridones.

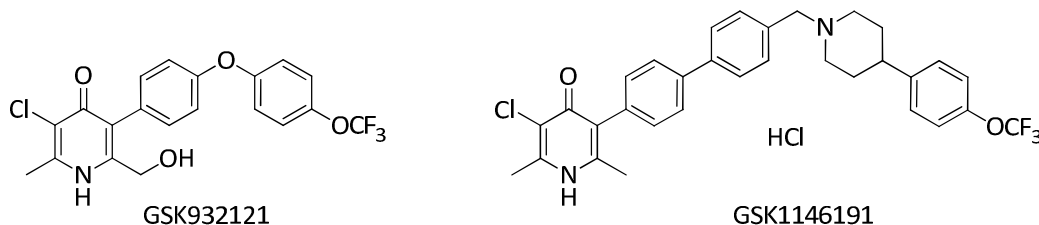
## 3.2 THE PRODRUG APPROACH

### 3.2.1 Previous work

The low solubility and low oral bioavailability in preclinical species were identified as the main issues for the development of 4(1*H*)-pyridones. On one hand, the introduction of polar moieties at position 6 led to the promising compound GSK932121, which showed better solubility and improved pharmacokinetic profile,<sup>142,138</sup> however it still demonstrated nonlinear pharmacokinetics in preclinical species with decreased oral bioavailability at high doses, required to evaluate the safety profile of the compound previous to its administration in humans.

In parallel, a new compound GSK1146191 was identified in our group as the most potent antimalarial 4(1*H*)-pyridone (*Pf* IC<sub>50</sub> = 0.0005 µg/mL This basic 4(1*H*)-pyridone displayed an outstanding *in vivo* efficacy when it was tested in the *P. falcip* mouse model (ED<sub>90</sub> = 0.6 mg/kg) (Table 3.3).

**Table 3.3** GSK932121 and GSK1146191 profiling



Compound	<i>In vitro</i>		<i>In vivo</i>							
	Whole cell IC <sub>50</sub> (µg/mL)		Therapeutic Efficacy in <i>P. falcip</i> (mg/kg)		PK in mouse					
	<i>P. falcip</i> 3D7A	Human HepG2	ED <sub>50</sub>	ED <sub>90</sub>	p.o (10 mg/kg)			i.v. (10 mg/kg)		
					C <sub>max</sub> (µg/mL)	DNAUC (µg·h/mL per mg/kg)	F <sup>a</sup> %	CL (mL/min/kg)	T <sub>1/2</sub> (h:s)	V <sub>d</sub> (L/kg)
GSK932121	0.006	10	0.5	0.6	3.1	5.2	94.3	3	3.8	1
GSK1146191	0.0005	>5	0.2	0.6	0.3	1.1	11	3.1	28.5	7.8

<sup>a</sup> suspension in 1% methylcellulose

The lower C<sub>max</sub> observed for GSK1146191 (0.3 vs. 3.1 µg/mL for GSK932121) as well as the higher V<sub>d</sub> (7.8 L/kg vs. 1 L/kg) could explain that the *in vivo* efficacy observed for both compounds was very similar. Again, the low absorption of the compound GSK1146191 could be related to the low solubility (PBS: ≤ 0.1 µg/mL; FASSIF sol: 5.4 µg/mL) and in the case of GSK1146191, the low permeability (Passive Papp: <20 nm/sec)

GSK932121 and GSK1146191 were the result of a Medicinal Chemistry program focused on the improvement of the 4(1*H*)-pyridones by introduction of polar hydroxyl groups (GSK932121)<sup>142</sup> and ionizable tertiary amines (GSK1146191).<sup>155</sup> Both compounds, were potent 4(1*H*)-pyridones with excellent *in vitro* and *in vivo* efficacies however, pharmacokinetic studies showed that despite the good clearance values, low oral exposures were obtained (DNAUC = 5.2 and 1.1 µg·h/mL per mg/kg, respectively).

The use of solubilizing excipients<sup>156</sup> and special formulations, such as nanomilled particles,<sup>157</sup> enhanced the solubility of the 4(1*H*)-pyridones in the media and therefore improved the bioavailability values, however this approach may significantly increase the cost of goods of the final drug, moving away of the main goal of seeking a Malaria treatment affordable to the populations hardest hit by the disease. For these reasons, a back-up program was directed towards finding water-soluble prodrugs of the most promising 4(1*H*)-pyridones.<sup>158</sup>

### 3.2.2 The Prodrug Theory

The term prodrug was first used by A. Albert et al.<sup>159</sup> in the late 1950's and was defined as pharmacologically inactive derivatives of drug molecules or drug candidates, that undergo enzymatic or chemical transformation to release the active drug molecule upon administration (Figure 3.6). Prodrugs are used as an approach to overcome pharmaceutical, pharmacokinetic or pharmacodynamic barriers that prevent the effective administration of drug candidates.<sup>160</sup> These barriers may include: low aqueous solubility; chemical instability, poor dissolution rates;<sup>161</sup> insufficient oral absorption due to poor permeability across the intestinal cell wall, low lipophilicity, high presystemic metabolism and high toxicity.

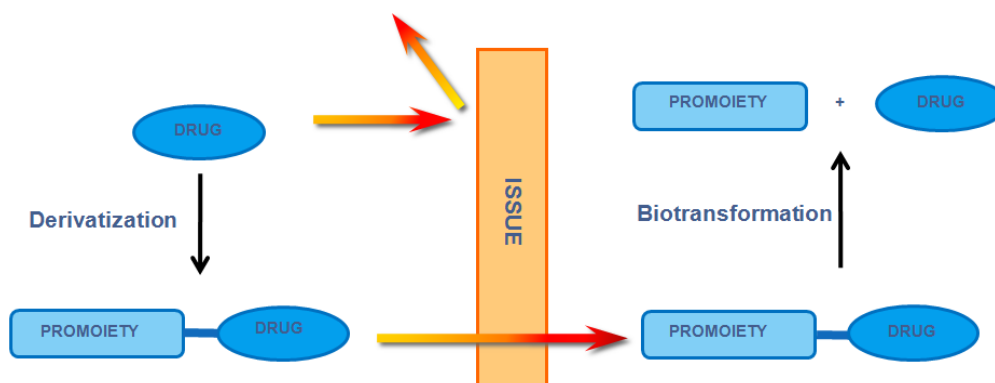


**Figure 3.6** Illustration of the prodrug concept

The oral bioavailability of a drug is usually limited by its aqueous solubility or low permeability but before embarking on a prodrug strategy, it is necessary to understand the physicochemical and biological factors that are limiting the oral bioavailability of a compound. The Biopharmaceutical Classification System (BCS)<sup>162</sup> classifies drugs based on solubility and permeability measures (Figure 3.7). The x-axis shows the volume (mL) required to dissolve the highest dose strength of the parent drug at the lowest solubility over the pH 1–7.5 and permeability is represented in the y-axis.

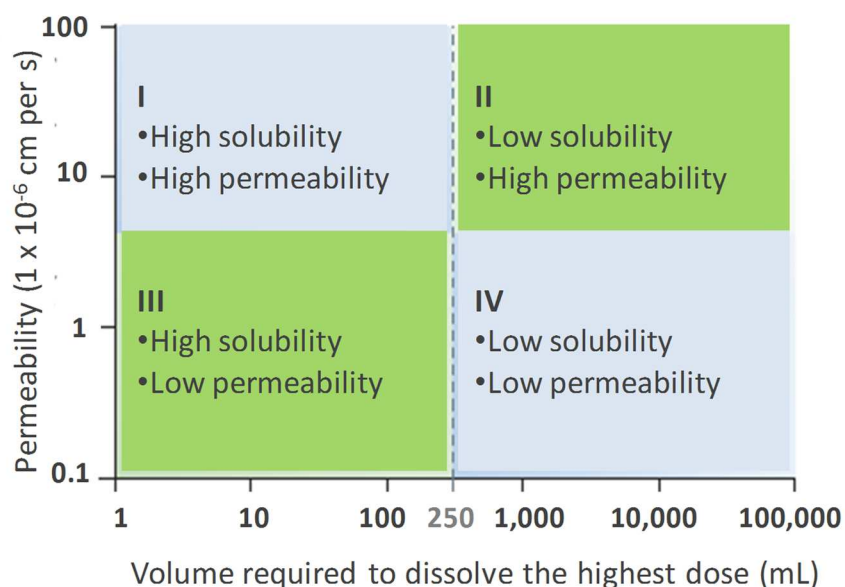


**Figure 3.7** Biopharmaceutical Classification System (BCS) characterization of drugs based on solubility and permeability measures<sup>163</sup>

BCS Class I compounds are soluble and well absorbed after oral administration. In contrast, totally opposite properties are represented by BCS Class IV compounds which have both low solubility and low permeability. Parent drugs belonging to the BCS Classes II and III (shown in green) are those with a higher probability of success in a prodrug strategy to enhance solubility (in BCS Class II compounds) or permeability (in the case of the BCS Class III compounds).

### 3.2.3 Prodrug Classification

Two different prodrugs classification are described in the literature:<sup>160</sup>

1) *BASED ON THE CHEMICAL ATTACHED*. A conventional classification based on derivatization and the type of carriers attached to the drug. This method is subdivided in two sub-major classes:

a. Carrier-linked prodrugs: where the active drug is linked to a carrier or promoiety, which can be cleaved by hydrolytic or oxidation/reduction enzymes (such as an ester, labile amide, imines etc.) or nonenzymatically (chemically) to provide the parent drug. Ideally, the group removed is pharmacologically inactive and nontoxic. Carrier-linked prodrugs can be subdivided into:

- *bipartite*: where the active drug is attached directly to one carrier (promoiety);
- *tripartite*: where a spacer is utilized to connect the active drug and a promoiety. Generally, a tripartite prodrug approach is used when the bipartite prodrug is unstable due to the inherent nature of the drug-promoiety linkage;
- *mutual prodrugs*, which consist of two active drugs that are linked together

b. Bioprecursors which are chemical entities that do not contain a promoiety yet are activated by oxidation, reduction or hydrolysis into new compounds that may be active or be further activated into active metabolites. In this prodrug approach, there is no linker attached to the drug; however, the prodrug should be readily metabolized to provide the active drug.



2) *BASED ON THE CELLULAR SITE BY WHICH THE INTERCONVERSION TAKES PLACE*. In addition, prodrugs can be classified based on the cellular site of interconversion into the active drug. This classification strategy include two types:<sup>164</sup>

- a. type I conversion to their active drugs occurs intracellularly (e.g., antiviral nucleoside analogues, lipid-lowering statins)
- b. type II conversion occurs extracellularly, especially in digestive fluids or in the systemic circulation (e.g., etoposide phosphate, valganciclovir, fosamprenavir)

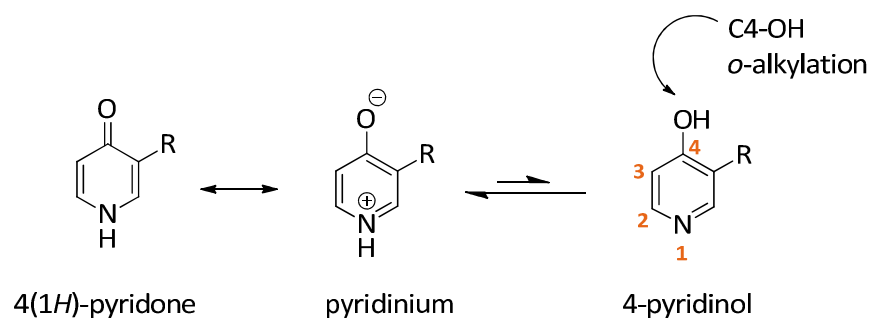
Both types can be further categorized into Subtypes: Type IA, IB and Type IIA, IIB, and IIC based on whether or not the intracellular converting location is also the site of therapeutic action, or the conversion occurs in the gastrointestinal (GI) fluids or systemic circulation.

Type IA prodrugs refer to those that are converted at the cellular targets of therapeutic actions, whereas Type IB prodrugs' conversion occurs in the primary metabolic tissues such as liver, gut, or lung. For Type II prodrugs, the conversion process could either take place extracellularly in the milieu of gastrointestinal fluids (Type IIA), in the systemic circulation and/or other systemic extracellular fluid compartments (Type IIB), or near therapeutical target cells (Type IIC). However, a prodrug may belong to multiple categories and be recognized as a Mixed-Type prodrug.

### **3.2.4 Prodrug rational for GSK932121 and GSK1146191**

Several key factors should be carefully examined when designing a prodrug, one of them concerns the parent drug: which functional groups are amenable to chemical prodrug derivatization? GSK932121 and GSK1146191 have in common the 4(1*H*)-pyridone core. Structural studies of 4(1*H*)-pyridones using X-ray crystallography, IR and liquid NMR suggest that the keto tauto-isomer is favored in both solid and liquid states.<sup>165–167</sup> 4(1*H*)-Pyridones are aromatic as long as the lone pair of the nitrogen electrons can be delocalized into the ring and the degree of the aromaticity depends on the contribution of the pyridinium form to the overall structure.

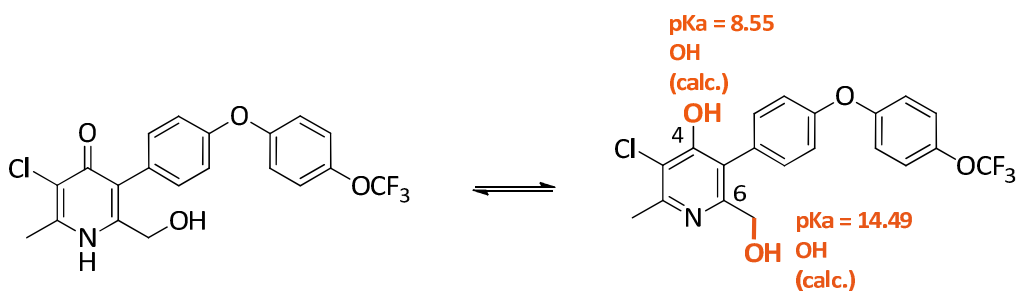
Despite the predominance of the keto-form in the 4(1*H*)-pyridones, the enol character suggests the existence of a tautomeric equilibrium (Scheme 3.4).



**Scheme 3.4** Tautomer forms of 4(1*H*)-pyridones

Different strategies aimed at increasing the solubility in water (e.g. salt formation) proved to be unsuccessful in 4(1*H*)-pyridones because of the weak acidic and basic character of the pyridone nucleus. 4(1*H*)-Pyridones act like classical aromatic compounds with electrophilic aromatic substitutions (halogenation, nitration, etc.) occurring selectively at position 3. Whereas position 4 presented at the 4-pyridinol tautomeric form undergoes nucleophilic substitutions, providing a suitable position where a promoiety can be attached to the 4(1*H*)-pyridone via *O*-alkylation.

In the case of GSK932121, the presence of a new primary hydroxyl group offered new opportunities for the preparation of suitable prodrugs. In this case, there were two acidic positions able to undergo nucleophilic substitutions, two different hydroxyl moieties which showed different calculated  $pK_a$  values:  $pK_a = 8.55$  for the C4-OH and  $pK_a = 14.49$  for the C6-CH<sub>2</sub>OH (Scheme 3.5), as expected due to their aromatic and aliphatic character, respectively.



**Scheme 3.5** GSK932121 phosphate prodrug approach

Another important factor that should be examined is, how the prodrug will be used? what problem must be overcome? At this point, the absorption, distribution, metabolism, excretion (ADME) and pharmacokinetic properties of both, parent and prodrug, need to be comprehensively understood.

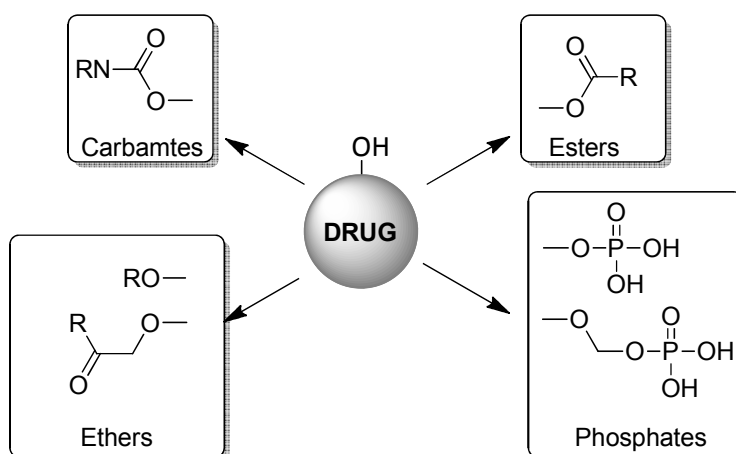
GSK932121 belong to the classical BCS Class II compounds: low aqueous solubility and high permeability.<sup>162</sup> This class of drugs have a high probability of success in a prodrugging strategy to improve solubility. On the other hand, GSK1146191 belong to the classical BCS Class IV compounds: low aqueous solubility and low permeability.<sup>162</sup> Although drugs belonging to this class are problematic and are rarely described, some BCS Classes IV drugs exist in the pharmaceutical market.<sup>168</sup>

GSK932121 and GSK1146191, were identified as extremely potent oral antimalarial drugs but both presented pharmacokinetic issues due to their low solubility. The common absorption routes in oral drugs require the total dissolution of the drug in the contents of the gut. A prodrug approach to link GSK932121 and GSK1146191 to ionizable or polar functional groups offered an excellent alternative way to improve drug solubility and hence its bioavailability. In the case of GSK1146191, low permeability added an extra handicap. An ideal prodrug for GSK1146191 should be able to mask hydrogen bonding groups in the molecule to improve permeability as well as solubility.

### ***3.2.5 Prodrugs for hydroxyl functionalities***

The choice of the promoiety should be considered with respect to the chemical versatility of the parent drug and in the case of GSK932121 and GSK1146191, this promoiety could be attached to the -OH functionality present in the minor tautomer, 4-hydroxypyridine of the 4(1*H*)-pyridone core. Ideally, the final prodrug must be inactive, nontoxic and once in solution, it should avoid extensive chemical and enzymic degradation.

The -OH functionality, has the potential to undergo a variety of chemical modifications for the preparation of a prodrug, such as esters, carbamates, ethers and phosphates (Scheme 3.6).



**Scheme 3.6** Prodrugs for hydroxyl functionalities

Each option must be considered with respect to the problem to be overcome (in this case, low oral bioavailability) and where and how we want the drug to be released.

### PHOSPHATE ESTER AS PRODRUG

This approach increases solubility by often several orders of magnitude, by virtue of the dianionic phosphate group.<sup>169</sup> They undergo rapid *in vivo* bioconversion at the intestinal brush border by action of membrane-bound alkaline phosphatases<sup>170</sup>, releasing the parent drug in the vicinity of the mucosal membrane ( Figure 3.8).

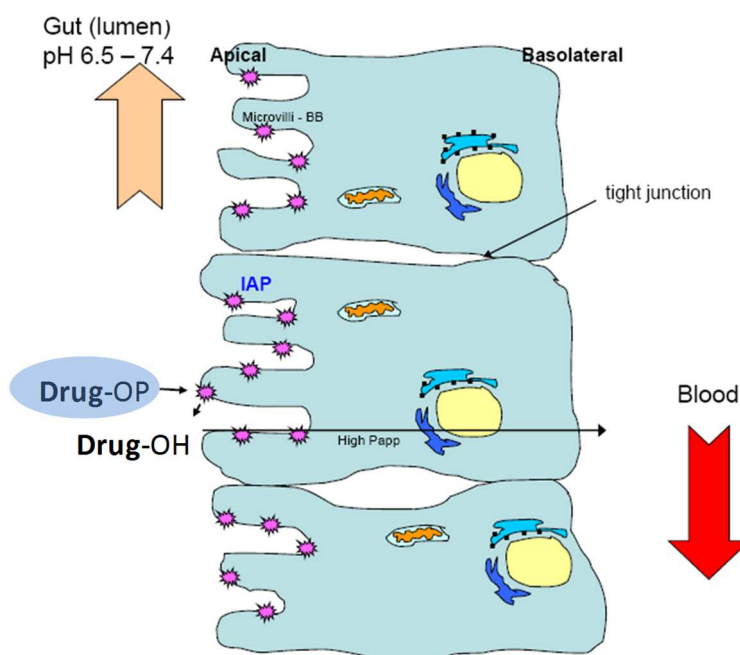
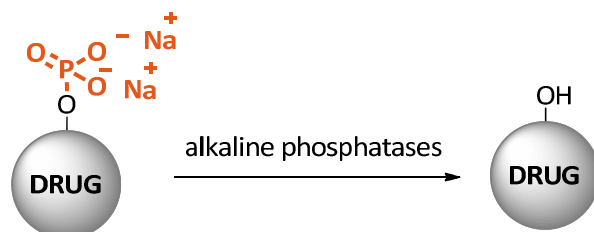


**Figure 3.8** Bioconversion of a prodrug (**Drug-OP**) to the generic drug (**Drug-OH**) by intestinal alkaline phosphatases (**IAP**)

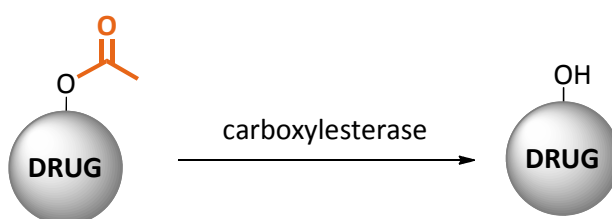
Alkaline phosphatase (AP) is a non-specific phosphomonoesterase that produces free inorganic phosphate or transfers the phosphoryl group to other alcohols<sup>171</sup> and its intestinal form (IAP) is highly conserved across mammals<sup>172</sup> (Scheme 3.7).



**Scheme 3.7** Bioconversion of a generic prodrugs by alkaline phosphatases.

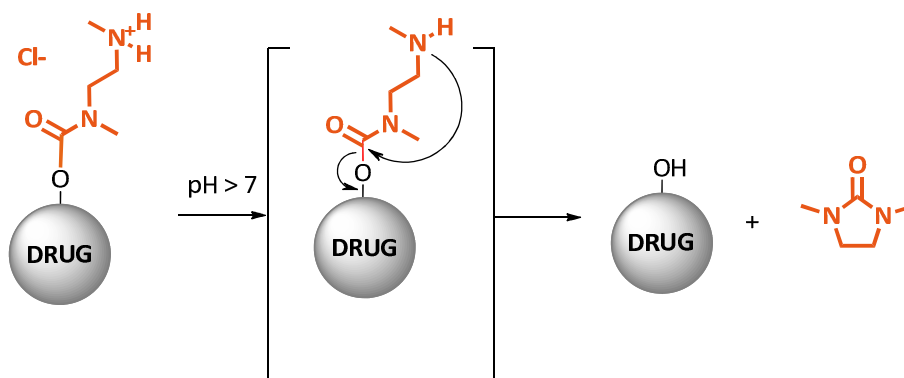
### *ESTERS AND CARBAMATES AS PRODRUGS*

The introduction of both esters<sup>170</sup> and basic carbamates<sup>173</sup> can be considered in order to improve the permeability and solubility by modifying the hydrocarbon moiety. The rationale behind the ester prodrug strategy is to mask hydrogen bonding group in the active compound.<sup>174</sup> The synthesis is often straightforward and once in the body ester-prodrugs are readily bioconverted into their active species by ubiquitous esterases (Scheme 3.8).<sup>175</sup>



**Scheme 3.8** Bioconversion of a generic prodrug by enzyme-regulated drug delivery

Carbamates differ from esters by the presence of an oxygen or nitrogen on both sides of the carbonyl carbon and they are often enzymatically more stable than the corresponding esters. For the prodrug approach-study we considered the synthesis of a carbamate able to regenerate the parent drug through a non-enzymatic pathway. Basic carbamates like methyl(2-(methylamino)ethyl)carbamates are used as prodrugs who release the parent compound by intramolecular cyclization reaction, resulting in imidazolidin-2-ones. In this way, generation of the active drug is not dependent upon the enzymatic host's environment but rather solely upon the rate of the cyclization reaction.



**Scheme 3.9** Bioconversion of a generic prodrugs by pH regulated cyclization.

This basic amino carrier was found to be stable toward murine plasma esterases and also at low pH but it was reactive in neutral and alkaline medium. Basic media leaves the basic amine free to attack the carbamate moiety promoting the final cyclization-elimination reaction (Scheme 3.9).<sup>176</sup>

The medicinal chemistry described herein was focused on the synthesis and biological evaluation of new water-soluble prodrugs. This strategy was based on the rationales described above. In this study, compounds GSK932121 and GSK1146191, were used as tool compounds to validate the prodrug strategy as a feasible approach to improve the oral bioavailability of the 4(1*H*)-pyridones (Figure 3.9).

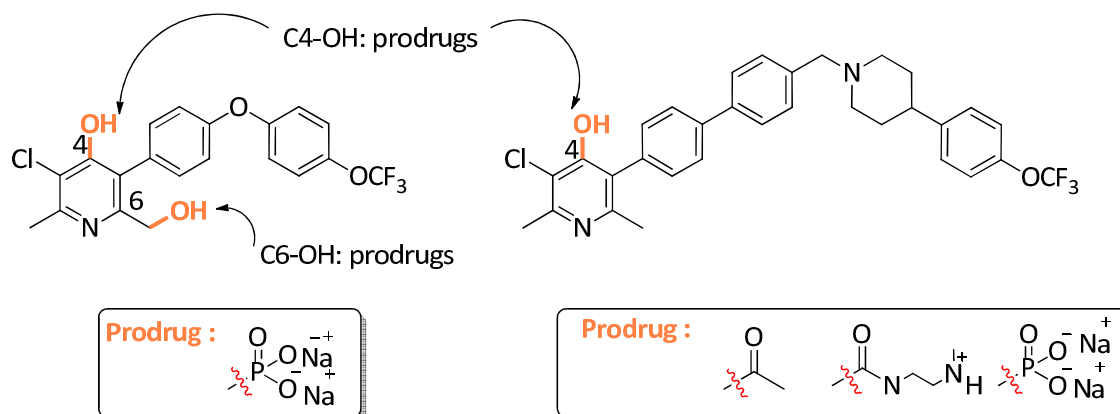
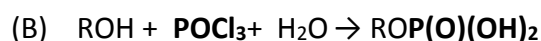


**Figure 3.9** Prodrug strategy for GSK932121 and GSK1146191

### 3.2.6 Synthesis of GSK932121 Prodrugs

#### PHOSPHATE PRODRUG

Phosphate monoesters are commonly prepared by two different methods. Method (A), involves hydrolysis of triesters. Phosphoric acid chloride reacts with the hydroxy moiety to give the corresponding triester. Subsequent hydrolysis leads to the desired phosphate monoester. The second approach, Method (B), consists of the reaction of phosphorus oxychloride with the alcohol to provide the monoester after hydrolysis (Scheme 3.10):<sup>177</sup>.



**Scheme 3.10** Phosphate monoesters: synthetic approaches

Different approaches for the synthesis of the monophosphate of GSK932121 were studied and the results are summarized in Table 3.4. Reaction progress from GSK932121 to the corresponding phosphate ester was determined by LCMS. In this study, three reaction's products were detected: the two different monophosphate derivatives (one at the pyridone ring (**16**) and another at primary hydroxyl group (**17**) and the diphosphate derivative (**18**) (Figure 3.10). Ratios for the different products (**16**, **17** and **18**) and yields for the corresponding isolated compound are also included in Table 3.4.

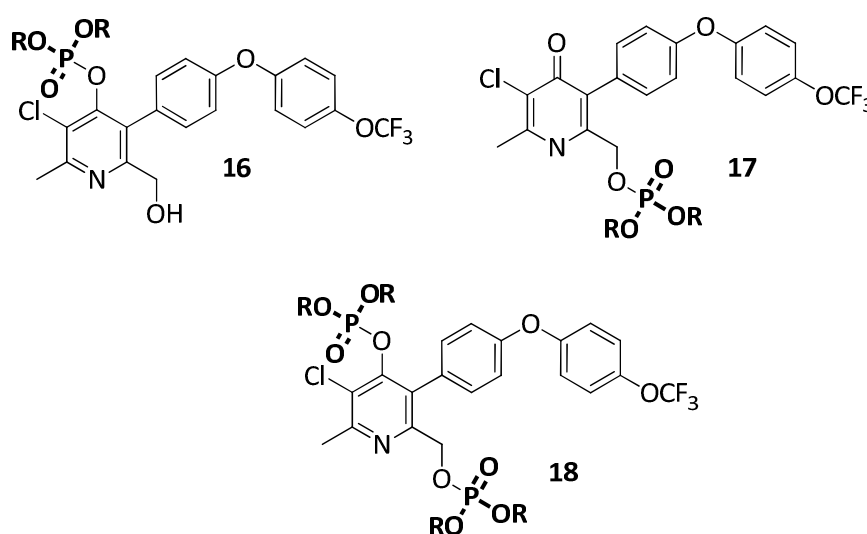
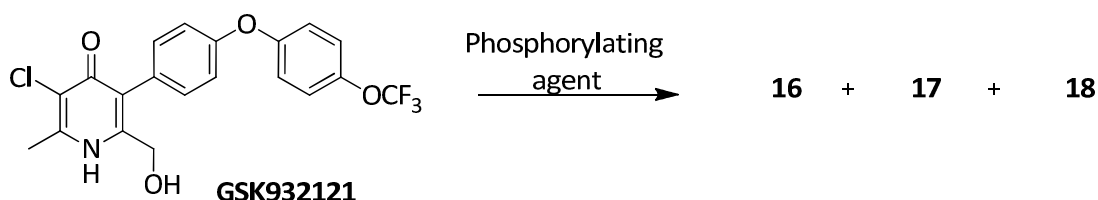


**Figure 3.10** Monophosphate (**16** and **17**) and diphosphate (**18**) esters

Direct phosphorylation using POCl<sub>3</sub> (Method (B)) was soon discarded due to the undesired chlorination at position 6 and chemistry was focus on preparing the phosphate monoesters following the strategy described in Method (A) (Scheme 3.10).

A standard method for acylation reactions involves pyridine-catalyzed acylation. In order to find a selective phosphorylation methodology, the reaction was performed in the presence of 4-dimethylaminopyridine (DMAP). Et<sub>3</sub>N was used as a proton scavenger and THF as solvent. Under these conditions different phosphorylating agents were investigated ((EtO)<sub>2</sub>P(O)Cl), Entry 1-2; (BnO)<sub>2</sub>P(O)Cl, Entry 3; (MeO)<sub>2</sub>P(O)Cl; Entry 2-5; Table 3.4) Mainly monophosphate ester **16** was obtained in all the cases. (MeO)<sub>2</sub>P(O)Cl proved to be the most selective agent, when the number of equivalents of phosphorylating agent was increased (from 1.5 eq. to 2.5 eq.), giving compound **16** in good yield (61%), (Entry 6, Table 3.4). However, the phosphate at position 4 proved to be chemically unstable; hydrolysis to the corresponding starting material GSK932121 was always observed when the product was analyzed by HNMR. Another base-catalyst, *N*-methylimidazole (NMIM),<sup>178</sup> was investigated but only starting material GSK932121 was recovered (Entry 7-8, Table 3.4).

**Table 3.4** Phosphorylation conditions for GSK932121

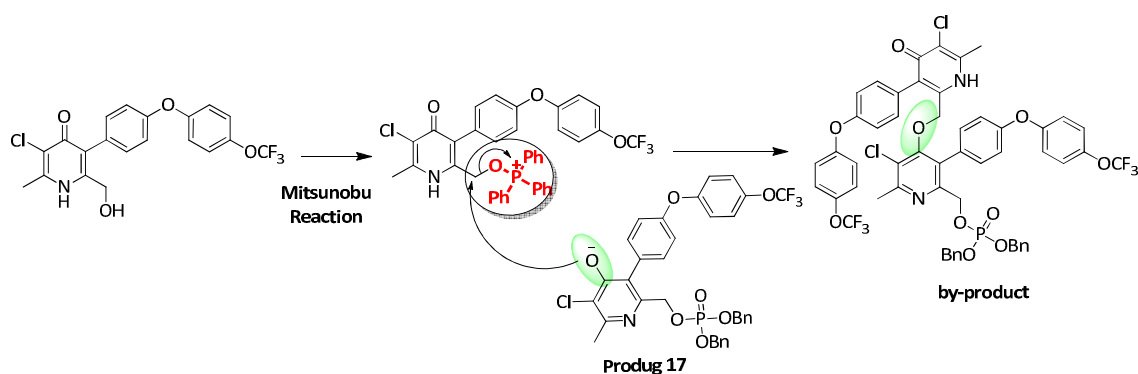


Entry	Phosphorylating agents	Reaction conditions	Solvent	Product	
				Reaction Ratios	Yield
				<b>16: 17:18</b>	
1	(EtO) <sub>2</sub> P(O)Cl (1.1eq)	DMAP/Et <sub>3</sub> N	DCM	75:0:25	NIC
2	(EtO) <sub>2</sub> P(O)Cl (4eq)	DMAP/Et <sub>3</sub> N	DCM	20:0: <b>80</b>	6% of <b>18</b>
4	(BnO) <sub>2</sub> P(O)Cl (2.5eq)	DMAP/Et <sub>3</sub> N	DCM	95:0:5	NIC
5	(MeO) <sub>2</sub> P(O)Cl (1.5eq)	DMAP/Et <sub>3</sub> N	DCM	<b>100</b> :0:0	52% of <b>16</b>
6	(MeO) <sub>2</sub> P(O)Cl (2.5eq)	DMAP/Et <sub>3</sub> N	DCM	<b>100</b> :0:0	61% of <b>16</b>
7	(EtO) <sub>2</sub> P(O)Cl	NMIM/Et <sub>3</sub> N	DCM	SM	-
8	(MeO) <sub>2</sub> P(O)Cl	NMIM Et <sub>3</sub> N	DCM	SM	-
9	(BnO) <sub>2</sub> P(O)OH (3eq)	DEAD, PPh <sub>3</sub>	THF	0: <b>83</b> :00	65% of <b>17</b>
10	(BnO) <sub>2</sub> P(O)Cl (3eq)	NaH	THF	0: <b>60</b> :40	40:6% <b>17:18</b>
11	(BnO) <sub>2</sub> P(O)Cl (3eq)	NaH + NaOH	THF	0: <b>100</b> :0	70% of <b>17</b>

NIC: No Isolated Compound



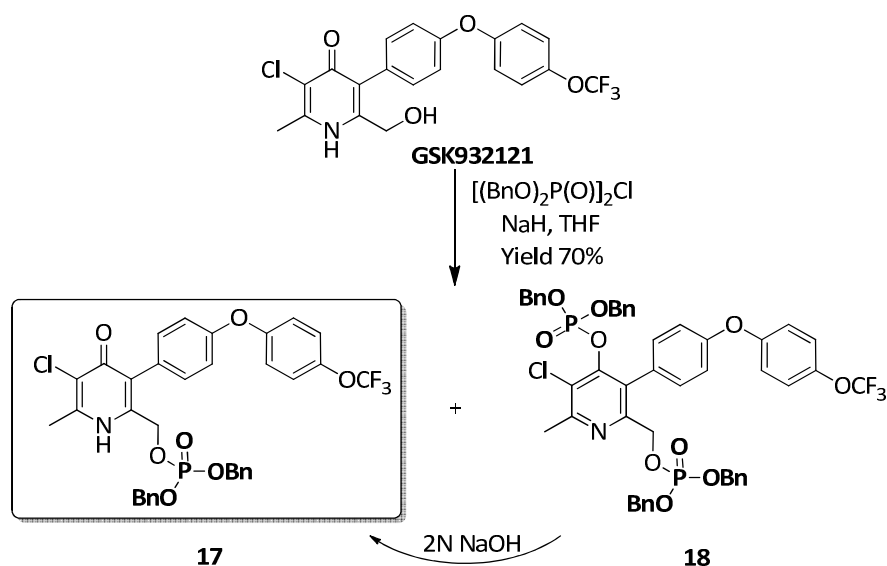
Due to the low stability observed for the phosphate ester at the position 4, a selective phosphorylation at the C6-CH<sub>2</sub>OH position to obtain only monophosphate ester **17** was explored. Mitsunobu conditions, which facilitate the conversion of primary and secondary alcohols to esters, were considered. Using dibenzyl phosphate as phosphorylating agent, Mitsunobu reaction was induced by triphenylphosphine and diethyl azodicarboxylate (DEAD) in THF. A side product was also obtained and column chromatography purification was required to give the desired monophosphate ester **17** in 65% yield (Entry 9, Table 3.4). This byproduct was the result of a second substitution reaction conducted by the alkoxide ion generated at position 4 of the pyridone (Scheme 3.11).



**Scheme 3.11** Mitsunobu reaction by-product

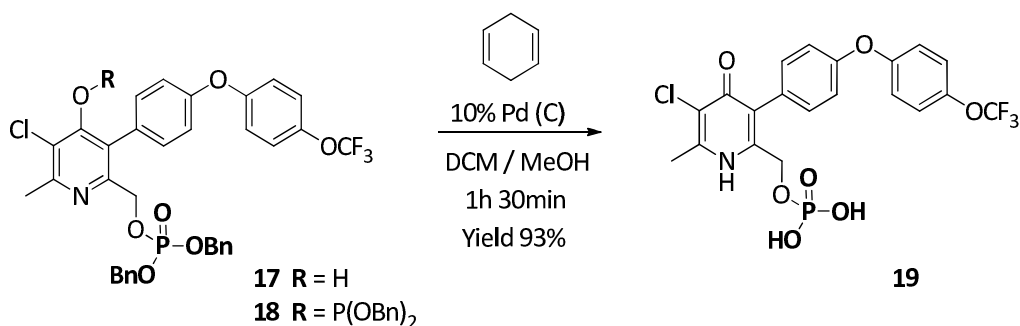
In our eagerness to obtain selectively the monophosphate ester **17** at position 6, we proposed a different approach. This strategy consisted of bis-phosphorylation using a strong base to obtain compound **18** and then hydrolysis of the phosphate ester at position 4. When NaH (3 eq) was used in THF, reaction of GSK932121 and (BnO)<sub>2</sub>P(O)Cl led to a mixture 60 : 40 (**17** : **18**) after 24h (Entry 10, Table 3.4). Then 2N NaOH (aq.) solution was added and the reaction stirred for 24h at room temperature. Only desired monophosphate **17** was detected and it was successfully purified by trituration in *tert*-butyl methyl ether in good yield (70%) (Entry 11, Table 3.4).

A reliable synthesis for the monophosphate ester **17** was finally identified and is summarized in scheme 3.12.



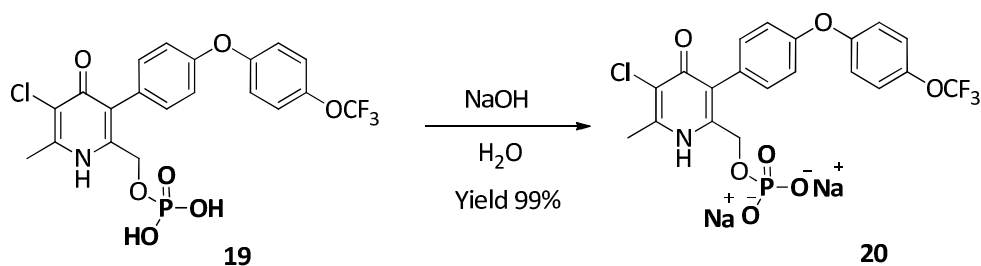
**Scheme 3.12** Final synthesis of the monophosphate **17**

Removal of the two benzyl esters was easily achieved through hydrogenation using 1,4-cyclohexadiene as hydrogen source and 10% Pd(C) as catalyst. Compound **19** was obtained and isolated by trituration in *tert*-butyl methyl ether in very good yield (93%). In order to study the stability of the phosphate ester at the two different positions, cleavage of diphosphate **18** was studied under the same chemical conditions: 1,4-cyclohexadiene, 10% Pd(C) and MeOH as solvent. As expected, due to the low stability showed by the phosphate at position 4 (**16**) only dihydrogen phosphate **19** was obtained (Scheme 3.13).



**Scheme 3.13** Hydrolysis of the diphosphate ester

The di-sodium salt was prepared by reaction of **19** with 2 equivalents of NaOH in water leading to the corresponding disodium salt **20** after lyophilization in 99% yield (Scheme 3.14).

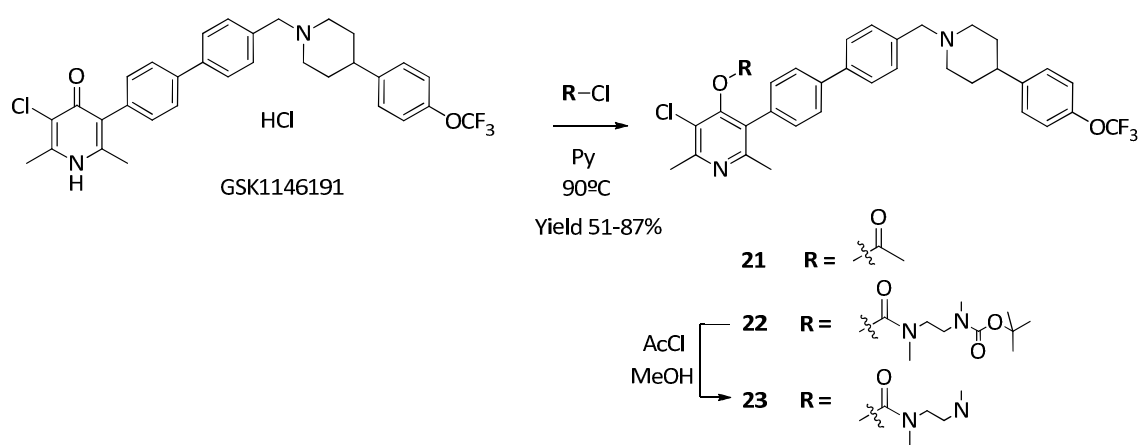


Scheme 3.14 Sodium salt formation

### 3.2.7 Synthesis of GSK1146191 Prodrugs

#### ESTERS AND CARBAMATES PRODRUGS

The synthesis of the different prodrugs of the parent compound GSK1146191 was achieved via acylation with the corresponding acid chlorides. The reaction was performed heating at 90 °C in anhydrous pyridine and, leading to the expected compounds **21** and **22** in good yields, 51% and 87% respectively. Final compound **23** was obtained by deprotection of **22** with acetyl chloride in MeOH at room temperature (yield 72%) (Scheme 3.15).



Scheme 3.15 Synthesis of esters and basic carbamates prodrugs

#### PHOSPHATE PRODRUG

In parallel to GSK932121's phosphate prodrug studies, we explored the synthesis of a suitable phosphate prodrug for GSK1146191. Using GSK1146191 as starting material and dibenzyl phosphorochloridate ((BnO)<sub>2</sub>P(O)Cl) as phosphorylating agent, different bases were investigated to obtain the phosphate ester prodrug. No reaction was observed when K<sub>2</sub>CO<sub>3</sub> and DIPEA (weak bases with pKa ~10) were used (Entries 1 and 2, Table 3.5)



hydrogenation, with 10% Pd(C) as catalyst and different solvent mixtures; the use of 1,4-cyclohexadiene as hydrogen source and also cleavage in acid media, but GSK1146191 was always recovered. Unfortunately, we were unable to hydrolyze the benzyl esters. All the attempts were unsuccessful and only the parent compound was recovered. This study, along with the results obtained for the synthesis of GSK932121's phosphate prodrug, confirmed the low chemical stability of a phosphate ester moiety directly attached to the 4(1*H*)-pyridone at position 4.

The structure of all the compounds synthesized in this section was elucidated by proton Nuclear Magnetic Resonance Spectroscopy (<sup>1</sup>H-NMR) and Liquid chromatography–mass spectrometry (LC/MS). Proton and carbon assignment for compound **19** used HMQC and HMBC spectra analysis (see Appendix I).

### 3.2.8 Biological activity and analysis results

#### PRODRUG OF GSK932121

As mentioned previously, the optimal profile of the pyridone prodrug is inactive and nontoxic compounds that improve the ADME profile (absorption in this case) with the aim of increasing systemic exposure levels of the parent drug. Solubility and chemical stability studies were performed on the GSK932121 phosphate prodrug **20** (Table 3.6)., As expected, its lipophilicity was reduced by the introduction of the phosphate moiety (ChromLogD<sub>pH7.4</sub> = 1.7), which translated into an outstanding solubility. Solubility was determined in different biorelevant media (PBS, phosphate buffered saline; FeSSIF; FaSSIF and SGF, simulated gastric fluids) and in all media, prodrug **20** was significantly more soluble than parent GSK932121. It proved not to be active as antimalarial and

**Table 3.6.** *In vitro* profile and solubility in different biorelevant media of prodrug **20**

Compound	Structure	IC <sub>50</sub> (μM)	ChromLogD	Solubility (mg/mL)			
				PBS pH 7.4	FESSIF pH 5	FASSIF pH 6.5	SGF pH 1.3
GSK932121		0.003	5.24	<0.0001	0.002	0.0007	0.3
<b>20</b>		N.A.	1.7	>1	>0.8	>1	>0.6

N.A.: Not active

Solubility profile of GSK932121 and its prodrug **20** at different pH is represented in Figure 3.11. Solubility curves exhibit the pH effect for both compounds and prodrug **20** showed to be  $>10^5$  fold more soluble than the parent GSK932121 at pH = 5 (the pH of the stomach should range between 1-5 but it varies throughout the day).<sup>179</sup>

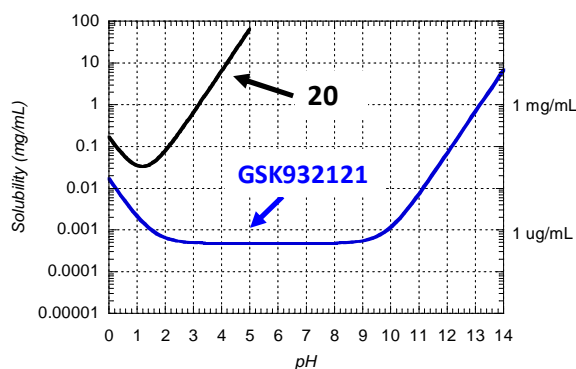


**Figure 3.11** Solubility of **20** and GSK932121 at different pH

Chemical stability was studied in 1% aqueous methyl cellulose (pH = 6.1) and water (pH = 6.4) during 15 days at room temperature (Figure 3.12). As shown in the chromatograms, HPLC-DAD analysis confirmed that the prodrug **20** was chemically stable in solution and no signs of hydrolysis were detected in any of the samples analysed up to 10 days after their preparation at room temperature.

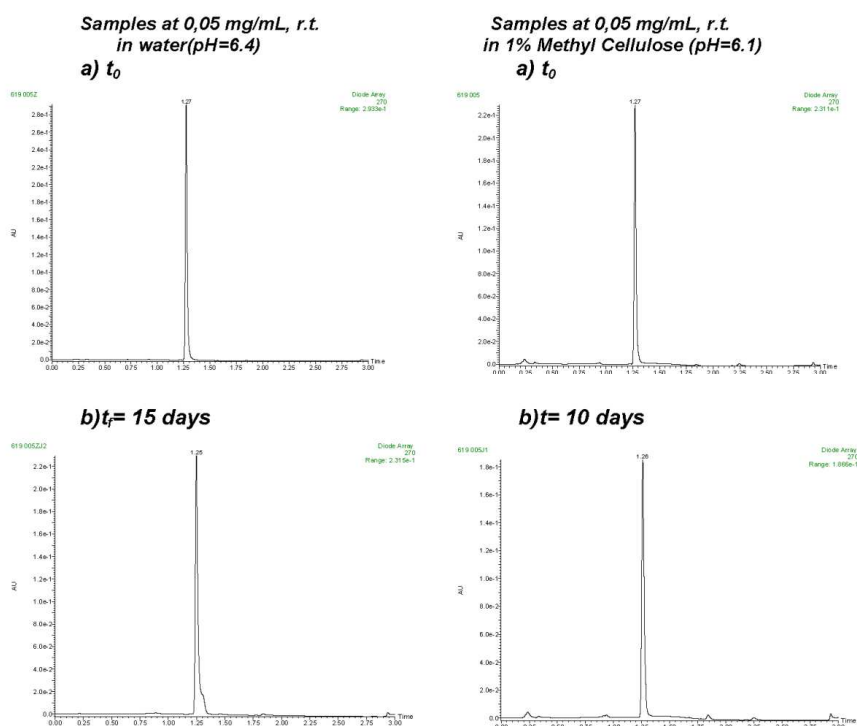


**Figure 3.12** Chemical stability of **20** in MC 1% by HPLC-DAD

The next step was to evaluate the prodrug behaviour in the intestinal gut: specifically, permeability and drug release. Drug permeability through the intestinal membrane is one of the most important factors in defining oral drug absorption, and the human intestinal epithelial cell (CaCo2) monolayers have been widely accepted as a useful *in vitro* model membrane to study drug absorption in the large intestine (Figure 3.13).<sup>180,181</sup>

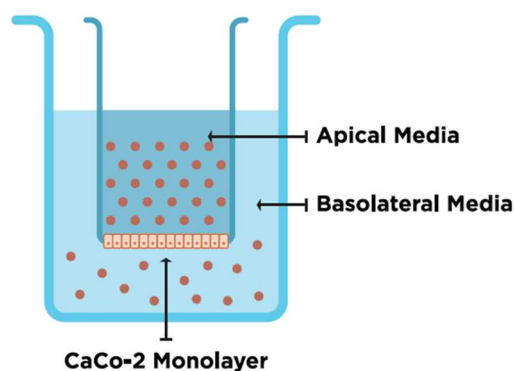


**Figure 3.13** Sketch for Caco2 monolayer assay

Using CaCo-2 monolayer model, coefficients for the passive permeability ( $P_{app}$ ) were calculated for prodrug **20** in both the apical to basolateral ( $A \rightarrow B$ ) and basolateral to apical ( $B \rightarrow A$ ) directions according to the following equation:

$$P_{app} = \frac{dQ}{dt} \times \frac{1}{A \cdot C_0}$$

where  $dQ/dt$  is the rate of appearance of drugs on the basolateral side ( $\mu\text{mole} \cdot \text{s}^{-1}$ ),  $C_0$  is the initial drug concentration on the apical side ( $\mu\text{M}$ ), and  $A$  is the surface area of the monolayer ( $\text{cm}^2$ ). The amount or concentration of compound on each side was measured by LC/MS. The high, moderate and low classification for CaCo2 permeability were determined from in house studies with marketed compounds for which % absorption in humans has been published. The relative value of  $P_{app}$  will give us an idea on the absorption of the drug through the human intestinal epithelia cells. Results of the permeability assay of prodrug **20** in Caco-2 cells were summarized in Table 3.7.

**Table 3.7** Permeability across Caco2 cell line

Compound	Papp (nm/s)	Permeability classification
<b>20</b>	0	LOW
<b>GSK932121</b>	105.3	HIGH

This permeability assay allowed the quantitation of both compounds, GSK932121 and its phosphate prodrug **20** in apical and basolateral compartments. In the apical-basolateral direction, GSK932121 is generated at the apical side (GSK932121 contribution: 98.9 %) from **20** due to the prodrug hydrolysis by alkaline phosphatases (AP) and crosses the monolayer effectively (Papp = 105.3 nm/s). Prodrug **20** doesn't cross the CaCo2 monolayer and showed a minimal permeability value (Papp = 0 nm/s) (Table 3.8). From basolateral-apical direction, prodrug **20** remains mainly unchanged due to the absence of AP at the basolateral side (prodrug **20** contribution: 86.4 %).

**Table 3.8** GSK932121A and **20** amounts in apical and basolateral compartments following application of **20** to CaCo-2 monolayers

Initial compound amount (nmol)	APICAL		BASOLATERAL		Mass Balance %
	<b>20</b>	GSK932121	<b>20</b>	GSK932121	
<b>A -&gt; B</b> 0.6 (2 uM)	0.02 (4.1)	0.44 (89.8)	0.00	0.03 (6.1)	82
<b>B -&gt; A</b> 1.4 (2 uM)	0.01 (0.8)	0.09 (7.2)	1.08 (86.4)	0.07 (5.6)	89

Donor compartment

Acceptor compartment

In brackets: Compound contribution (%) to total Mass Balance

We can conclude that the dianionic phosphate prodrug **20** increases significantly the aqueous solubility, displays adequate chemical stability and rapid bioconversion by membrane bound alkaline phosphatases releasing high concentration of drug in the vicinity of the mucosal membrane. In addition, its low permeability leads to low systemic exposure to the prodrug. All these properties made monophosphate ester **20** an adequate water soluble prodrug for the antimalarial compound GSK932121.



The synthesis of water soluble prodrugs aimed to address the issue of low oral bioavailability of 4(1H)-pyridones administered orally at doses >10 mg/kg. Pharmacokinetic studies of GSK932121 and its prodrug **20** were performed in parallel. Both compounds were administered to rats at 10 mg/kg, the parent drug compound as a nanomilled suspension in 1% MC, whereas the prodrug **20** was administered as a solution in water. Figure 3.14 shows the blood concentration of GSK932121 when the parent compound was administered (in red) and when the prodrug was administered (in dark blue). These results confirmed that the prodrug approach was very successful and significant high levels of GSK932121 were achieved using the prodrug **20**, allowing to perform the dose escalation studies in rats, which are needed to calculate the safety dose of the drug in anticipation to human studies.

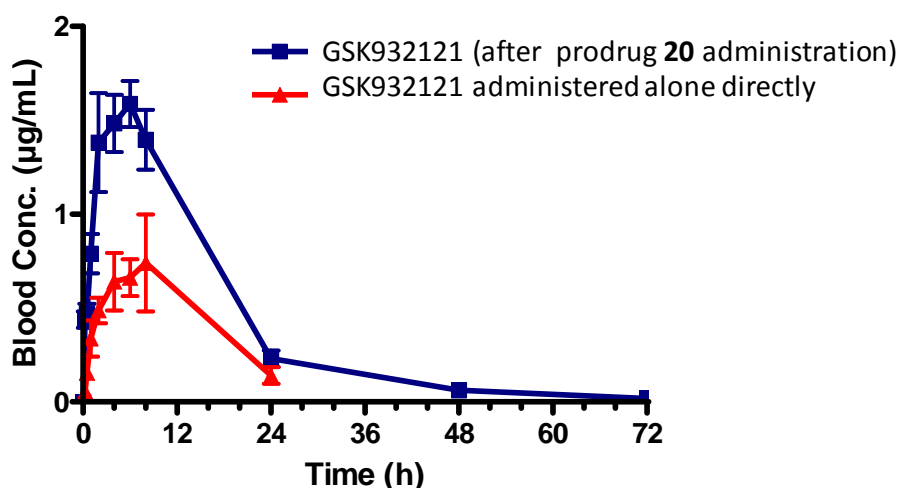


**Figure 3.14** PK in rat of GSK932121 and **20** after oral administration at 10 mg/Kg.

Blood levels (DNAUC) of the drug GSK932121 were three-fold higher when its prodrug was administered as a sodium salt in solution (3.9 and 1.16  $\mu\text{g}\cdot\text{h}/\text{mL}$  per mg/kg, prodrug **20** and parent GSK932121, respectively) and the same improvement was observed in the  $C_{\text{max}}$  value (1.78 and 0.8  $\mu\text{g}\cdot\text{h}/\text{mL}$ , prodrug **20** and parent GSK932121, respectively) (Table 3.9).

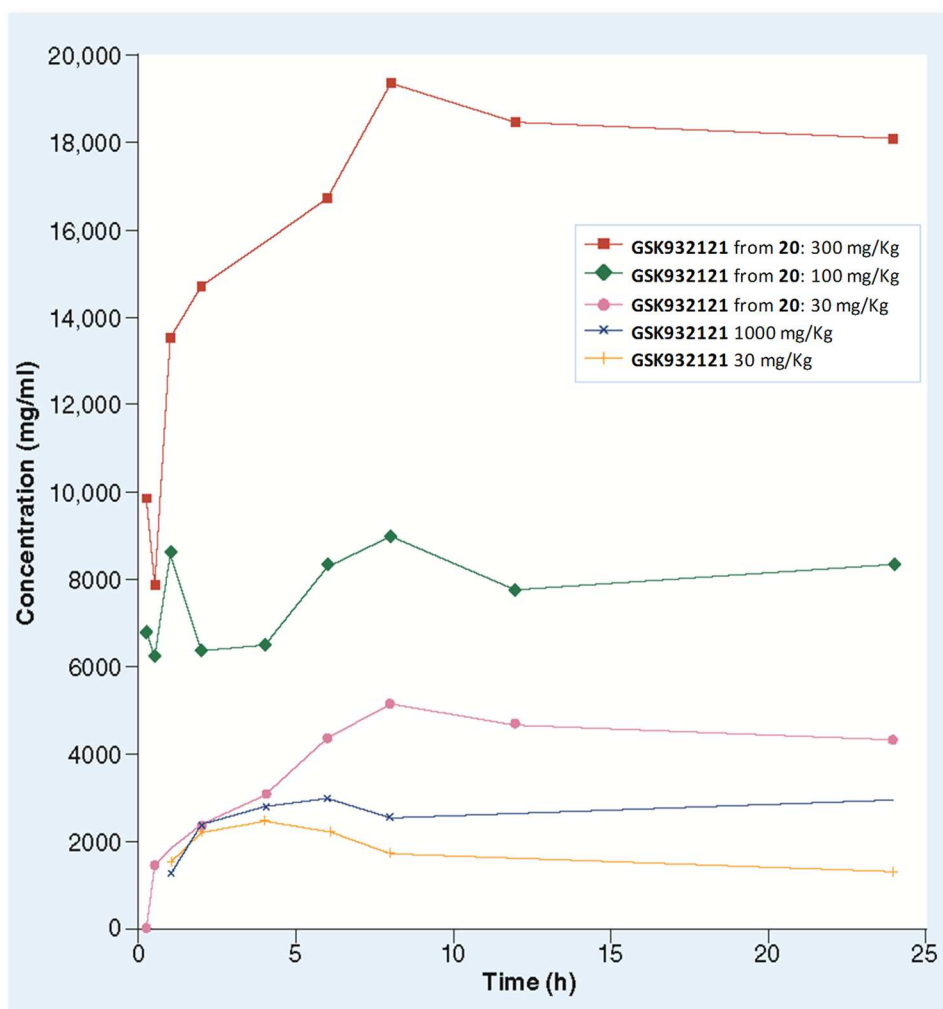
**Table 3.9** Pharmacokinetic in male rats

Route	Compound administered	Compound administered	Dose (mg / Kg)	Cmax (ug/mL)	Tmax (h)	AUC (0-inf) (mg ·h/mL)	DNAUC
oral	<b>20</b> <sup>(1)</sup>	<b>GSK932121</b>	<b>10</b>	1.78	6	24.6	3.19
	<b>GSK932121</b> <sup>(2)</sup>		10	0.8	6	11.6	1.16

1) Prodrug **20** administered orally in solution.

2) Parent GSK932121 administered orally in suspension (1% MC)

The required dose escalation studies in rats were performed with the prodrug **20**. Oral exposures to parent GSK932121 were measured when its corresponding prodrug **20** was administered orally over a wide range of doses in rats.



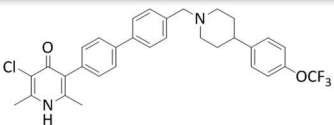
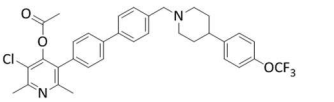
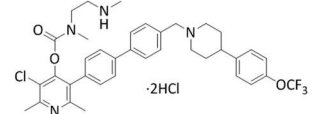
**Figure 3.15** Prodrug effect: blood levels of GSK932121 measured in rats after oral administration of its prodrug **20** in buffered aqueous solution at 30, 100 and 300 mg/kg. Blood levels of GSK932121 administered orally at 30 and 1000 mg/kg in suspension (20%PEG/20% captisol) are also included for comparison.

Figure 3.15 shows the blood levels of GSK932121 after oral administration of **20** in buffered aqueous solution at different doses compared with the blood levels of GSK932121 administered orally. Although the exposure increase was not perfectly linear over the range of doses administered, significantly higher blood levels of parent GSK932121 were detected after administration of its soluble phosphate prodrug **20**.

### PRODRUGS OF GSK1146191

Solubility and stability studies were also performed for the different prodrugs of GSK1146191. The solubility was determined in sodium citrate buffer (pH = 4.4) at room temperature and showed a significant improvement for prodrug **23** (carbamate of GSK1146191) versus the solubility of its corresponding parent compound in aqueous media. Solubility of prodrug **21** (acetate of GSK1146191) in the same medium remained very poor (< 1 ug/mL) (Table 3.10).

**Table 3.10** Solubility of GSK1146191's antimalarial prodrugs.

Compound	Structure	Solubility (mg/mL) <sup>a</sup>
GSK1146191		<0.001
<b>21</b>		<0.001
<b>23</b>		<b>1.33</b>

<sup>a</sup>Solubility Medium: 10 mM Citrate buffer pH=4,4

Prodrug, carbamate derivative **23**, was significantly more soluble in water than parent GSK1146191 in the absence of any additives, for this reason, chemical stabilities of prodrug **23** were determined in different media at rt; methyl cellulose (MC) 1% (Figure 3.17); Captisol 20% and Encapsine 20% (Figure 3.18), at two different pH values, pH = 6.06 (aqueous solution) and pH = 3.1 (solution in 2 μM Sodium Citrate buffer).

As expected for a pH regulated prodrug, compound **23** was more stable in acidic media (Sodium Citrate buffer pH 3.1) than in aqueous solution (Figure 3.16).

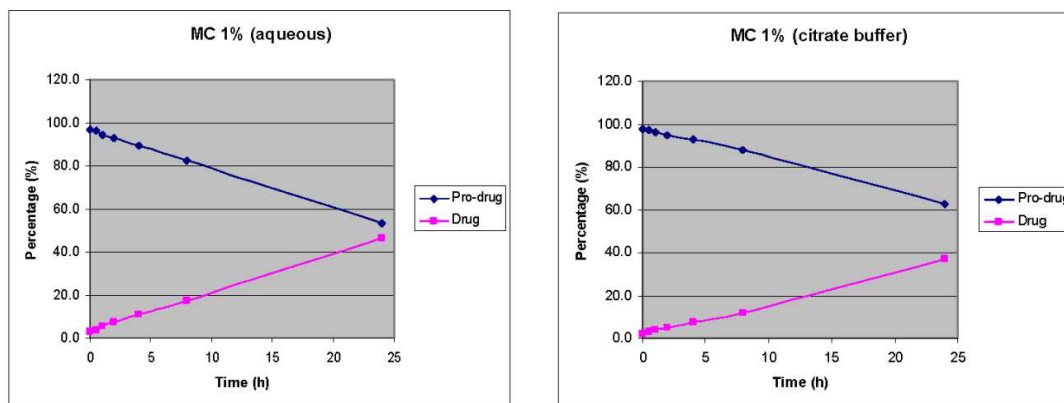


**Figure 3.16** Chemical stability of **23** in MC 1% in water and in aqueous 2 $\mu$ M Sodium Citrate buffer at pH 3.1

The use of cyclodextrins as excipients was not necessary to improve solubility and furthermore, the use of both cyclodextrins seemed to increase the prodrug instability. Encapsine 20% in aqueous solution showed the formation of the parent GSK1146191 immediately and prodrug **23** was almost not detected. Captisol 20% in Citrate buffered solution showed a slight increase in the prodrug's stability; it was 20h before the percentage of GSK1146191 overcome that of the prodrug (Figure 3.17).

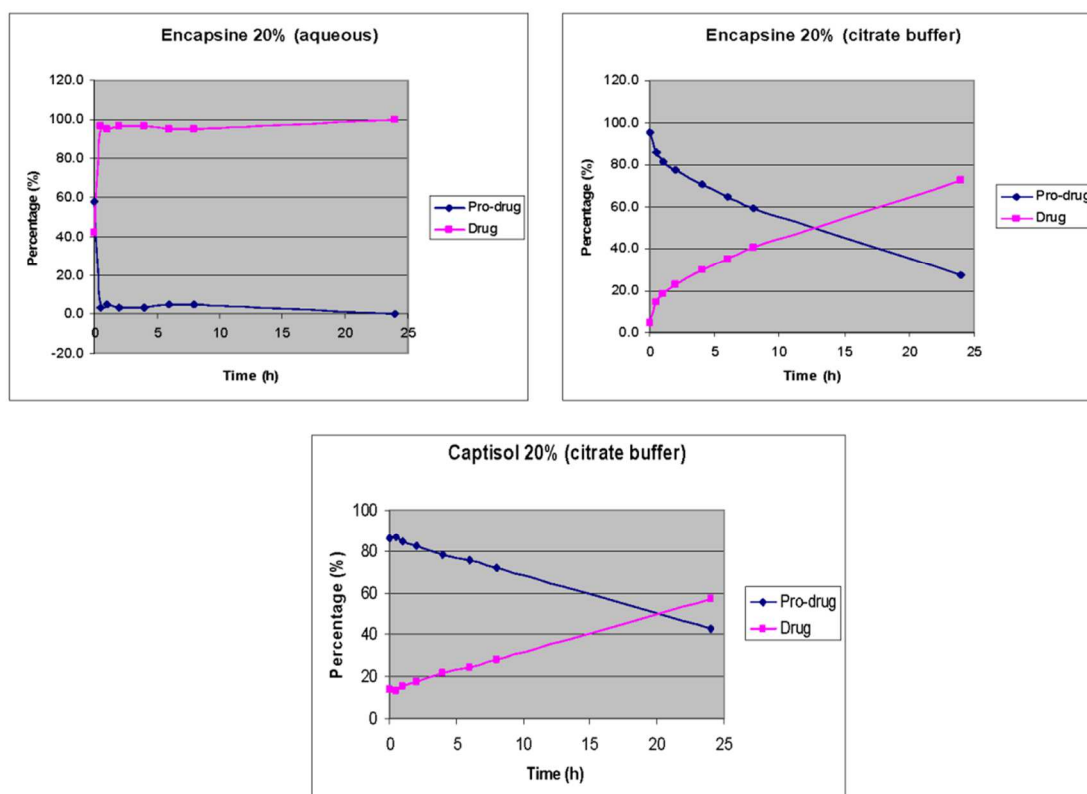


**Figure 3.17** Chemical stability of **23** in Encapsine 20% and Captisol 20%, in water and in aqueous 2 $\mu$ M Sodium Citrate buffer at pH 3.1.

As shown in the chromatograms, HPLC-DAD analysis confirmed decomposition after 2h leading to the parent drug in MC 1%. After 2h, solution in 1% MC in 2  $\mu$ M Sodium Citrate buffer (pH = 3.1), proved to be a suitable media for prodrug **23** (Figure 3.18).

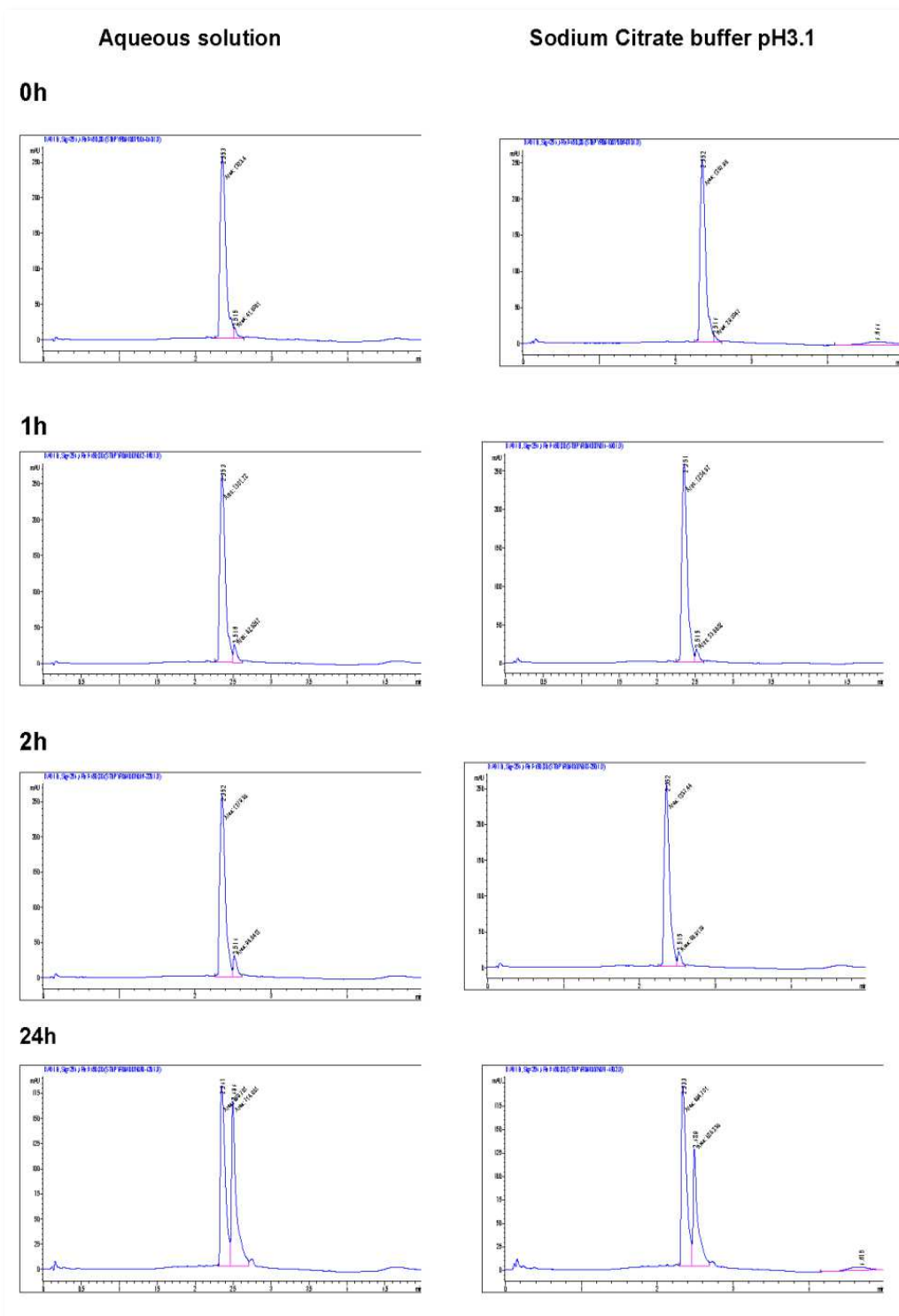
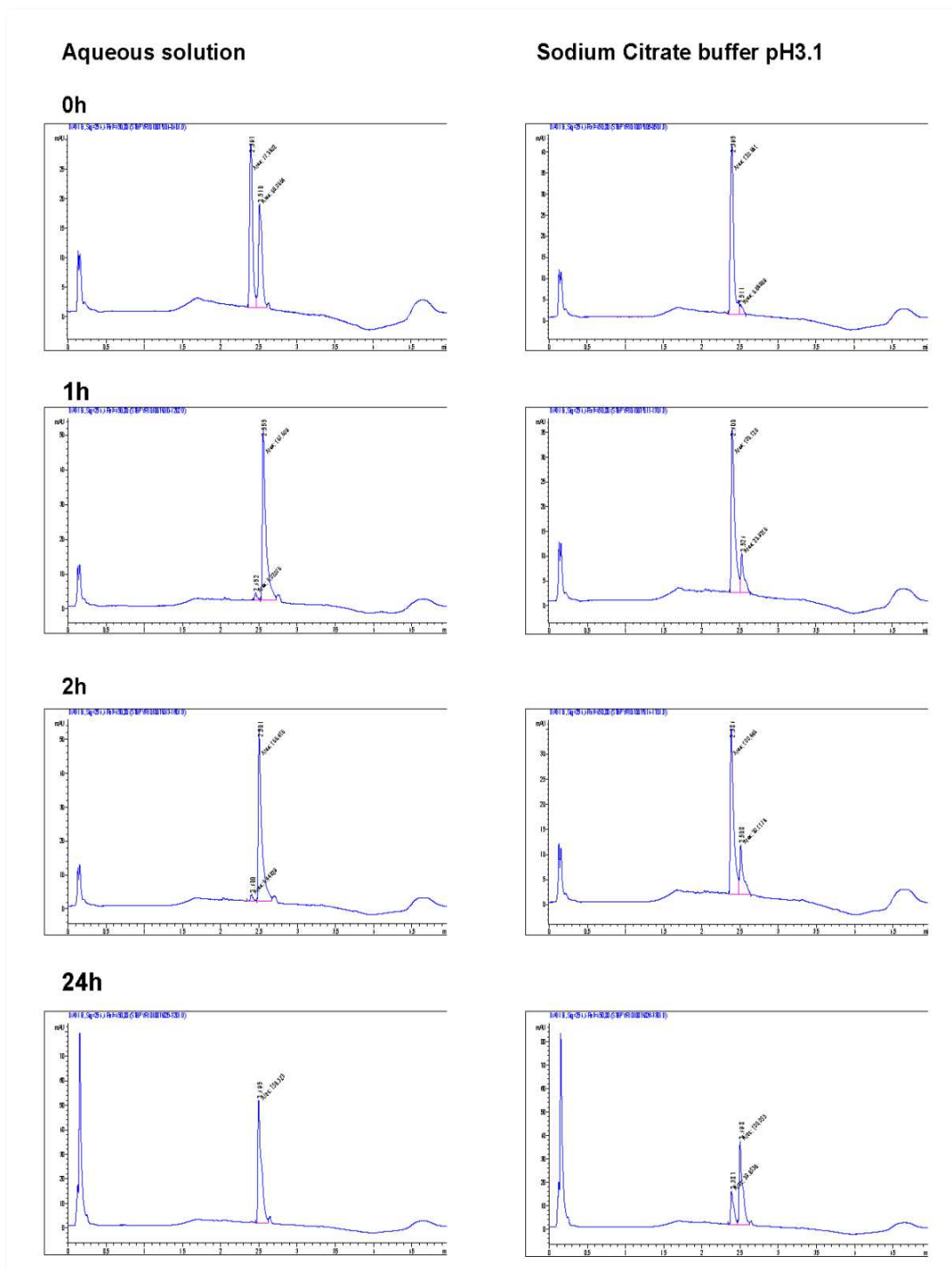


Figure 3.18 Chemical stability of **23** in MC 1% by HPLC-DAD

When the prodrug was dissolved in Encapsine 20% in citrate buffered solution, over half of the compound detected was the parent drug GSK1146191, 24h after preparing the solution (Figure 3.19).



**Figure 3.19** Chemical stability of 23 in Encapsine 20% by HPLC-DAD

Pharmacokinetic studies of GSK1146191 and its prodrug **23** were performed in order to assess the effect of increased solubility and, most importantly, to demonstrate an adequate release of the parent drug in the media after oral administration.

GSK1146191 and its prodrug **23** were administered orally in mice at 10 mg/kg using different administration vehicles. The parent drug GSK1146191 was administered as a suspension in 1% of MC to improve solubility and also as a solution, in DPE (DMSO/PEG-400/encapsine, 0.5 mg/mL). Prodrug **23** was administered as a solution using the most suitable vehicle previously identified, 1% MC in 2  $\mu$ M Sodium Citrate buffer (pH = 3.1).

The pharmacokinetic studies showed better drug exposures when the parent drug was administered directly as a DPE solution (in pink) than as a suspension in 1% MC (in black). On the other hand, the parent drug GSK1146191 released by prodrug **23** (in blue), did not achieve the expected increase in blood concentration (Figure 3.20).

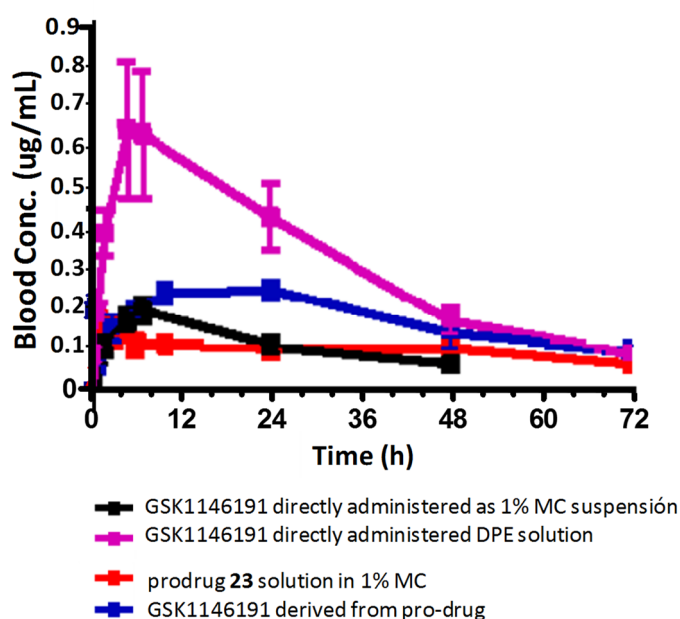


**Figure 3.20** PK in rat of GSK1146191 and **23** after oral administration at 10 mg/Kg.

Pharmacokinetic results showed that oral AUC for GSK1146191 was four-fold higher when it was directly administered in DPE solution in comparison to the 1% MC suspension (22.39 and 5.48  $\mu$ g·h/mL, in DPE and in 1% MC, respectively) and the same improvement was observed in the C<sub>max</sub> value (0.64 and 0.19  $\mu$ g/mL, DPE and 1% MC, respectively). When GSK1146191 was administered as a prodrug, AUC exposures of the

parent drug were slightly better than when it was administered directly as a 1% MC suspension, two-fold higher (12.33 and 5.48  $\mu\text{g}\cdot\text{h}/\text{mL}$ , as a prodrug and in 1% MC, respectively) (Table 3.11).

However, these result were just the opposite compare with those obtained with the GSK932121's phosphate prodrug. In this case, the prodrug rational did not work expected and the prodrug **23** was not able to increase the oral bioavailability of GSK1146191.

**Table 3.11** Pharmacokinetic in male rats

Compound	C max (mg/mL)	T max (hours)	AUC (0-72h) (mg·h/mL)
GSK1146191 (1% MC)	0.19	7	5.486 <sup>(1)</sup>
GSK1146191 (DPE)	0.64	5	22.391
<b>23</b> (1% MC pH 3.1)	0.146	1	7.088
GSK1146191 (parent)	0.247	24	12.336

1) Last time point with compound concentration >LOQ was 48h so, in this case value show is AUC (0-48h)

### 3.2.9 Conclusions

The synthesis of the GSK932121 mono phosphate prodrug **20** was successfully performed and the development of a robust chemical approach allowed the synthesis of compound **20** in a multigram scale to complete the pharmacokinetic and toxicity studies. Pharmacokinetic results demonstrated that a prodrug approach aimed at increasing the solubility in water, can help to solve the problems related with the dissolution-rate limited absorption in the antimalarial 4(1*H*)-pyridones. And what is more, in the case of the GSK932121 prodrug **20** we demonstrated that the phosphate ester is an excellent prodrug to overcome solubility problems, improving the linearity in the dose-escalation studies.



However, unexpected acute toxicity was observed in rats after oral administration of prodrug **20**, which was subsequently replicated by dosing GSK932121 alone through intraperitoneal administration at similar exposure levels to those achieved with its prodrug. The FTIH study with GSK932121 was placed on hold and later terminated despite its uneventful progress through the first two dose levels, requiring the development of new 4(1*H*)-pyridones with better therapeutic window.

A basic carbamate for GSK1146191 attached at position 4 of the 4(1*H*)-pyridone core was prepared and further studied as a suitable prodrug designed to improve solubility. Prodrug, carbamate derivative **23**, showed to be more soluble in water than its parent compound GSK1146191 in the absence of any additives, however, pharmacokinetic studies showed an ineffective release of the parent drug in the media which was translated in a slight improvement of the oral bioavailability of the drug GSK1146191.

### 3.3 AZAFLUORENONES

Azafluorenones are fused tricyclic compounds that are pyridine analogs to fluorenones (Figure 3.21). The azafluorenone scaffold is found in natural alkaloids and is considered a “privileged structure” due to its biological properties, for example they are known for their antifungal,<sup>182,183</sup> antimicrobial,<sup>184–187</sup> and antimalarial<sup>185,188–190</sup> activities as well as their role in the treatment of neurodegenerative disorders.<sup>191</sup>

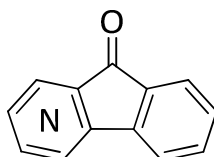


**Figure 3.21** Azafluorenone scaffold

Antimalarial activity of azafluorenone alkaloids has been reported for the 4-azafluorenone alkaloids 5,8-dihydroxy-6-methoxyonychine (*analogue a*) and 5-hydroxy-6-methoxyonychine (*analogue b*) (Figure 3.22). Both compounds are Onychine analogues and were isolated from the roots of the Australian tree *Mitrephora diversifolia* (Annonaceae). *Analogue b* is the more active, displaying IC<sub>50</sub> values of 9.9 and 11.4 μM against 3D7 and Dd2 strains of the malaria causing parasite *Plasmodium falciparum*.<sup>188</sup> The synthesis of azafluorenones derivatives at different positions of the tricyclic structure has been published<sup>192–194</sup> but only 4-azafluorenone alkaloids were reported as potent antimalarials.

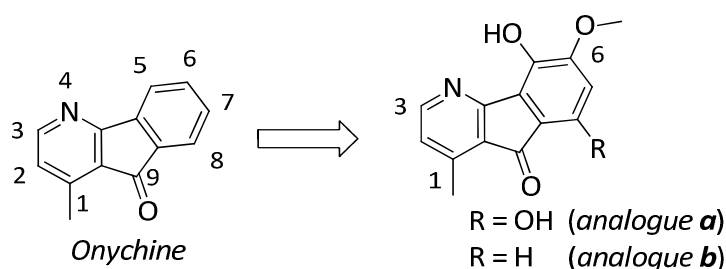


**Figure 3.22** Antimalarial 4-azafluorenones

### 3.3.1 Previous work.

In our group azafluorenones **26** and **27** were isolated as side products during the scale-up synthesis of GW308678 and GW844520 respectively (Figure 3.23). Both compounds are fused 4(1*H*)-pyridones and can be defined as a new 1-azafluorenone alkaloid compounds and not related scaffolds have been previously described in the literature. Compound **26** was isolated as a red solid and it displayed an outstanding *in vitro* antimalarial activity,  $IC_{50} = 0.039 \mu\text{M}$ , compared to the known 4-azafluorenones (unit of  $\mu\text{M}$ ). Likewise, the corresponding GW844520's tricyclic derivative **27** was also isolated providing the same range of antimalarial potency,  $IC_{50} = 0.045 \mu\text{M}$ .

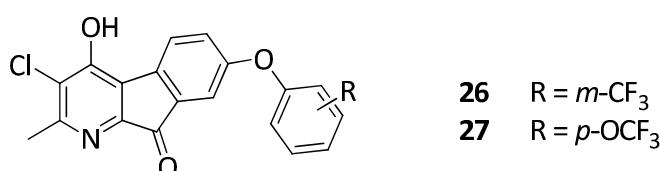


**Figure 3.23** Antimalarial 1-azafluorenones

Compound **27** was progressed to further studies in order to assess the antimalarial potential of this new tricyclic scaffold. It showed inhibition of the plasmodial ubiquinol: cytochrome c oxidoreductase (Cyt *bc*<sub>1</sub>) with potencies in the low nanomolar range ( $IC_{50} = 0.0038 \mu\text{M}$ ), confirming the same mode of action than the classical pyridones, as well as inhibition in the whole-cell *in vitro* assay against *P.falciparum* cultures ( $IC_{50} = 0.045 \mu\text{M}$ ). This potency translated into a good *in vivo* efficacy when it was tested in the *P.yoelii* murine model ( $ED_{50}$  &  $ED_{90} = 0.2$  &  $0.25 \text{ mg/kg}$ ). The maximal non-lethal dose MNLD was also calculated to determine the safety margin for **27** (Table 3.12).

**Table 3.12** Antimalarial profile of compound **27**

Compound	<i>P.falciparum</i> In vitro $IC_{50}$ ( $\mu\text{M}$ )		<i>P. yoelii</i> CD1 mice In vivo (mg/kg)		
	Target Cyt <i>bc</i> <sub>1</sub>	Whole cell 3D7A	$ED_{50}$	$ED_{90}$	MNLD
<b>27</b>	0.0038	0.045	0.2	0.25	37.3

Due to these encouraging results with compounds **26** and **27**, the work described herein was focused on the study of the structure-activity relationships (SAR) of this novel tricyclic scaffold on two key positions for the classical antimalarial 4(1*H*)-pyridones (Figure 3.24); position 3, where the halogen atom showed to be important for the potency, and position 9, where some polar groups are tolerated but not protonable groups (see Chapter 1.4.2)

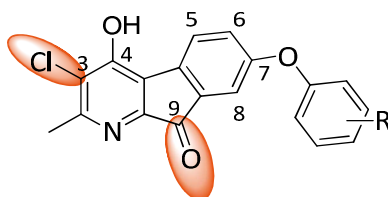
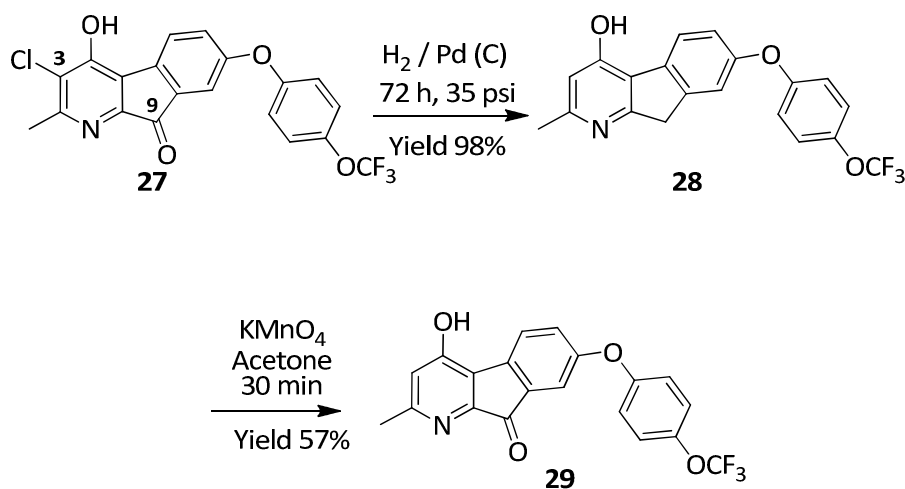


Figure 3.24 Chemical basic modifications of the 1-azafluorenone

### 3.3.2 Chemical synthesis of the 1-azafluorenone series

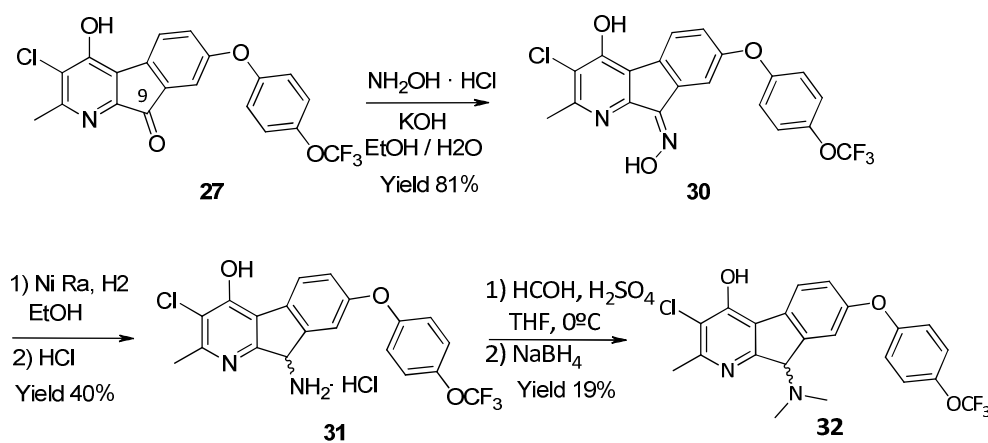
For this study, compound **27** was used as starting material and the exploratory SAR was started by removing the chloro atom at position 3. Hydrogenation of compound **27** in presence of Pd (C) at 35 psi for 72h led to the desired de-halogenation at position 3 of the pyridone ring but also to the reduction of the ketone to methylene at position 9 of the tricyclic skeleton (**28**). Compound **28** was obtained in good yield (98%), further oxidation with  $\text{KMnO}_4$  in acetone afforded the desired de-halogenated derivative **29** (yield 57%) (Scheme 3.16):



Scheme 3.16 1-Azafluorenone analogues

This new scaffold allowed us to explore the relevance of the new carbonyl group at position 9 and looking for a GSK932121 cyclic analogue. However all the attempts to prepare the corresponding hydroxy analogue at position 9 were unsuccessful and starting material **27** was always recovered probably due to a spontaneous oxidation of the alcohol.

With the aim of synthesising analogues at position 9 we investigated the introduction of ionizable moieties such as basic amines. To achieve such modifications we considered the synthesis of the corresponding oxime at position 9 and further reduction to prepare the amine **31**. This amine could be used as starting material to obtain stable derivatives at position 9 (Scheme 3.17):



**Scheme 3.17** 1-Azafluorenone analogues at position C9

Oxime **30** was prepared in good yields (81%) by reaction of **27** with hydroxylamine hydrochloride in basic media. Reduction with Ni-Raney<sup>195</sup> and further purification by trituration in ACN led to compound **31** in moderate yields (40%). Compound **32** was prepared by reductive amination using  $\text{NaBH}_4$  as reductive agent.<sup>196</sup> Purification by column chromatography led to compound **32** in a poor 19% yield (Scheme 3.17).

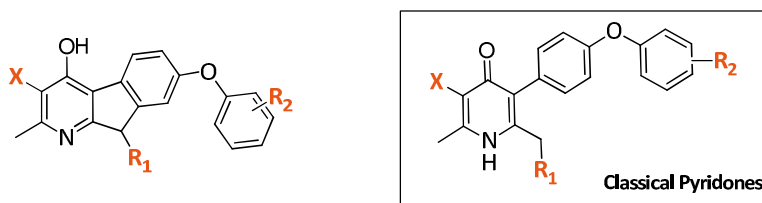
The structure of all the compounds synthesized in this section was elucidated by proton Nuclear Magnetic Resonance Spectroscopy ( $^1\text{H-NMR}$ ) and Liquid chromatography–mass spectrometry (LC/MS) (see Appendix I).

### 3.3.3 Biological analysis of the 1-azafluorenone series

#### *In vitro* PROFILE

Antimalarial potency of the compounds (*Pf* IC<sub>50</sub>) and cytotoxicity values against HepG2 cells are summarized in Table 3.13. In order to make the analysis of these results as efficient as possible, key analogues previously prepared in our group but not included in the work presented in this thesis, are included in the table and duly indicated (\*).

**Table 3.13** *In vitro* Antimalarial activity of 1-Azafluorenones



Compound	X	R <sub>1</sub>	R <sub>2</sub>	IC <sub>50</sub> (μM)	HepG2 (μM)	SI.
26	Cl	=O	4-CF <sub>3</sub>	0.039	> 3	> 76
27	Cl	=O	4-OCF <sub>3</sub>	0.045	> 25	> 555
28	H	-H	4-OCF <sub>3</sub>	0.021	16.77	798
29	H	=O	4-OCF <sub>3</sub>	0.009	24.86	2673
30	Cl	=N-OH	4-OCF <sub>3</sub>	0.017	>25	1470
32	Cl	-N(Me) <sub>2</sub>	4-OCF <sub>3</sub>	0.027	13.38	1115
<b>GW844520</b>	Cl	-H	4-OCF <sub>3</sub>	0.005	> 61	>12200
<b>GW308678</b>	Cl	-H	4-CF <sub>3</sub>	0.003	> 63	>21000
<b>33*</b>	H	-H	4-OCF <sub>3</sub>	0.016	-	-
<b>14h*</b>	Cl	-N(Me) <sub>2</sub>	4-OCF <sub>3</sub>	>0.5	-	-
<b>GSK932121</b>	Cl	-OH	4-OCF <sub>3</sub>	0.006	10	>1666
<b>Atovaquone</b>	-	-	-	0.0002	-	-
<b>Chloroquine</b>	-	-	-	0.03	-	-

*Classical Pyridones*

SI.: Selectivity Index= HepG2 IC<sub>50</sub>/*Pf*IC<sub>50</sub>.

Interesting information could be drawn from this SAR analysis. The de-halogenated derivative at position 3 in the pyridone ring led to even more potent compounds (**29**,  $IC_{50} = 0.0093 \mu\text{M}$ ) in comparison with the corresponding chloro derivative **27** ( $IC_{50} = 0.045 \mu\text{M}$ ), which differs from the classical 1(*H*)-pyridones, in which halogen substitution at position 3 was mandatory to obtain good antimalarial activity (**33\***).

Another interesting observation was that removal of the carbonyl substitution at position 9 gave a compound in the same range of potency that original compounds **26** and **27** (**28**,  $IC_{50} = 0.021 \mu\text{M}$ ), suggesting that carbonyl substitution at position 9 was not essential for the antimalarial activity. Also, we observed that modifications at position 9 were allowed, maintaining or improving the activity of the 1-azafluorenone (**30** y **32**,  $IC_{50}=0.017$  and  $0.027 \mu\text{M}$ , respectively), which also differs from the classical 1(*H*)-pyridones, in which the introduction of tertiary amines at position 6 lead to inactive compounds (**14h\***).

Compounds **28**, **29**, **30** and **32** were evaluated against HepG2 human cell line showing moderate cytotoxicity, however, due to the excellent antimalarial activity displayed, good SI were obtained in all cases. It is important to highlight the effect in the SI when modifications were performed at position 9 of the 1-azafluorenone. The replacement of the carbonyl moiety by other functionalities such as hydroxyl oxime (**30**) or dimethyl amine (**32**) led to selective compounds (SI = >1470 and 1115, respectively), with selectivity indexes in the range of the potent antimalarial GSK932121 (SI = >1666).

### *In vivo PROFILE*

These encouraging results prompted us to evaluate compounds **29** ( $IC_{50}=0.0093 \mu\text{M}$ ; HepG2  $24.86 \mu\text{M}$ ) and **30** ( $IC_{50}=0.017 \mu\text{M}$ ; HepG2  $>25 \mu\text{M}$ ) in the *P.yoelii* CD1 mice model. A promising *in vivo* antimalarial profile was confirmed for the 1-azafluorenone **29** with  $ED_{50}$  and  $ED_{90}$  values of 1.86 and 3.92 mg/Kg respectively and a MNLD  $>100$  mg/Kg. However, compound **30** did not show the expected dose-response after intraperitoneal administration in mouse.

In order to understand the lack of *in vivo* activity displayed by compound **30**, pharmacokinetic studies were performed. Intraperitoneal administration (i.p.) was chosen to avoid oral absorption issues and the selection of the doses was based on the

maximal non-lethal dose (MNL) study. The MNL in mice treated with **30** (single i.p. dose) was 30 mg/Kg and therefore the doses for PK studies were established at 15 mg/Kg and 8 mg/Kg. PK data are shown in Table 3.14.

**Table 3.14** Pharmacokinetic Parameters of **30** in CD1 mice after intraperitoneal administration

Dose	AUC(0-48h) ( $\mu\text{g}\cdot\text{h}/\text{mL}$ )	C <sub>max</sub> ( $\mu\text{g}/\text{mL}$ )	t <sub>max</sub> (h)	DNAUC(0-48h) ( $\mu\text{g}\cdot\text{h}/\text{mL}$ per mg/Kg)	C <sub>max</sub> /Dose ( $\mu\text{g}/\text{mL}$ per mg/Kg)
8	2.62	0.471	1	0.336	0.0604
15	2.07	0.189	1	0.135	0.0123

Similar exposure levels at 8 and 15 mg/Kg doses were achieved, likely due to incomplete absorption, with remaining non-absorbed compound found in the peritoneum of the mice after 48 hours, post-dosing in both tested doses (Figure 3.25). In conclusion, low exposure of compound **30** was determined after the PK studies and this feature was in agreement with the lack of dose-response observed when **37** was tested in the *P.yoelii* efficacy mice model.

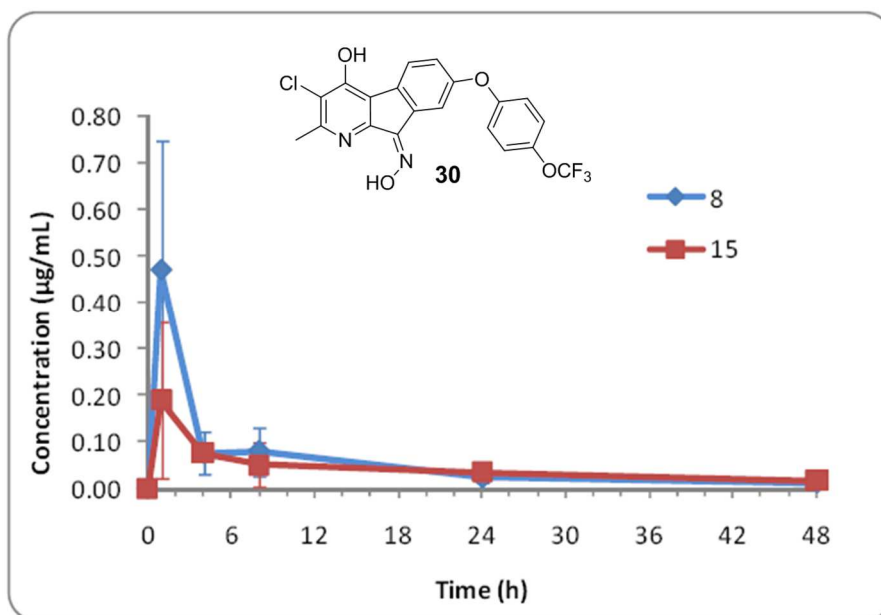


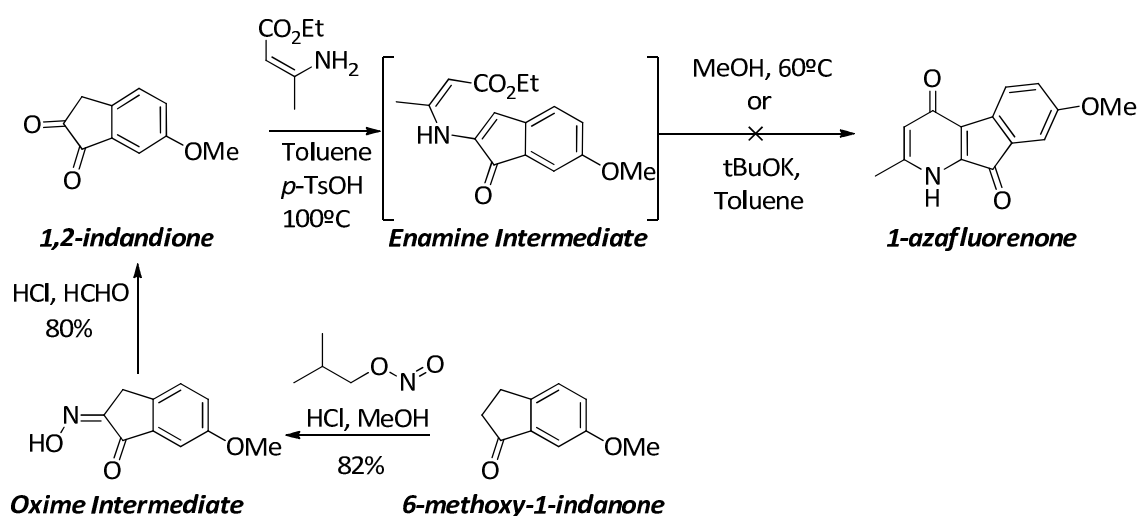
**Figure 3.25** Pharmacokinetic profiles of **30** after intraperitoneal administration of 8 mg/kg and 15 mg/kg to CD1 mice.



### 3.3.4 Chemical synthesis of the 1-azafluorenone scaffold

#### Background: synthetic studies

Different approaches to synthesize these tricyclic compounds were performed in our group. Intramolecular cyclization of the enamine intermediate formed from 6-methoxy-1*H*-indene-1,2(3*H*)-dione was studied (Scheme 3.18). The required oxime intermediate was obtained by reaction of 6-methoxy-1-indanone with isopentyl nitrite and concentrated hydrochloric acid in methanol under gentle warming.<sup>197</sup> Subsequent acidic hydrolysis, in the presence of formaldehyde, led to the key 1,2-indandione derivative.<sup>198</sup> Nucleophilic addition of the corresponding amine, ethyl 3-aminocrotonate, would lead to the enamine intermediate able to promote the intramolecular base-mediated cyclization to obtain the 1-azafluorenone. After different attempts, this approach was finally discarded. Enamine intermediate was detected by LCMS but the desired 1-azafluorenone was never obtained.

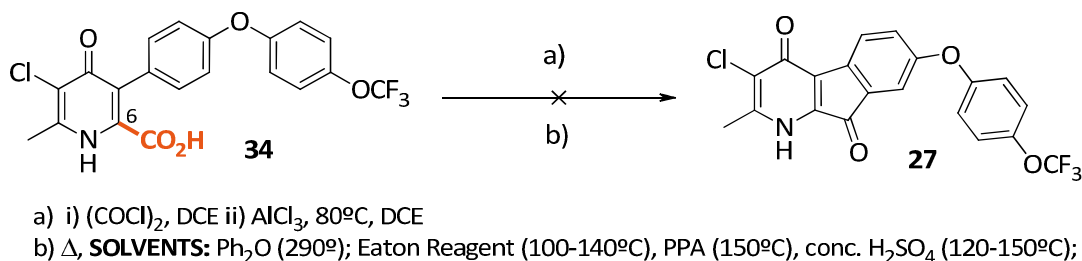


**Scheme 3.18** Enamine formation and intramolecular cyclization

Direct ring closure approach of the corresponding pyridone was also explored. In our group a synthetic approach was optimized in order to prepare different analogues at position 6 of the classical pyridones.<sup>139</sup>

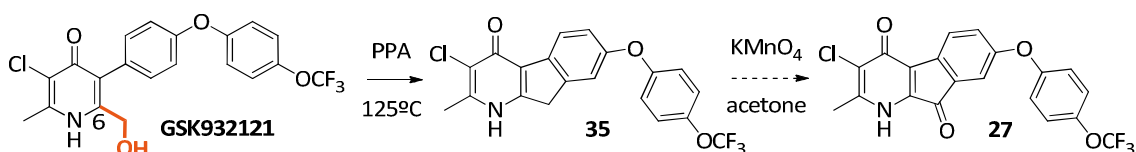
Aromatic substitution via Friedel-Craft acylation was studied using the carboxylic acidic derivative **34** as starting material (Scheme 3.20). Different Lewis acids were tested but only AlCl<sub>3</sub> allowed us to identify **27** by LCMS analysis, unfortunately only traces of the desired compound **27** were obtained. Thermal cyclization using different conditions

such as, Ph<sub>2</sub>O (at 290°); Eaton Reagent (at 100-140 °C), PPA (at 150 °C) and conc. H<sub>2</sub>SO<sub>4</sub> (at 120-150 °C); were also explored but **27** was never obtained, with starting material decomposition being the main result Scheme 3.19).<sup>199</sup>



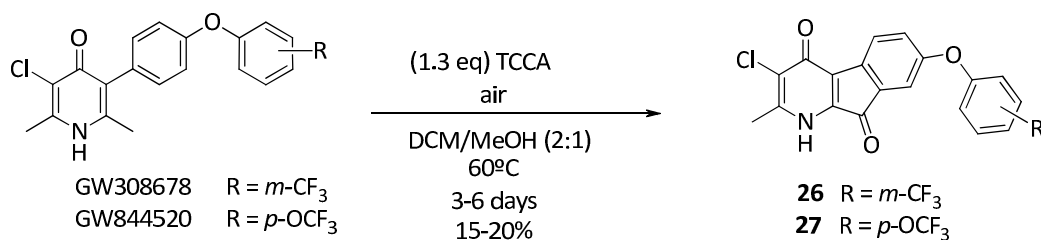
**Scheme 3.19** Nucleophilic ring closure via Friedel-Craft acylation

GSK932121 was used as starting material to prepare the tricyclic intermediate **35**, able to afford **27** by oxidation with KMnO<sub>4</sub>. Reaction of GSK932121 with PPA led to the desired intermediate **35** only when reaction was heated at high temperatures (150-205 °C), however reagents decomposition led to unpracticable mixtures and only traces of tricyclic **35** were isolated (Scheme 3.20).<sup>199</sup>



**Scheme 3.20** . Nucleophilic ring closure

Our group also examined the original reaction where the desired tricyclic derivative was formed. Different reagent amount, reaction times, solvents and radical initiators were studied. The best results were obtained by reaction of the corresponding 4(1*H*)-pyridone with 1.3 equivalents of TCCA under continuous air stream in DCM/MeOH (2:1) as solvent. In this manner, the desired 1-azafluorenones were obtained but in low yield (15-20% yield) (Scheme 3.21):



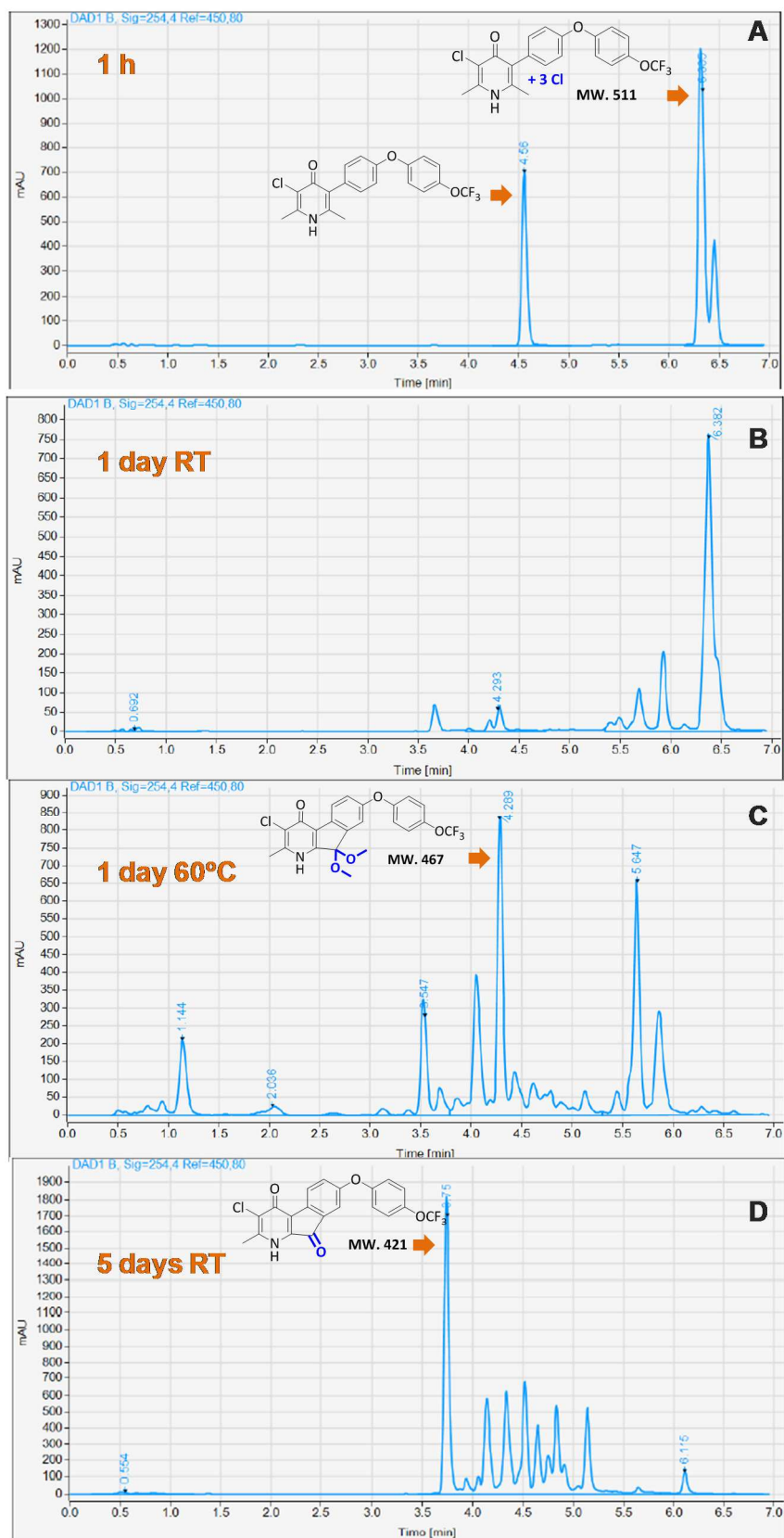
**Scheme 3.21** Synthesis of 1-azafluorenones

### 3.3.5 Mechanistic study for the synthesis of the 1-azafluorenone scaffold

For this thesis the intramolecular cyclization process for the synthesis of the 1-azafluorenone **27** (Scheme 3.21), was studied by HPLC and LCMS analysis at different times along the reaction process (Figure 3.26).

GW844520 was dissolved in a mixture of DCM / MeOH (2:1) and 1.3 equivalent of TCCA was added at 0 °C. Reaction was allowed to reach RT and one hour later a new signal was identified by HPLC (RT 6.32 min) and LCMS (MS ES+ 511.9, MS ES- 510.9, isotope pattern showed four chlorine atoms). This new signal could correspond to a trichlorinated intermediate of GW844520 (MS ES<sup>+</sup> + 3Cl) (see Figure 3.26 (A)).

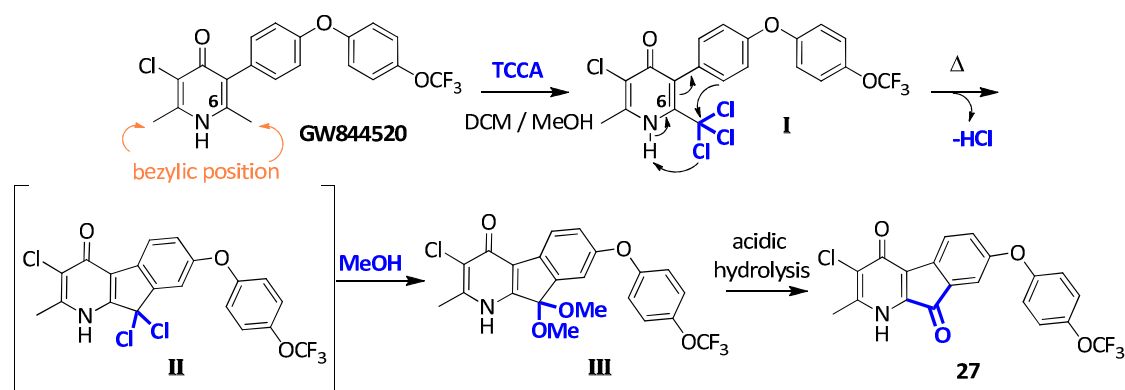
After 24 h stirring at room temperature, the chlorination reaction was complete (see Figure 3.26; (B)). The reaction was then heated at 60 °C and a complex mixture was obtained but one signal was mainly detected by HPLC (RT 4.29 min). This signal was identified by LCMS (MS ES+ 468.1, MS ES- 466.1) as the dimethylketal tricyclic intermediate (MW 467) (see Figure 3. 27 (C)). Finally, the reaction was stirred at RT for 5 days and desired compound (MW 421) was detected by HPLC (RT 3.75 min) and LCMS (MS ES+ 422.0, MS ES- 421.0) as the main product (see Figure 3. 26; (D)). After filtration of the solid and different washes **27** was obtained in 23% yield.



\*HPLC conditions. COLUMN: XBRIDGE 3.5 $\mu$  RP18 , 4.6 x 50 mm. GRADIENT: 10 $\mu$ M NH<sub>4</sub>HCO<sub>3</sub>-ACN. 0-1 min 75:25; 1-5 min 0:100; 5-6.4 min 0:100; 6.4-7min 75:25. FLOW: 1 mL / min. WAVELENGTH: 254 and 210 nm. Temp 30 °C

Figure 3.26 HPLC Reaction progression to obtain the tricyclic azafluorenone

Based on the experimental results, we propose the mechanism depicted in Scheme 3.22. After polychlorination of the benzylic positions at the pyridone core with TCCA, the trichlorinated intermediate **I** undergoes an intramolecular Friedel Craft alkylation to furnish intermediate **II**.



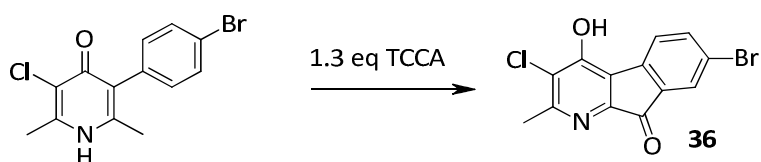
**Scheme 3.22** Proposed mechanism for the tricyclic formation.

LCMS analysis allowed us to identify the dimethylketal **III** as one of the tricyclic intermediates, being obtained by substitution of the chlorine atom by MeOH (although it could happen before or after the cyclization). The formation of the dimethylketal **III** is consistent with the observation that the evaporation of the co/solvent (DCM) under a continuous air stream, favored the reaction rate. To conclude this process, acidic hydrolysis of dimethylketal **III** provide the desired 1-azafluorenone **27**.

To discard a radical or an oxygen mediated cyclization, the reaction was performed in absence of oxygen (under N<sub>2</sub> atmosphere) or in presence of a radical inhibitor (TEMPO). In both cases the tricyclic compound was obtained, indicating that cyclization reaction does not proceed via radicals or is promoted by the presence of oxygen.

### 3.3.6 Synthesis of a suitable intermediate for SAR studies.

Following a similar reaction and in order to explore the SAR around the 1-azafluorenone lipophilic tail, the synthesis of the suitable Bromo intermediate **36** was studied (Scheme 3.23).



**Scheme 3.23** Study of reaction conditions to obtain **36**

Standard conditions previously used for the synthesis of the 1-azafluorenone **27** were applied to prepare **36**. The mixture DCM/MeOH (2:1) allowed us to obtain a total dissolution of the compound but precipitation was observed when the polychlorinated derivatives were formed after addition of the 1.3 eq of TCCA. The use of aprotic solvents like DMF or NMP led to homogeneous polychlorinated mixtures but when they were heated to complete the intramolecular ring closure any change was observed. The same unsuccessful result was obtained when AcOH was used as solvent. Polychlorinated derivatives were detected by LCMS, however, after heating to induce the cyclization, the expected tricyclic **36** was not detected. We conclude that the synthesis to obtain the intermediate **36** was unfruitful probably due to the deactivating effect of the Bromo substitution in the aromatic ring.

### 3.3.7 Conclusions

The 1-azafluorenone series, a novel tricyclic scaffold based on the 4(1H)-pyridone ring, has been validated as potent antimalarial. New analogues, in addition to the parent compounds **26** and **27**, have been synthesized at positions 3 and 9 of the azafluorenone, and data reported not only suggested a clear SAR for this new tricyclic skeleton but also a slightly different behaviour to the classical 4(1H)-pyridones when similar substituents were introduced at these two positions (Figure 3.27).

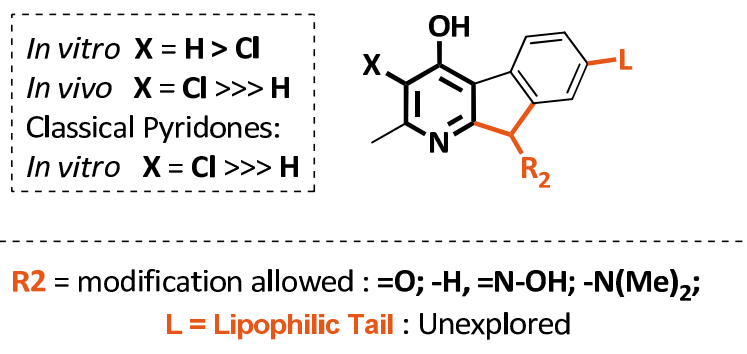


**Figure 3.27** Antimalarial structure-activity relationships (SAR) for 1-azafluorenones

The excellent *in vitro* and *in vivo* antimalarial activity, together with the good selectivity index observed, pointed at the 1-azafluorenones as a novel and promising sub-series able to overcome the safety issues found in the classical 4-(1*H*)-pyridones, raising the opportunity of a back-up series. However, the low synthetic tractability for this series remained a major problem, precluding exploration around the lipophilic tail.

### 3.4 TRICYCLIC BENZOTHIENOPYRIDINONES

#### 3.4.1 “Confidential Section”

Building upon our studies with the 1-azafluorenone scaffold and with the aim of identifying more tractable scaffolds to complete the SAR studies, a new tricyclic scaffold was designed and prepared able to maintain the good antimalarial properties. The work here in described was focus on the optimization of a robust and tractable synthetic pathway for this new tricyclic chemical class. This new chemical diversity allowed to introduce modifications at different positions, including the yet unexplored tail region (L) and to study its effect in the antimalaria activity.

More than 50 final compounds were designed and synthesized using different chemical approaches (Suzuki coupling, Ullman reaction and Shonogashira coupling). *In vitro* and *in vivo* profiling for final compounds were completed and also analysed in order to evaluate this novel family of tricyclic 4(1*H*)-pyridone series as a feasible antimalarial drug. This profiling included:

- *In vitro* *P.falciparum* and human HepG2 activities (whole cell assays);
- *In vitro* profiling against the plasmodial ubiquinol (enzymatic assays);
- *In vitro* profiling against *P.falciparum* atovaquone-resistant strain FCR3-A;
- *In vivo* Pharmacokinetic Parameters (solubility, Vd, Cl, NDAUC, Cmax, Tmax, %F);
- *In vivo* Antimalarial Activity in the *P.Yoelli* mouse model.
- *In vivo* Antimalarial Activity in the in the *P.falciparum* humanized mouse model.

Analysis and visualization of the biological data for all the derivatives obtained was performed using TIBCO Spotfire (Data Visualization & Analytics Software). Molecular modelling for the key analogues was also carried out using MOE (Molecular Operating Environment, software for Molecular Modelling and Simulations).

The structure of all the compounds synthesized in this section was elucidated by proton Nuclear Magnetic Resonance Spectroscopy (<sup>1</sup>H-NMR) and Liquid chromatography–mass spectrometry (LC/MS)



---

## **4 CONCLUSIONS**

---

## 4.1 Conclusiones

El presente trabajo se ha llevado a cabo dentro de un proyecto de investigación perteneciente a la compañía farmacéutica GlaxoSmithKline (GSK) y ha sido enfocado al desarrollo de nuevos fármacos antimaláricos pertenecientes a la familia de las 4(1H)-piridonas, identificadas como potentes inhibidores de la cadena de transporte de electrones mitocondrial de *P. falciparum* en el complejo III del citocromo *bc1*.

El principal objetivo de este trabajo ha consistido en la síntesis de nuevos derivados de la serie de las 4(1H)-piridonas diseñados para mejorar las propiedades farmacológicas de los cabeza de serie GW844520, GW308678 y GSK932121.

Así, en el Capítulo 3.1 se exploró la posición 2 de las 4(1H)-piridonas. Para este estudio se prepararon análogos de GW844520 y GW308678 diseñados para reducir la lipofilia mediante la incorporación de grupos polares, como hidroxilo, o grupos ionizables, como las aminas básicas (Figure 4.1):

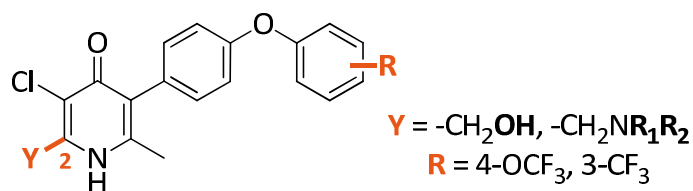


**Figure 4.1** 4(1H)-Piridonas modificadas en posición 2

Este trabajo reveló que la incorporación de grupos polares (-OH o -N=OH) permitía obtener compuestos con ligeras mejorías en las propiedades fisicoquímicas de la molécula, manteniendo la potencia antimalárica, sin embargo, este efecto no fue extensible a las aminas básicas, las cuales fueron inactivas. En general, los datos generados en el Capítulo 3.1 muestran que ciertas modificaciones en la posición 2 de las 4(1H)-piridonas pueden ser toleradas, pero ni las actividades antimaláricas ni las propiedades fisicoquímicas suponían una mejora significativa con respecto a los cabeza de serie GW844520, GW308678 o GSK932121. Por tanto, el trabajo químico en esta posición fue descartado.

En este Capítulo 3.1 también se han generado y analizado modelos de docking y cálculos teóricos de distintas 4(1H)-piridonas. Estos modelos teóricos han permitido identificar los límites estéricos a los que está sujeta la posición 2 de la 4-piridona como

una de las causas de la pérdida de actividad antimalárica observada en los resultados biológicos, justificándose también la pérdida total de la potencia de aquellos sustituyentes más voluminosos.

Continuando con el estudio para mejorar las propiedades fisicoquímicas de las 4(1H)-piridonas, en el Capítulo 3.2, se exploró la síntesis de profármacos para mejorar la solubilidad. Con este fin, se preparó con éxito el profármaco para el cabeza de serie GSK932121 (su correspondiente éster fosfato, **20**) (Figure 4.2).

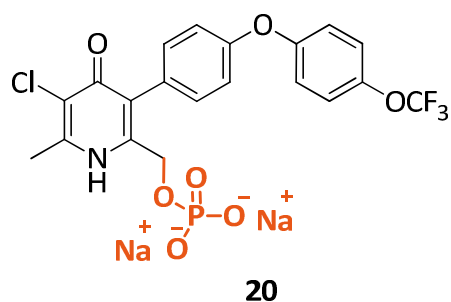


**Figure 4.2** Profármaco de GSK932121

La síntesis de la sal sódica estable del éster fosfato **20** (profármaco de GSK932121) se llevó a cabo con éxito y los estudios realizados con esta sal fueron críticos para la toma de decisiones en la progresión del compuesto GSK932121. La solubilidad del profármaco mostró ser  $10^5$  veces superior a la del compuesto original y la buena liberación del fármaco en las proximidades de la pared intestinal permitió aumentar la biodisponibilidad de la droga incluso a altas dosis.

El uso del profármaco **20** permitió completar los estudios de tolerabilidad a altas dosis y calcular el margen de seguridad del fármaco. Por desgracia este margen de seguridad no fue suficiente a dosis superiores a 0.3 mg/kg lo que detuvo la progresión de este compuesto a los estudios clínicos. Por tanto, podemos concluir que el uso de profármacos es una herramienta útil y que debe considerarse al principio del proceso de desarrollo de un fármaco y así poder asegurar una alta exposición de aquellos compuestos cuya dosificación oral se vea limitada por las bajas exposiciones.

La última parte de este trabajo fue enfocado a la validación y estudio de las versiones cíclicas de las 4(1H)-piridonas. En el Capítulo 3.3 se llevó a cabo la preparación de diferentes análogos a 1-azafluorenona **26** y **27**, permitiendo la validación de esta sub-

serie como potenciales antimaláricos que, al igual que sus precursores no cíclicos, actuaban en el citocromo *bc1*. de *P. falciparum*, inhibiendo el transporte de electrones mitocondrial (Figure 4.3).

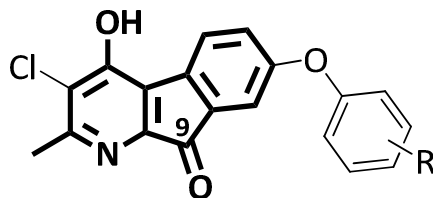


**Figure 4.3** 4(1*H*)-Piridonas tricíclicas

Los buenos resultados biológicos obtenidos nos llevaron a la exploración de posibles rutas sintéticas que nos permitieran sintetizar otros derivados y avanzar en el estudio de relación estructura-actividad. Finalmente, estudios mecanísticos de la reacción de ciclación llevados a cabo en este capítulo nos llevan a pensar que las 4(1*H*)-piridonas tricíclicas fueron obtenidas mediante una reacción de ciclación intramolecular de tipo Friedel Craft.

En general, las 1-azafluorenonas han sido validadas en el Capítulo 3.3. Sin embargo, estos estudios se vieron limitados por la baja accesibilidad química que ofrecía el esqueleto tricíclico de 1-azafluorenona. Por esta razón se decidió explorar la síntesis de otras 4(1*H*)-piridonas tricíclicas que presenten una mejor tractabilidad química.

En el Capítulo 3.4 se ha llevado a cabo un trabajo de exploración de los derivados cíclicos de las 4(1*H*)-piridonas. Así una nueva familia de 4(1*H*)-piridonas tricíclicas, fácilmente escalable, ha sido identificada y permitió llevar a cabo el estudio de relación estructura-actividad (SAR) que no había podido ser completado anteriormente con las 1-azafluorenonas.

Como resultado de este trabajo se prepararon más de cincuenta derivados que permitieron explorar el efecto de la cadena lipófila en la actividad antimalárica, la cual permitía modular tanto la potencia y selectividad, como las propiedades físico-químicas de la molécula.

La química médica reportada en el Capítulo 3.4 ha validado las 4(1*H*)-piridonas tricíclicas como un nuevo quimio tipo dentro de las piridonas siendo también inhibidores de *P. falciparum* en el complejo III del citocromo *bc1*. En concreto, una de las subseries

tricíclicas dio lugar a los derivados más potentes y más selectivos frente al citocromo *bc1* humano dentro de las 4(1*H*)-piridonas, tanto clásicas y como cíclicas descritas hasta el momento.

Los modelos de docking y cálculos teóricos permitieron identificar un ligero giro de la estructura dentro de la proteína. Esta distinta interacción dentro del centro activo, así como los resultados obtenidos en los estudios de farmacología y actividad en cepas resistentes a las 4(1*H*)-piridonas clásicas, apuntan a que esta nueva familia de 4(1*H*)-piridonas tricíclicas podrían presentar un distinto modo de unión a la proteína del complejo *bc1*. Este resultado abre una puerta a poder mitigar los problemas de selectividad y toxicidad encontrados con las 4(1*H*)-piridonas clásicas.

El trabajo descrito en esta tesis ha dado lugar a las siguientes publicaciones:

1. - Bueno, J. M.; Manzano, P.; García, M. C.; Chicharro, J.; Puente, M.; Lorenzo, M.; García, A.; Ferrer, S.; Gómez, R. M.; Fraile, M. T.; Lavandera, J. L.; Fiandor, J. M.; Vidal, J.; Herreros, E.; Gargallo-Viola, D. Potent Antimalarial 4-Pyridones with Improved Physico-Chemical Properties. *Bioorganic Med. Chem. Lett.* **2011**, *21* (18), 5214–5218
2. - Bueno, J. M.; Fernandez-Molina, J.; Leon, M.L.; Mallo, A.; Manzano, M.P. 4(1H)-pyridones derivatives and their use as antimalaria agents. WO 2010/081904
3. - Bueno, J. M.; Fiandor, J. M.; Puente-Felipe, M.; Chicharro-Gonzalo, Jesus, Kusalakumari sukumar, S. K.; Maleki, M. Phosphate Ester of a 4-Pyridone derivative and its use in the chemotherapy of parasitic infections. WO 2010/094738
4. - Puente-Felipe, M; Esther Carranza, Silvia Padilla, Jaume Vidal, Maria J. Almela, Adolfo García-Perez, Maria J. Lafuente, Sara Prats, Laura M. Sanz, Cristina de Cozar, M. Belén Jimenez-Díaz, Esperanza Herreros, José M. Bueno and Pilar Manzano, \* Tricyclic Benzothienopyridinones: A Novel Chemotype within Antimalarial 4(1H)-pyridones. *Publication pending to be authorized.*

---

## **5 EXPERIMENTAL SECTION**

---

## 5.1 Instrumentation

All reagents were obtained commercially and used directly without further purification, unless stated otherwise. All solvents were obtained dry from commercial suppliers. After aqueous work-up of reaction mixtures, organic solutions were routinely dried with anhydrous magnesium sulphate. Solvents were removed under reduced pressure using a diaphragm pump or water aspirator with a Buchi rotary evaporator. Additional traces of solvent were removed by drying under high vacuum at 0.5 mmHg using a rotary oil pump. Reactions under microwave irradiation were performed using a Biotage Initiator microwave with a maximum pressure of 220 psi.

Flash chromatography was carried out using prepacked Isolute Flash or Biotage silica gel columns as the stationary phase and analytical grade solvents as the eluent unless otherwise stated. Flash thin layer chromatography (TLC) was performed using precoated plates (Merck), with the stated solvent system and visualised under U.V. irradiation.

HPLC analyses were carried out on a Dionex HPLC system using a Thermo Electron Corporation Hyperprep HS C18 column (8  $\mu$ M, 250 x 4.6 mm) and diode array as a detector. A gradient of water and acetonitrile (5-95%) was used as a solvent at a flow rate of 1 mL/min for 8 minutes.

Total ion current traces were obtained for electrospray positive and negative ionization (ES+/ES-) on a Waters ZMD 2000. **ESIMS**

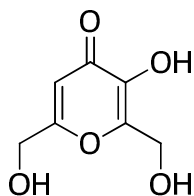
Analytical chromatographic conditions used for the LC/MS analysis e.g. column type, stationary phase particle size and solvents are described for each compound. Common chromatographic parameters were as follows: flow rate, 1.5 mL/min; injection volume, 5  $\mu$ L; column temperature, 30 °C; UV wavelength range, 220-330 nm for ACE and flow rate, 1.5 mL/min; injection volume, 10  $\mu$ L; column temperature, 40 °C; UV wavelength range, 220-330 nm for Sunfire. The purity of all tested compounds was  $\geq$ 95 % using the analytical method described above unless stated otherwise.



$^1\text{H}$  and  $^{13}\text{C}$  NMR spectra were determined on a Varian Unity spectrometer (300 MHz). Chemical shifts were recorded downfield from tetramethylsilane (TMS) defined as 0 in parts per million (ppm). Chemical shifts are reported in parts per million (ppm) in  $\delta$  units and coupling constants ( $J$ ) are reported in Hertz (Hz). In reporting  $^1\text{H}$  and  $^{13}\text{C}$  NMR data the following abbreviations will be used; br (broad), s (singlet), br s (broad singlet), d (doublet), t (triplet), q (quartet), dd (doublet of doublets), dt (doublet of triplets), td (triplet of doublets), ddd (double of double of doublets), and m (multiplet).

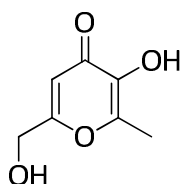
## 5.2 General methods and experimental data

### Preparation of 3-hydroxy-2,6-bis(hydroxymethyl)-4H-pyran-4-one (2).



In a 250 mL round bottom flask were added Kojic acid **1** (Fluka, 10 g) and 1 N NaOH aq. (84 mL, 1.2 eq.). The mixture was cooled (ice/water bath) and 37 % aqueous formaldehyde (Aldrich, 26.8 mL, 1.3 eq.) was added dropwise. After 48 h at room temperature the mixture was cooled down until 0 °C and acidified by adding HCl aq. The precipitated solid was collected by filtration and dried in vacuo to give 9.13 g of the title compound as a yellowish solid. Yield: 75 %.  $^1\text{H NMR}$  (300 MHz,  $\text{CD}_3\text{OD}$ )  $\delta$  6.47 (s, 1H), 4.62 (s, 2H), 4.44 (s, 2H).  $^1\text{H NMR}$  (400 MHz,  $\text{DMSO}-d_6$ )  $\delta$  8.95 (s, 1H), 6.31 (s, 1H), 5.67 (t,  $J=5.94$  Hz, 1H), 5.35 (t,  $J=5.81$  Hz, 1H), 4.40 (d,  $J=5.56$  Hz, 2H), 4.31 (d,  $J=5.81$  Hz, 2H).  $^{13}\text{C NMR}$  (101 MHz,  $\text{DMSO}-d_6$ )  $\delta$  174.7, 168.0, 149.8, 142.1, 109.3, 60.0, 55.5.

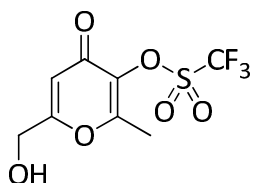
### Preparation of 3-hydroxy-6-(hydroxymethyl)-2-methyl-4H-pyran-4-one (3).



To a suspension of **2** (6.56 g) in water (22.8 mL, 0.6 mL/mmol) at 50 °C was added zinc dust (Panreac, 4.98 g, 2 eq.) and HCl aq. (11.43 mL, 0.3 mL/mmol) dropwise and the mixture heated at 70-80 °C for 5 h. The excess zinc was removed by hot filtration through Celite and the filter cake washed with chilled water. To the aqueous solution was added solid NaCl until a solid separated. This solid was filtered off and dried under vacuum to obtain 3.16 g of the title compound. Yield: 53 %.  $^1\text{H NMR}$  (300 MHz,  $\text{CD}_3\text{OD}$ )  $\delta$  6.43 (d,  $J=0.88$  Hz, 1H), 4.40 (d,  $J=0.88$  Hz, 2H), 2.35 (s, 3H).  $^{13}\text{C NMR}$  (101 MHz,  $\text{DMSO}-d_6$ )

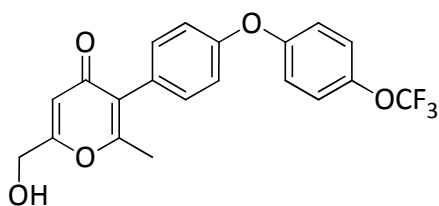
$\delta$  173.6, 167.3, 148.5, 142.3, 109.4, 60.0, 14.4. **ESIMS**  $m/z$ : 157  $[M+H]^+$ . Purity was determined as >95 % by HPLC ( $\lambda$  274 nm), Rt: 0.77 min (Ace C18; 3  $\mu$ ; 30 x 4.6 mm; formic acid 0.1 % pH 2.4 / Acetonitrile).

**Preparation of 6-(hydroxymethyl)-2-methyl-4-oxo-4H-pyran-3-yltrifluoromethane sulfonate (4).**



To a solution of **3** (475 mg) in anhydrous N,N-dimethylformamide (8.3 mL, 2.7 mL/mmol) under a N<sub>2</sub> atmosphere were added potassium carbonate (Aldrich, 497 mg, 1.2 eq.) and N-phenyltrifluoromethanesulfonimide (Fluka, 1.17 g, 1.08 eq.). After stirring for 1 h at room temperature, salts were filtered and washed with tBuOMe. The organic layer was washed with 1 N NH<sub>4</sub>Cl aq. (4x), 10 % Na<sub>2</sub>CO<sub>3</sub> aq. (4x) and then brine, dried over Mg<sub>2</sub>SO<sub>4</sub>, filtered and concentrated under vacuum to obtain 733 mg of the title compound as a yellow oil. Yield: 85 %. **<sup>1</sup>H NMR** (300 MHz, CDCl<sub>3</sub>)  $\delta$  6.57 (d,  $J=0.59$  Hz, 1H), 4.51 (d,  $J=6.59$  Hz, 2H), 2.42 (s, 3H). **ESIMS**  $m/z$ : 289  $[M+H]^+$ . Purity was determined as >95 % by HPLC ( $\lambda$  254 nm), Rt: 2.49 min (Ace C18; 3  $\mu$ ; 30 x 4.6 mm; formic acid 0.1 % pH 2.4 / Acetonitrile).

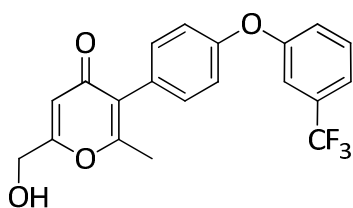
**Preparation of 6-(hydroxymethyl)-2-methyl-3-(4-(4-(trifluoromethoxy)phenoxy)phenyl)-4H-pyran-4-one (5a).**



To a solution of the intermediate **4** (1.45 g) in toluene (15 mL, 3 mL/mmol) and under inert atmosphere was added bis(triphenylphosphine) palladium(II)chloride (Aldrich, 176.5 mg, 0.05 eq.) at room temperature. To this, was added dropwise a solution of 4-(4-trifluoromethoxyphenoxy)phenylboronic acid **11a** (previously prepared in our group 1.95 g, 1.3 eq.) in EtOH (55.86 mL, 7 mL/mmol) and sodium carbonate (2.13 g, 4 eq.). The mixture was heated at 85 °C for 40 min, cooled, filtered through a pad of Celite and evaporated. The crude was dissolved in EtOAc, washed with 1 N NH<sub>4</sub>Cl aq. (1x), H<sub>2</sub>O (1x), NaHCO<sub>3</sub> aq. sat. (1x) and brine (1x), dried (MgSO<sub>4</sub>) and concentrated under vacuum.

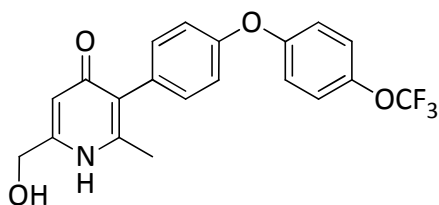
Purification by column chromatography (SiO<sub>2</sub> 100g, EtOAc-hexane) gave the title compound (1.16 g) as a beige solid. Yield: 58 %. <sup>1</sup>H-NMR (300 MHz, CDCl<sub>3</sub>) δ 7.24-7.16 (m, 4H), 7.05 (dd, *J*=7.47, 8.93 Hz, 4H), 6.50 (s, 1H), 4.50 (s, 2H), 2.23 (s, 3H). **ESIMS** *m/z*: 393 [M+H]<sup>+</sup>. Purity was determined as >95 % by HPLC (λ 254 nm), Rt: 3.07 min (Ace C18; 3 μ; 30 x 4.6 mm; formic acid 0.1 % pH 2.4 / Acetonitrile).

**Preparation of 6-(hydroxymethyl)-2-methyl-3-(4-{[3(trifluoromethyl)phenyl]oxy}phenyl)-4H-pyran-4-one (5b).**



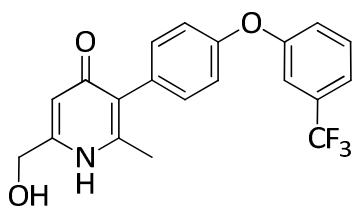
The compound was prepared following the procedure described for Intermediate **6a** but using the boronic acid **11b** as starting material. Compound **5b** was obtained as a yellow solid. Yield: 48 %. <sup>1</sup>H-NMR (300 MHz, CDCl<sub>3</sub>) δ 7.50-7.31 (m, 3H), 7.25-7.20 (m, 3H), 7.09-7.03 (m, 2H), 6.53 (s, 1H), 4.51 (s, 2H), 2.25 (s, 3H). **ESIMS** *m/z*: 377 [M+H]<sup>+</sup>. Purity was determined as >95 % by HPLC (λ 240 nm), Rt: 3.25 min (Ace C18; 3 μ; 30 x 4.6 mm; formic acid 0.1 % pH 2.4 / Acetonitrile).

**Preparation of 6-(hydroxymethyl)-2-methyl-3-(4-(4-(trifluoromethoxy)phenoxy)phenyl)pyridin-4(1H)-one (6a).**



To a solution of the pyranone **5a** (195 mg) in methanol (2 mL) was added commercial 30% aqueous ammonia (Aldrich, 3 mL) with stirring. The reaction was run at 140 °C (max. pressure 16 bar) for 1800 s in a Personal Chemistry Emrys microwave reactor. Reaction was diluted with water and the precipitate filtered and washed with acetonitrile to afford the title compound (92 mg) as a whitish solid. Yield: 48 %. <sup>1</sup>H NMR (300 MHz, DMSO-d<sub>6</sub>) δ 11.07 (br. s., 1H), 7.36 (d, *J*=8.93 Hz, 2H), 7.19 (d, *J*=8.64 Hz, 2H), 7.11 (d, *J*=9.08 Hz, 2H), 7.01 (d, *J*=8.64 Hz, 2H), 6.07 (s, 1H), 5.49 (t, *J*=6.00 Hz, 1H), 4.32 (d, *J*=6.00 Hz, 2H), 2.09 (s, 3H). **ESIMS** *m/z*: 392 [M+H]<sup>+</sup>. Purity was determined as >95 % by HPLC (λ 254 nm), Rt: 2.78 min (Ace C18; 3 μ; 30 x 4.6 mm; formic acid 0.1 % pH 2.4 / Acetonitrile).

**Preparation of 6-(hydroxymethyl)-2-methyl-3-(4-{[3(trifluoromethyl)phenoxy]oxy}phenyl)-pyridin-4(1H)-one (6b).**

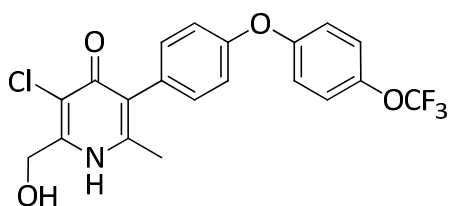


The compound was prepared following the procedure described for Intermediate **6a** but using **5b** as starting material. Compound **6b** was obtained as a white solid.

Yield: 52 %. <sup>1</sup>H-NMR (300 MHz, DMSO-d<sub>6</sub>): 11.21-10.92

(m, 1H), 7.68-7.58 (m, 1H), 7.52-7.46 (m, 1H), 7.36-7.27 (m, 2H), 7.22 (d, *J*=8.49 Hz, 2H), 7.07 (d, *J*=8.49 Hz, 2H), 6.15-6.00 (m, 1H), 5.62-5.39 (m, 1H), 4.33 (br. s., 2H), 2.10 (s, 3H).). **ESIMS** *m/z*: 376 [M+H]<sup>+</sup>. Purity was determined as >95 % by HPLC (λ 271 nm), Rt: 2.66 min (Ace C18; 3 μ; 30 x 4.6 mm; formic acid 0.1 % pH 2.4 / Acetonitrile).

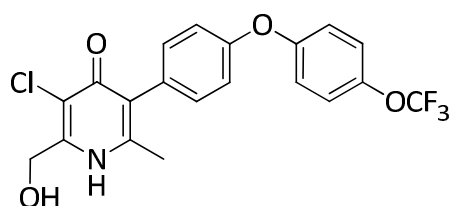
**Preparation of 3-chloro-2-(hydroxymethyl)-6-methyl-5-(4-(4-(trifluoromethoxy)phenoxy)phenyl) pyridin-4(1H)-one (7a).**



To a solution of **6a** (245 mg) in a mixture of dichloromethane/methanol (v/v 2:1) at 0 °C, was added trichloroisocyanuric acid (Aldrich, 58.4 mg, 1.2 eq.). The mixture was stirred at this

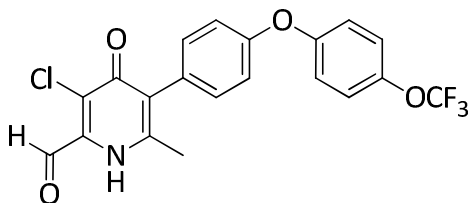
temperature for 60 min. The crude was filtered, concentrated and the mixture obtained purified by column chromatography (SiO<sub>2</sub> 20g, dichloromethane/methanol 5 %) to afford the title compound (123 mg) as a white solid. Yield: 46 %. <sup>1</sup>H NMR (300 MHz, DMSO-d<sub>6</sub>) δ 11.31 (br. s., 1H), 7.41 (d, *J*=8.64 Hz, 2H), 7.24 (d, *J*=8.64 Hz, 2H), 7.16 (d, *J*=8.49 Hz, 2H), 7.06 (d, *J*=9.23 Hz, 2H), 5.91 (br. s., 1H), 4.59 (s, 2H), 2.17 (s, 3H). **ESIMS** *m/z*: 426 [M+H]<sup>+</sup>. Purity was determined as >95 % by HPLC (λ 254 nm), Rt: 3.08 min (Ace C18; 3 μ; 30 x 4.6 mm; formic acid 0.1 % pH 2.4 / Acetonitrile).

**Preparation of 3-chloro-2-(hydroxymethyl)-6-methyl-5-(4-{{3(trifluoromethyl)phenyl}oxy}phenyl)-pyridin-4(1H)-one (7b).**



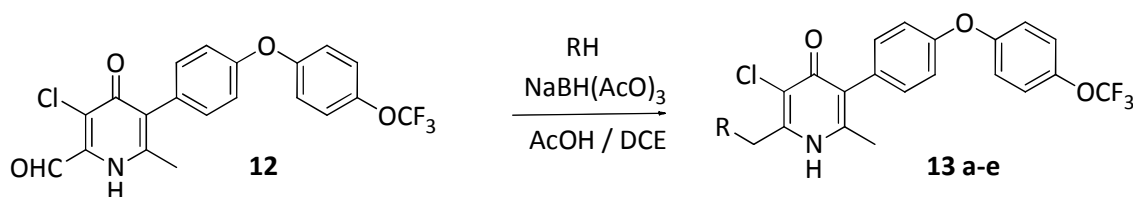
The compound was prepared following the procedure described for Example **7a** but using **6b** as starting material. A final trituration with acetonitrile was required to afford the compound **7b** (85 mg) as a white solid. Yield: 36 %. <sup>1</sup>H-NMR (300 MHz, DMSO-d<sub>6</sub>) δ 11.31 (br. s., 1H), 7.68-7.59 m, 1H), 7.54-7.44 (m, 1H), 7.37-7.30 (m, 2H), 7.27-7.19 (m, 2H), 7.12-7.05 (m, 2H), 5.93-5.83 (m, 1H), 4.59 (d, *J*=4.98 Hz, 2H), 2.16 (s, 3H). <sup>13</sup>C NMR (101 MHz, DMSO-d<sub>6</sub>) δ 170.9, 157.8, 155.0, 146.1, 135.86, 132.9, 132.0, 131.9, 126.1, 125.5, 122.7, 120.3, 119.0(2C), 118.7, 118.8, 115.2(q), 58.9, 18.2. ESIMS *m/z*: 410 [M+H]<sup>+</sup>. Purity was determined as >95 % by HPLC (λ 254 nm), Rt: 2.96 min (Ace C18; 3 μ; 30 x 4.6 mm; formic acid 0.1 % pH 2.4 / Acetonitrile).

**Preparation of 3-chloro-6-methyl-4-oxo-5-[4-{{4-((trifluoromethyl)oxy)phenyl}oxy}phenyl]-1,4-dihydro-2-pyridinecarbaldehyde (12).**



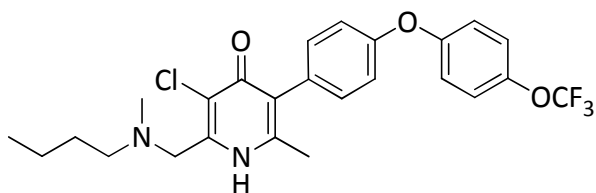
To a suspension of **7a** (0.422 g) in dichloromethane (4.25 mL, 4.25 mL/mmol) was added under argon atmosphere anhydrous DMSO (3 mL, 2 mL/mmol). The resulting solution was cooled in an ice-water bath and triethylamine (Aldrich, 1 mL, 1.06 mL/mmol) was added followed by sulfur trioxide-pyridine 15 complex (Aldrich, 0.788 g, 5 eq.). The mixture was allowed to warm to room temperature overnight. After 20 h of stirring the mixture was washed with H<sub>2</sub>O (5x), dried over Na<sub>2</sub>SO<sub>4</sub> and concentrated to dryness. 380 mg of the title compound were obtained as a yellow powder. This compound was used in next steps without further purification.

• **General method for the reductive aminations:**



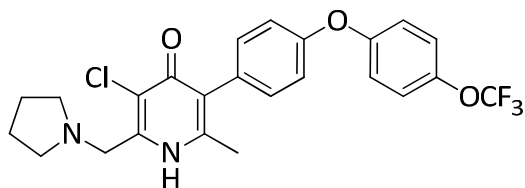
To a solution of 3-chloro-6-methyl-4-oxo-5-[4-(4-(trifluoromethyl)oxy)phenyl]oxyphenyl]-1,4-dihydro-2-pyridinecarbaldehyde (**12**) (1 eq.) in DCE (4.6 mL/mmol) and under N<sub>2</sub> atmosphere, the corresponding amine (1.1 eq.) and Acetic acid (1.0 eq.) were added at room temperature. After 30 min, sodium triacetoxyborohydride (Acros, 1.5 eq.) was added. After 2 h, the reaction was treated at room temperature with sat NaHCO<sub>3</sub> aq. and then extracted with AcOEt (x3). Organic phases were combined and washed with brine (x1), dried over Na<sub>2</sub>SO<sub>4</sub>, filtered and concentrated. Purification was carried out by column chromatography (NH<sub>2</sub>·SiO<sub>2</sub> 5g, eluent: DCM, 100 %) to give the title compound.

**Preparation of 2-((butyl(methyl)amino)methyl)-3-chloro-6-methyl-5-(4-(4-(trifluoromethoxy)phenoxy)phenoxy)phenyl)pyridin-4(1H)-one (13a).**



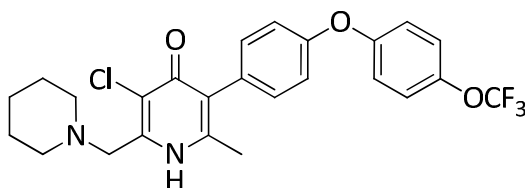
The compound was prepared following the general procedure for reductive amination using *n*-methylbutylamine (Aldrich, 7.3  $\mu$ l, 0.061 mmol, 1.1 eq.). Compound **13a** was obtained as a white solid. Yield: 36 %. <sup>1</sup>H NMR (300 MHz, CDCl<sub>3</sub>)  $\delta$  7.26 (d, *J*=8.64 Hz, 2H), 7.19 (d, *J*=9.08 Hz, 2H), 7.06 (d, *J*=8.93 Hz, 2H), 7.03 (d, *J*=8.35 Hz, 2H), 3.69 (s, 2H), 2.57 (t, *J*=7.32 Hz, 2H), 2.40 (s, 3H), 2.23 (s, 3H), 1.59-1.46(m, 2H), 1.43-1.31 (m, 2H), 0.96 (t, *J*=7.32 Hz, 3H). **ESIMS** *m/z*: 495 [M+H]<sup>+</sup>; 493 [M-H]<sup>-</sup>. Purity was determined as >95 % by HPLC ( $\lambda$  240 nm), Rt: 2.92 min (Ace C18; 3  $\mu$ ; 30 x 4.6 mm; formic acid 0.1 % pH 2.4 / Acetonitrile).

**Preparation of 3-chloro-6-methyl-2-(pyrrolidin-1-ylmethyl)-5-(4-(4-(trifluoromethoxy)phenoxy)phenyl)pyridin-4(1H)-one (13b).**



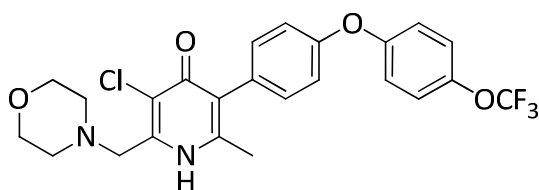
The compound was prepared following the general procedure for reductive amination and using pyrrolidine (Aldrich, 22.53  $\mu$ l, 0.267 mmol, 1.1 eq.). Compound **13b** was obtained as a white solid. Yield: 43 %.  $^1\text{H NMR}$  (300 MHz, DMSO- $d_6$ )  $\delta$  11.80-10.75 (br. s, 1H), 7.41 (d,  $J=9.23$  Hz, 2H), 7.24 (d,  $J=8.79$  Hz, 2H), 7.16 (d,  $J=9.08$  Hz, 2H), 7.05 (d,  $J=8.35$  Hz, 2H), 3.74 (s, 2H), 2.59 (br. s., 4H), 2.15 (s, 3H), 1.74 (br. s., 4H). **ESIMS**  $m/z$ : 479  $[\text{M}+\text{H}]^+$ ; 477  $[\text{M}-\text{H}]^-$ . Purity was determined as >95 % by HPLC ( $\lambda$  230 nm),  $R_t$ : 2.67 min (Ace C18; 3  $\mu$ ; 30 x 2.0 mm; formic acid 0.1 % pH 2.4 / Acetonitrile).

**Preparation of 3-chloro-6-methyl-2-(piperidin-1-ylmethyl)-5-(4-(4-(trifluoromethoxy)phenoxy)phenyl)pyridin-4(1H)-one (13c).**



The compound was prepared following the general procedure for reductive amination and using piperidine (Aldrich, 17.96  $\mu$ l, 0.182 mmol, 1.1 eq.). Compound **13c** was obtained as a white solid. Yield: 32 %.  $^1\text{H NMR}$  (300 MHz, DMSO- $d_6$ )  $\delta$  11.66-10.89 (br. s, 1H), 7.41 (d,  $J=9.23$  Hz, 2H), 7.24 (d,  $J=8.35$  Hz, 2H), 7.16 (d,  $J=8.64$  Hz, 2H), 7.05 (d,  $J=8.49$  Hz, 2H), 3.56 (s, 2H), 2.15 (s, 3H), 1.61-1.48 (m, 4H), 1.40 (br. s., 2H). **ESIMS**  $m/z$ : 493  $[\text{M}+\text{H}]^+$ . Purity was determined as >95% by HPLC ( $\lambda$  254 nm),  $R_t$ : 2.75 min (Ace C18; 3  $\mu$ ; 30 x 4.6 mm; formic acid 0.1 % pH 2.4 / Acetonitrile).

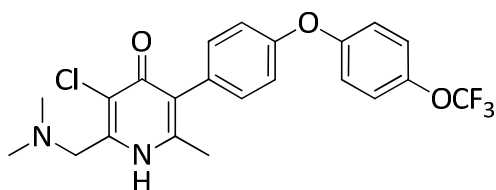
**Preparation of 3-chloro-6-methyl-2-(morpholinomethyl)-5-(4-(4-(trifluoromethoxy)phenoxy)phenyl)pyridin-4(1H)-one (13d).**



The compound was prepared following the general procedure for reductive amination and using morpholine (Aldrich, 24.22  $\mu$ l, 0.277 mmol, 1.1 eq.). Compound

**13d** was obtained as a white solid. Yield: 48 %.  $^1\text{H NMR}$  (300 MHz, DMSO- $d_6$ )  $\delta$  11.34 (br. s, 1H), 7.41 (d,  $J=8.79$  Hz, 2H), 7.24 (d,  $J=8.79$  Hz, 2H), 7.16 (d,  $J=8.93$  Hz, 2H), 7.05 (d,  $J=8.79$  Hz, 2H), 3.63-3.58 (m, 6H), 2.55-2.43 (m, 4H), 2.15 (s, 3H). **ESIMS**  $m/z$ : 495  $[\text{M}+\text{H}]^+$ . Purity was determined as >95 % by HPLC ( $\lambda$  240 nm), Rt: 3.03 min (Ace C18; 3  $\mu$ ; 30 x 4.6 mm; formic acid 0.1 % pH 2.4 / Acetonitrile).

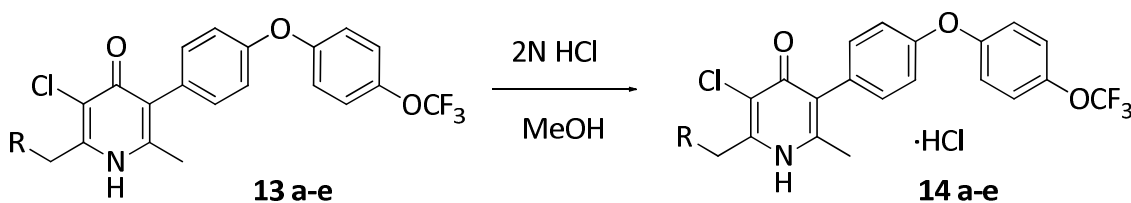
**Preparation of 3-chloro-2-((dimethylamino)methyl)-6-methyl-5-(4-(4-(trifluoromethoxy)phenoxy)phenyl)pyridin-4(1H)-one (13e).**



The compound was prepared following the general procedure for reductive amination and using dimethylamine in THF (Aldrich, 138  $\mu$ l, 0.277 mmol, 1.1 eq.). Compound **13e** was

obtained as a white solid. Yield: 35 %.  $^1\text{H NMR}$  (300 MHz, DMSO- $d_6$ )  $\delta$  12.01-10.78 (m, 1H), 7.42 (d,  $J=8.79$  Hz, 2H), 7.23 (d,  $J=8.79$  Hz, 2H), 7.16 (d,  $J=9.37$  Hz, 2H), 7.05 (d,  $J=8.79$  Hz, 2H), 3.56 (s, 2H), 2.27 (s, 6H), 2.15 (s, 3H). **ESIMS**  $m/z$ : 453  $[\text{M}+\text{H}]^+$ . Purity was determined as >95 % by HPLC ( $\lambda$  254 nm), Rt: 2.61 min (Ace C18; 3  $\mu$ ; 30 x 4.6 mm; formic acid 0.1 % pH 2.4 / Acetonitrile).

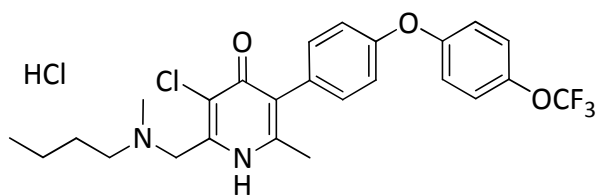
- General method for the hydrochloride salt formation:**



The corresponding amine was suspended in MeOH (1 mL/mmol) and a 2 N HCl solution (2.2 eq.) was added. The solution obtained was stirred at room temperature for 2 h and then concentrated *in vacuo* to leave the desired compound as a hydrochloride salt.



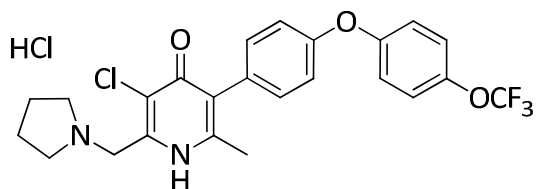
**Preparation of 2-((butyl(methyl)amino)methyl)-3-chloro-6-methyl-5-(4-(4-(trifluoromethoxy)phenoxy)phenyl)pyridin-4(1H)-one hydrochloride (14a).**



The compound was prepared from **13a** following the general procedure for the hydrochloride salt formation.

Compound **14a** was obtained as a white solid. Quant. yield. <sup>1</sup>H NMR (300 MHz, CDCl<sub>3</sub>) δ 11.73 (br. s., 1H), 7.21 (d, *J*=8.64 Hz, 4H), 7.11-7.00 (m, 4H), 4.77 (br. s., 1H), 4.62 (br. s., 1H), 3.37-3.13 (m, 2H), 3.04-2.89 (m, 3H), 2.43 (s, 3H), 1.91 (br. s., 2H), 1.47 (br. s., 2H), 1.00 (t, *J*=7.10 Hz, 3H). <sup>13</sup>C NMR (101 MHz, DMSO-*d*<sub>6</sub>) δ 155.9(2C), 144.2(2C), 132.6(2C), 130.7(2C), 126.5, 123.5(2C), 121.8, 120.6(2C), 119.3, 118.8(2C), 56.3(2C), 49.0, 25.9, 19.8, 14.0(2C). ESIMS *m/z*: 495 [M+H]<sup>+</sup>. Purity was determined as >95% by HPLC (λ 254 nm), Rt: 2.91 min (Ace C18; 3 μ; 30 x 4.6 mm; formic acid 0.1 % pH 2.4 / Acetonitrile).

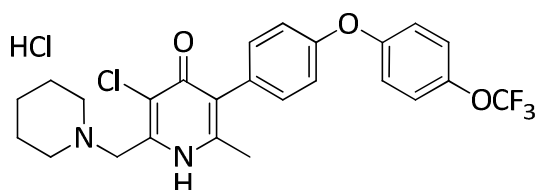
**Preparation of 3-chloro-6-methyl-2-(pyrrolidin-1-ylmethyl)-5-(4-(4-(trifluoromethoxy)phenoxy)phenyl)pyridin-4(1H)-one hydrochloride (14b).**



The compound was prepared from **13b** following the general procedure for the hydrochloride salt formation. Compound **14b** was obtained as a white solid. Quant.

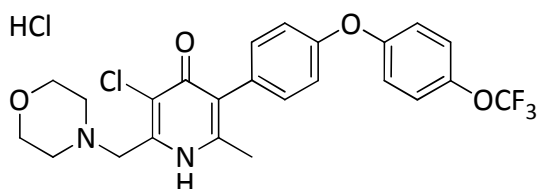
yield. <sup>1</sup>H NMR (300 MHz, DMSO-*d*<sub>6</sub>) δ 10.55 (br. s., 1H), 7.43 (d, *J*=9.08 Hz, 2H), 7.26 (d, *J*=8.64 Hz, 2H), 7.18 (d, *J*=9.23 Hz, 2H), 7.10 (d, *J*=8.49 Hz, 2H), 4.64 (br. s., 2H), 3.46 (br. s., 4H), 2.22 (s, 3H), 2.01 (br. s., 4H). <sup>13</sup>C NMR (101 MHz, DMSO-*d*<sub>6</sub>) δ 155.9(2C), 144.2(2C), 132.6(2C), 130.7(2C), 126.5, 123.5(2C), 121.8, 120.6(2C), 119.3, 118.8(2C), 54.4, 26.8(2C), 23.1(2C), 18.7. ESIMS *m/z*: 479 [M+H]<sup>+</sup>. Purity was determined as >95% by HPLC (λ 254 nm), Rt: 2.70 min (Ace C18; 3 μ; 30 x 4.6 mm; formic acid 0.1 % pH 2.4 / Acetonitrile).

**Preparation of 3-chloro-6-methyl-2-(piperidin-1-ylmethyl)-5-(4-(4-(trifluoromethoxy) phenoxy)phenyl)pyridin-4(1H)-one hydrochloride (14c).**



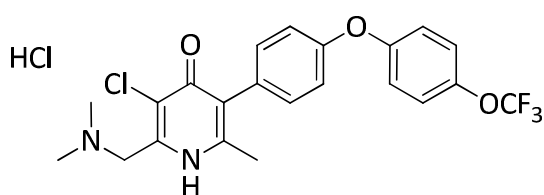
The compound was prepared from **13c** following the general procedure for the hydrochloride salt formation. Compound **14c** was obtained as a whitish solid. Quant. yield.  $^1\text{H NMR}$  (300 MHz, DMSO- $d_6$ )  $\delta$  12.82-12.10 (m, 1H), 10.29 (br. s., 1H), 7.42 (d,  $J=9.37$  Hz, 2H), 7.26 (d,  $J=8.79$  Hz, 2H), 7.18 (d,  $J=9.08$  Hz, 2H), 7.09 (d,  $J=8.64$  Hz, 2H), 4.52 (s, 2H), 3.50-3.11 (m, 4H), 2.22 (s, 3H), 1.82 (br. s., 4H), 1.62 (br. s., 2H).  $^{13}\text{C NMR}$  (101 MHz, DMSO- $d_6$ )  $\delta$  155.9, 155.9, 144.3(2C), 132.6(2C), 130.7(2C), 126.5(2C), 123.5(2C), 121.85, 120.6(2C), 119.3, 118.8(2C), 54.5, 53.1(2C), 22.9(2C), 21.4, 18.81. **ESIMS**  $m/z$ : 493  $[\text{M}+\text{H}]^+$ . Purity was determined as >95 % by HPLC ( $\lambda$  254 nm),  $R_t$ : 2.74 min (Ace C18; 3  $\mu$ ; 30 x 4.6 mm; formic acid 0.1 % pH 2.4 / Acetonitrile).

**Preparation of 3-chloro-6-methyl-2-(morpholinomethyl)-5-(4-(4-(trifluoromethoxy) phenoxy)phenyl)pyridin-4(1H)-one hydrochloride (14d).**



The compound was prepared from **13d** following the general procedure for the hydrochloride salt formation. Compound **14d** was obtained as a white solid. Quant. Yield.  $^1\text{H NMR}$  (300 MHz, DMSO- $d_6$ )  $\delta$  11.48-10.30 (m, 1H), 7.43 (d,  $J=8.49$  Hz, 2H), 7.26 (d,  $J=8.64$  Hz, 2H), 7.18 (d,  $J=8.93$  Hz, 2H), 7.09 (d,  $J=8.64$  Hz, 2H), 4.57 (s, 2H), 3.90 (br. s., 4H), 3.40 (br. s., 4H), 2.22 (s, 3H).  $^{13}\text{C NMR}$  (101 MHz, DMSO- $d_6$ )  $\delta$  155.9, 155.9, 144.2(2C), 132.6(2C), 130.7(2C), 126.4, 123.5(2C), 121.8, 120.6(2C), 119.3, 118.8(2C), 63.09(2C), 61.63, 52.4(2C), 26.8. **ESIMS**  $m/z$ : 495  $[\text{M}+\text{H}]^+$ . Purity was determined as >95 % by HPLC ( $\lambda$  254 nm),  $R_t$ : 2.58 min (Ace C18; 3  $\mu$ ; 30 x 4.6 mm; formic acid 0.1 % pH 2.4 / Acetonitrile).

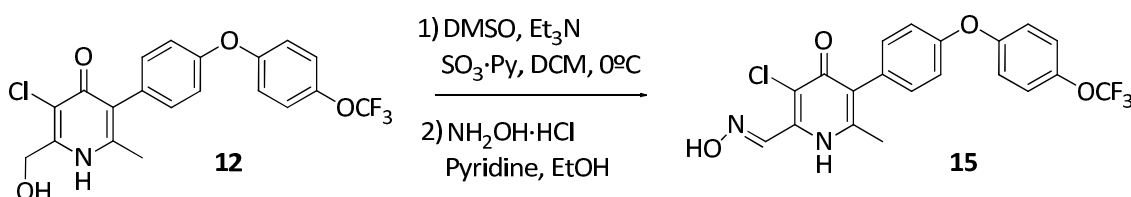
**Preparation of 3-chloro-2-((dimethylamino)methyl)-6-methyl-5-(4-(4-(trifluoromethoxy)phenoxy)phenyl)pyridin-4(1H)-one hydrochloride (14e)**



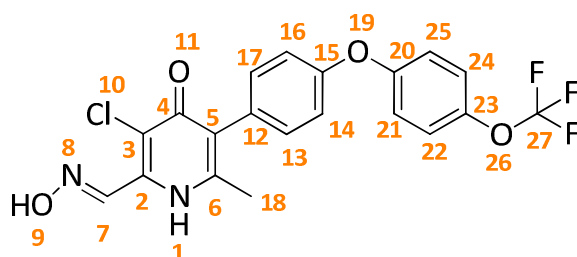
The compound was prepared from **13e** following the general procedure for the hydrochloride salt formation. Compound **14e** was obtained as a white solid. Quant.

Yield. <sup>1</sup>H NMR (300 MHz, DMSO-d<sub>6</sub>) δ 10.32 (br. s., 1H), 7.41 (dd, *J*=1.03, 8.05 Hz, 2H), 7.26 (dd, *J*=2.20, 8.79 Hz, 2H), 7.16 (dd, *J*=2.20, 9.08 Hz, 2H), 7.08 (dd, *J*=2.12, 8.71 Hz, 2H), 4.55 (s, 2H), 2.90 (s, 6H), 2.20 (d, *J*=2.20 Hz, 3H). <sup>13</sup>C NMR (101 MHz, DMSO-d<sub>6</sub>) δ 155.9(2C), 144.2(2C), 132.6(2C), 130.7 (2C), 126.5, 123.5(2C), 121.8, 120.6(2C), 119.3, 118.8(2C), 43.35(2C), 26.8, 17.62. ESIMS *m/z*: 453 [M+H]<sup>+</sup>. Purity was determined as >95 % by HPLC (λ 254 nm), Rt: 2.63 min (Ace C18; 3 μ; 30 x 4.6 mm; formic acid 0.1 % pH 2.4 / Acetonitrile).

• **Synthesis of the GW844520 hydroxyl oxime:**



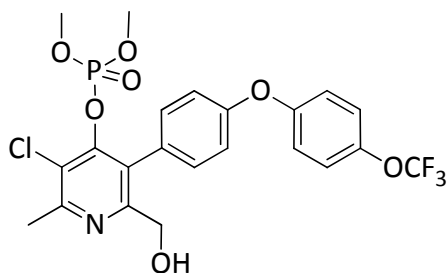
**Preparation of 3-chloro-6-methyl-4-oxo-5-[4-({4-[(trifluoromethyl)oxy]phenyl}oxy)phenyl]-1,4-dihydro-2-pyridinecarbaldehyde oxime (15).**



To a solution of (3-chloro-2-(hydroxymethyl)-6-methyl-5-[4-({4-[(trifluoromethyl)oxy]phenyl}oxy)phenyl]-pyridin-4(1H)-one) (**12**) (190 mg) in DCM (2 mL, 4.25 mL/mmol) was added dimethylsulfoxide (0.894 mL, 2 mL/mmol) under inert atmosphere (N<sub>2</sub>). The

resulting solution was cooling in ice/water bath and triethylamine (Aldrich, 0.474 mL, 1.06 mL/mmol) and then sulfur trioxide pyridine complex (Aldrich, 355 mg, 5eq.) was added portionwise. The mixture was allowed to warm to room temperature over 20 h. The resulting crude was washed with H<sub>2</sub>O (x5) and the organic solution dried over sodium sulphate. The solvent was eliminated under vacuum to give the aldehyde (170 mg) as a yellow solid. The crude pyridinecarbaldehyde was dissolved in EtOH under inert atmosphere. Then hydroxylamine hydrochloride (Aldrich, 139 mg, 5 eq.) and pyridine (Aldrich, 0.139 mL, 2 eq.) were added and the mixture heated under reflux for 2 h. After this, the crude solid was cooled, diluted with water, filtered and washed several times with water. The solid was stirred in acetonitrile for 2 h and then filtered, washed with more acetonitrile and dried to afford the title compound (50 mg) as a pale solid. Yield: 29 % <sup>1</sup>H NMR (400 MHz, CDCl<sub>3</sub>) δ 12.35 (s, 1H, OH), 11.52 (s, 1H, NH), 8.33 (s, 1H, CH-7), 7.42 (d, *J*=8.6 Hz, 2H, CH-25 and CH-21), 7.25 (d, *J*=8.8 Hz, 2H, 17CH and CH-13), 7.16 (d, *J*=9.1 Hz, 2H, CH-24 and CH-22), 7.06 (d, *J*=8.6Hz, 2H, CH-16 and CH-14), 2.18 (s, 3H, CH<sub>3</sub>-18). <sup>13</sup>C NMR (101 MHz, DMSO-d<sub>6</sub>) δ 170.6 (C-4), 155.5 (C-20), 155.1 (C-15), 144.8 (C-6), 143.7 (C-23), 141.0 (CH-7), 136.6 (C-2), 132.2 (CH-13 and CH-17), 130.7 (C-12), 125.9 (C-5), 122.9(CH-21 and CH-25), 121.8 (C-3), 120.0 (CF<sub>3</sub>), 119.9 (CH-24 and CH-22), 118.2 (CH-16 and CH-14), 17.9 (CH<sub>3</sub>-18). **ESIMS** *m/z*: 439 [M+H]<sup>+</sup>. Purity was determined as >95 % by HPLC (λ 254 nm), Rt: 3.19 min (Ace C18; 3 μ; 30 x 4.6 mm; formic acid 0.1 % pH 2.4 / Acetonitrile). Proton and carbon assignment for compound **15** was based on HMQC and HMBC spectra analysis (see Appendix I).

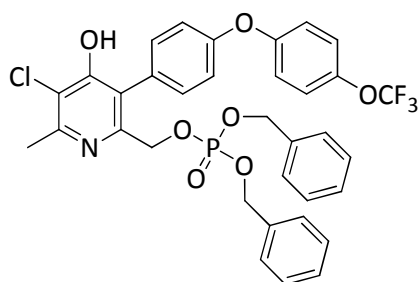
**Preparation of 3-chloro-6-(hydroxymethyl)-2-methyl-5-(4-(4-(trifluoromethoxy)phenoxy)phenyl)pyridin-4-yl dimethyl phosphate (16)**



GSK932121A (100 mg) was suspended in Dichloromethane (DCM) (2.5 mL) in a 25 mL round-bottomed flask under N<sub>2</sub> atmosphere. DMAP (Aldrich, 1.4 mg, 0.1 eq.) was added and the mixture was stirred for a few min. Finally, Et<sub>3</sub>N (Fluka, 0.098 mL, 3 eq.) and (MeO)<sub>2</sub>POCl (Aldrich, 0.038 mL, 2.5 eq.) were added

successively. 2h later reaction was allowed to react at rt and was diluted with Dichloromethane (DCM) (10 mL), washed with sat NH<sub>4</sub>Cl aq. (x3) and brine. The organic layer was dried over MgSO<sub>4</sub>, filtered and concentrated to lead a colorless oil. Crude sample was loaded in dichloromethane and purified on silica (Si) 2 g using a 0-100 % ethyl acetate-cyclohexane over 10 min to obtain the required product as a colorless (865 mg). Yield 65 %. <sup>1</sup>H NMR (300 MHz, DMSO-d<sub>6</sub>) δ 7.42 (d, *J*=8.64 Hz, 2H), 7.36 (d, *J*=8.35 Hz, 2H), 7.15 (dd, *J*=4.03, 8.42 Hz, 4H), 5.08 (t, *J*=5.60 Hz, 1H), 4.21 (d, *J*=5.57 Hz, 2H), 3.49 (s, 3H), 3.45 (s, 3H), 2.63 (s, 3H). **ESIMS** m/z: 534 [M+H]<sup>+</sup>. Purity was determined as >95 % by HPLC (λ 241 nm), Rt: 3.20 min (Sunfire 3.5 μ C18 4.6 x 50 mm; formic acid 0.1 % pH 2.4 / Acetonitrile).

**Preparation of Dibenzyl((5-chloro-4-hydroxy-6-methyl-3-(4-(4-(trifluoromethoxy)phenoxy) phenyl)pyridin-2-yl)methyl) phosphate (17)**



**Method A:** Table 3.7, Entry 9

GSK932121A (0.5 g), dibenzyl phosphate (Aldrich, 0.980 g, 3 eq.) and PPh<sub>3</sub> (0.924 g, 3 eq.) were suspended in dry Tetrahydrofuran (THF) (33 mL, 28 mL/mmol) under argon atmosphere. Diethyl azodicarboxylate (Fluka, 0.646 mL, 3 eq.) in Tetrahydrofuran (THF) (7 mL, 2 mL/mmol) was then added dropwise over 10 min and then stirred at rt for 24 h. Reaction mixture was evaporated under vacuo and the residue (3.4 g) was purified on a 70 g SPE silica cartridge, eluting manually with a step gradient 5-10 % Hexane-nBuOH. Desired compound was isolated as a white solid (0.524 g). Yield 65 %. <sup>1</sup>H NMR (300 MHz, DMSO-d<sub>6</sub>) δ 11.99 (br. s., 1H), 7.42-7.16 (m, 14H), 7.13-7.05 (m, 2H), 7.01-6.94 (m, 2H), 4.93 (d, *J*=7.76 Hz, 4H), 4.80 (d, *J*=6.88 Hz, 2H), 2.41 (s, 3H). **ESIMS** m/z: 686 [M+H]<sup>+</sup>. Purity was determined as >95 % by HPLC (λ 273 nm), Rt: 2.28 min (Sunfire 3.5 μ C18 4.6 x 50 mm; formic acid 0.1 % pH 2.4 / Acetonitrile).

**Method B:** Table 3.7, Entry 10

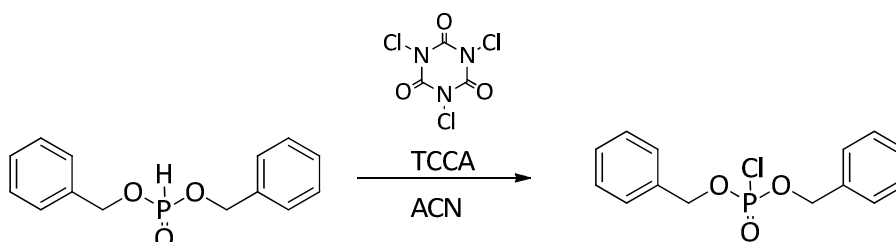
A suspension of GSK932121A (0.5 g, 1.174 mmol) in Tetrahydrofuran (THF) (35.1 mL) was stirred under nitrogen at rt and neat sodium hydride (0.141 g, 3.52 mmol) was added in one charge. The reaction mixture was stirred at rt for 30 min. This suspension was then cooled down until 0 °C and a solution of (BnO)<sub>2</sub>P(O)Cl in Tetrahydrofuran (THF) (2.336 mL), previously prepared in the laboratory, was added. A few minutes later the crude was allowed to reach rt and the suspension was completely dissolved. 24 h later, only diphosphate derivative and monophosphate derivative (-CH<sub>2</sub>O-P(OBn)<sub>2</sub>) were detected. The reaction mixture was partitioned between ethyl acetate and 2M hydrochloric acid. The organic phase was isolated and then was washed with saturated NaHCO<sub>3</sub> aq. and brine, dried over Na<sub>2</sub>SO<sub>4</sub> and evaporated in vacuum to give the crude product as a pale yellow solid. This crude was triturated with TBME and a white solid was obtained. This solid was filtered to lead the title compound (335 mg) as a white solid. Yield: 40 %.

**Method C:** Table 3.7, Entry 11

A suspension of GSK932121A (0.213 g, 0.500 mmol) in Tetrahydrofuran (THF) (12.83 mL) was stirred under nitrogen at rt and neat sodium hydride (0.060 g, 1.501 mmol) was added in one charge. The reaction mixture was stirred at rt for 30 min. This suspension was then cooled down until 0 °C and a solution of (BnO)<sub>2</sub>P(O)Cl in Tetrahydrofuran (THF) (2.57 mL), previously prepared, was added. A few minutes later the crude was allowed to reach rt and the suspension was completely dissolved. Desired monophosphate and diphosphate derivatives were detected 1.5 h later, remainder undesired monophosphate was still present. 4 h later no progression was observed so extra sodium hydride (0.020 g, 1 eq.) was added. 24 h later undesired monophosphate was not detected so NaOH (5mL, 10.00 mmol) was added to obtain the monophosphate prodrug by decomposition of the corresponding diphosphate derivative. 24h later, only the desired monophosphato derivative was detected. The reaction mixture was partitioned between ethyl acetate and 2M HCl aq. The organic phase was isolated and then was washed with saturated NaHCO<sub>3</sub> aq and brine, dried over Na<sub>2</sub>SO<sub>4</sub> and evaporated in

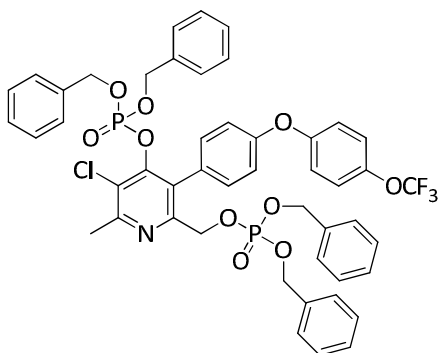
vacuum to give the crude product as a pale yellow gum. This crude was triturated with TBME and a white solid was obtained. This solid was filtered and the title compound was recovered as a white solid in 70 % yield.

- **General method for the preparation of dibenzyl phosphorochloridate (BnO)<sub>2</sub>P(O)Cl:**



To a solution of trichloroisocyanuric acid (Aldrich, 0.338 eq.) in acetonitrile (0.332 mol/l) stirred under nitrogen at 25 °C was added dropwise a solution of dibenzyl phosphite (BnO)<sub>2</sub>P(O)H (Aldrich, 1 eq.) in acetonitrile (0.332 mol/l) to give a yellow solution. The reaction mixture was stirred at rt for 15 min and a white solid appear (isocyanuric acid). This white solid was removed through a nylon filter and the solution containing dibenzyl phosphorochloridate was used for further reactions without isolation or purification.

**Preparation of {4-{{bis[(phenylmethyl)oxy]phosphoryl}oxy)-5-chloro-6-methyl-3-[4-{{4-[(trifluoromethyl)oxy]phenyl}oxy]phenyl}-2-pyridinyl]methyl bis(phenylmethyl) phosphate (18)**

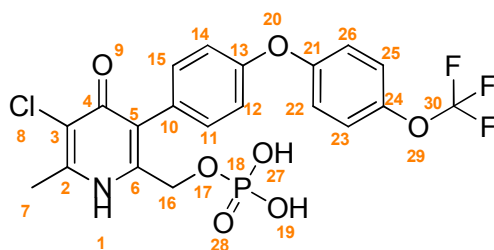


Using **method B** (Table 3.7, Entry 10) for the synthesis of compound **17**, the tittle compound was isolated as a side product from the TBME mother liquous which were concentrated to obtain a yellow oil. The crude compound was dissolved in dichloromethane and purified on silica (Si) 5 g using a 0-50 % ethyl acetate-cyclohexane gradient.

The appropriate fractions were combined and evaporated in vacuo to give the required product as colorless oil (73 mg). Yield 6 %. <sup>1</sup>H NMR (300 MHz, DMSO-d<sub>6</sub>) δ 40-

7.16 (m, 24H), 7.01 (d,  $J=8.64$  Hz, 2H), 6.91 (d,  $J=9.08$  Hz, 2H), 4.94 (d,  $J=7.76$  Hz, 4H), 4.85-4.68 (m, 6H), 2.58 (s, 3H). **ESIMS**  $m/z$ : 946  $[M+H]^+$ . Purity was determined as >95 % by HPLC ( $\lambda$  270 nm), Rt: 4.26 min (Sunfire 3.5  $\mu$  C18 4.6 x 50 mm; ammonium acetate 0.05 % pH 7 / Acetonitrile).

**Preparation of (5-chloro-4-hydroxy-6-methyl-3-(4-(4-(trifluoromethoxy)phenoxy)phenyl)pyridin-2-yl)methyl dihydrogen phosphate (19)**

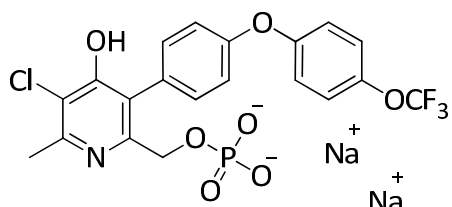


To a solution of dibenzyl((5-chloro-4-hydroxy-6-methyl-3-(4-(4-(trifluoromethoxy)phenoxy)phenyl)pyridin-2-yl)methyl)phosphate **17** (3 g) and 1,4-cyclohexadiene (21.72 mL, 52.5 eq.) in Methanol (3.56 L) was added 10 % Palladium on activated charcoal (0.465 g, 0.1eq). The mixture was stirred at rt under nitrogen atmosphere. 1.5 h later reaction was finished. Palladium on activated charcoal was filtered through a Celite and washed with MeOH. The filtrate was evaporated to lead a pale yellow solid. Then, the crude was suspended in toluene to obtain a gummy solid. Further evaporation of the solvent afforded a white solid which was triturated in TBME (60 mL) filtered and washed with more TBME to obtain the desired compound as a white solid (2.06 g). Yield 93 %. **<sup>1</sup>H NMR** (400 MHz, DMSO- $d_6$ )  $\delta$  12.54-11.27 (br. s., 1H, H-27 or H-19), 7.42 (d,  $J=8.6$  Hz, 2H, CH-26 and CH-22), 7.27 (d,  $J=8.6$  Hz, 2H, CH-15 and CH-11), 7.20 - 7.13 (m, 2H, CH-25 and CH-23), 7.06 (d,  $J=8.6$  Hz, 2H, CH-14 and CH-12), 4.64 (d,  $J=7.1$  Hz, 2H, CH<sub>2</sub>-16), 2.45 (s, 3H, CH<sub>3</sub>-7). **<sup>13</sup>C NMR** (101 MHz, DMSO- $d_6$ )  $\delta$  170.8 (C-4), 156.4 (C-13), 155.8 (C-21), 145.1 (C-2), 144.1 (C-24), 141.4 (C-6), 132.8 (CH-15 and CH-11), 129.8 (C-10), 126.2 (C-5) 123.4 (CH-26 and CH-22), 121.5 (C-3), 120.4 (CH-25 and CH-23), 118.6 (CH-14 and CH-12), 62.4 (CH<sub>2</sub>-16), 17.05 (CH<sub>3</sub>-7). **ESIMS**  $m/z$ : 506  $[M+H]^+$ . Purity was determined as >95 % by HPLC ( $\lambda$  268 nm), Rt: 1.99 min (Sunfire 3.5  $\mu$  C18 4.6



x 50 mm; ammonium acetate 0.05 % pH 7 / Acetonitrile). Proton and carbon assignment for compound **19** was based on HMQC and HMBC spectra analysis (see Appendix I).

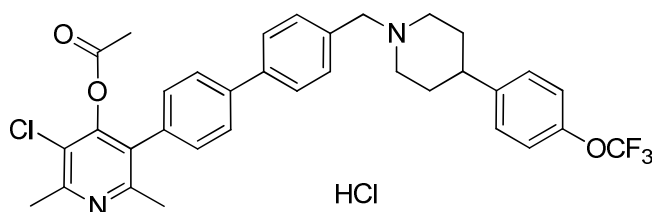
**Preparation of sodium (5-chloro-4-hydroxy-6-methyl-3-(4-(4-(trifluoromethoxy)phenoxy)phenyl)pyridin-2-yl)methyl phosphate (20)**



(5-chloro-4-hydroxy-6-methyl-3-(4-(4-(trifluoromethoxy)phenoxy)phenyl)pyridin-2-yl)methyl dihydrogen phosphate **19** (2.0 g) suspended in H<sub>2</sub>O (50.0 mL) was treated with

NaOH (0.326 g, 2.0 eq.) in H<sub>2</sub>O (50 mL) solution dropwise. The suspension was completely dissolved and stirred at rt for 20 min. Finally, the solution was lyophilized to give the corresponding disodium salt as a white solid (2.2 g). Yield 99 %. <sup>1</sup>H NMR (300 MHz, DMSO-d<sub>6</sub>) δ 7.31 (d, *J*=8.35 Hz, 2H), 7.18-7.05 (m, 4H), 6.94 (d, *J*=8.49 Hz, 2H), 4.48 (d, *J*=10.54 Hz, 2H), 2.24 (s, 3H). ESIMS *m/z*: 506 [M+H]<sup>+</sup>. Purity was determined as >95 % by HPLC (λ 238 nm), Rt: 1.70 min (Sunfire 3.5 μ C18 4.6 x 50 mm; ammonium acetate 0.05 % pH 7 / Acetonitrile).

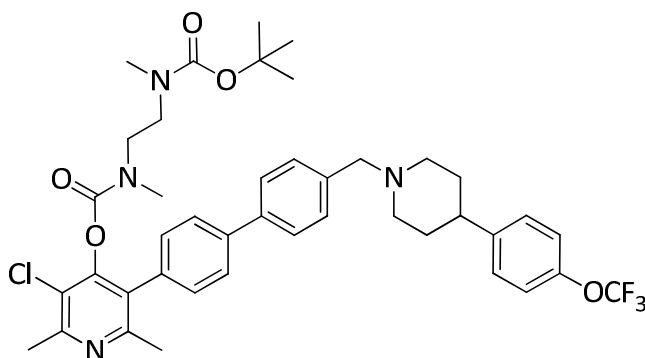
**Preparation of 3-chloro-2,6-dimethyl-5-{4'-[(4-{4-[(trifluoromethyl)oxy]phenyl}-1-piperidiny] methyl]-4-biphenyl}-4-pyridinyl acetate hydrochloride (21).**



A solution of GSK1146191B (110 mg) in anhydrous pyridine (Aldrich, 4 mL) was stirred. Acetic anhydride (Panreac, 517 μL, 30 eq.) was added and the mixture was heated under reflux (90 °C) for 30 min. The crude mixture was diluted in dichloromethane and washed with 1 N HCl aq. (x3) and brine (x1). The organic layer was dried over Na<sub>2</sub>SO<sub>4</sub> and evaporation gave the title compound (60 mg). Yield 51 %. <sup>1</sup>H NMR (300 MHz, DMSO-d<sub>6</sub>) δ 10.34 (br. s., 1H), 7.90-7.81 (m, 4H), 7.71 (d, *J*=8.20 Hz, 2H), 7.34 (s, 6H), 4.37 (br. s., 2H), 3.46 (br. s., 2H), 3.07 (br. s., 2H), 2.86 (br. s., 1H), 2.60 (s, 3H), 2.30 (s, 3H), 2.04 (s,

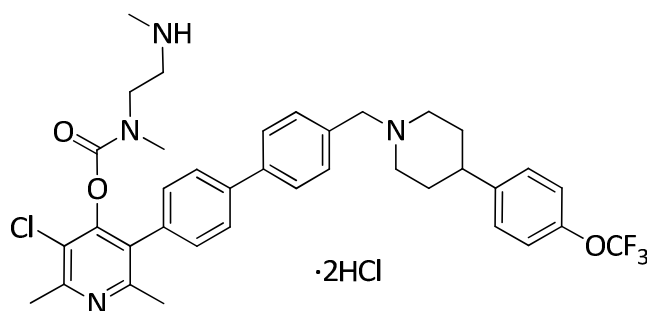
5H). **ESIMS**  $m/z$ : 609  $[M+H]^+$ . Purity was determined as >90 % by HPLC ( $\lambda$  261 nm), Rt: 2.53 min (Sunfire 3.5  $\mu$  C18 4.6 x 50 mm; formic acid 0.1 % pH 2.4 / Acetonitrile).

**Preparation of tert-butyl (3-chloro-2,6-dimethyl-5-(4'-((4-(4-(trifluoromethoxy)phenyl)piperidin-1-yl)methyl)-[1,1'-biphenyl]-4-yl)pyridin-4-yl)ethane-1,2-diylbis(methylcarbamate)(22).**



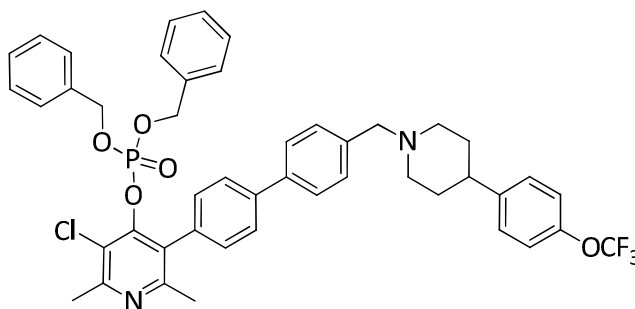
GSK1146191B (153 mg) and 1,1-dimethylethyl{2-[(chlorocarbonyl)(methyl) amino] ethyl}methylcarbamate (Prepared in our group, 81.5 mg, 1.3 eq.) were suspended under  $N_2$  atmosphere in anhydrous pyridine (Aldrich, 5 mL). DIPEA (Aldrich, 210  $\mu$ l, 1.2 eq.) was added and the mixture was stirred at rt for 1 h and then under reflux (90  $^{\circ}$ C) for 1 h. Reaction was cooled down, diluted in AcOEt and washed with 1 N HCl aq. (x3), 1 N NaOH aq. (x1) and brine (x1). The organic layer was dried over  $MgSO_4$  and concentrate under vacuum. Purification was carried out by column chromatography on silica (Si) 5 g, using a 0-10 % ethyl acetate-cyclohexane gradient over 20 min. Title compound was isolated as a white solid. Yield: 87 %.  **$^1H$  NMR** (300 MHz,  $CDCl_3$ )  $\delta$  7.65 (d,  $J=8.64$  Hz, 2H), 7.62-7.54 (m, 2H), 7.44 (d,  $J=8.05$  Hz, 2H), 7.30 (d,  $J=8.05$  Hz, 2H), 7.25-7.20 (m, 2H), 7.14 (d,  $J=9.08$  Hz, 2H), 3.61 (s, 2H), 3.43-3.13 (m, 4H), 3.06 (d,  $J=11.28$  Hz, 2H), 2.92-2.70 (m, 6H), 2.67 (s, 5H), 2.45-2.59 (m, 1H), 2.35 (d,  $J=3.51$  Hz, 3H), 2.12 (br. s., 2H), 1.81 (br. s., 4H), 1.41 (d,  $J=5.71$  Hz, 10H). **ESIMS**  $m/z$ : 780  $[M+H]^+$ . Purity was determined as >95 % by HPLC ( $\lambda$  254 nm), Rt: 4.87 min (X-Terra 3.5  $\mu$  C18 4.6 x 50 mm; trifluoroacetic acid / Acetonitrile).

**Preparation of 3-chloro-2,6-dimethyl-5-(4'-((4-(4-(trifluoromethoxy)phenyl)piperidin-1-yl)methyl)-[1,1'-biphenyl]-4-yl)pyridin-4-ylmethyl(2-(methylamino)ethyl) carbamate di hydrochloride (23).**



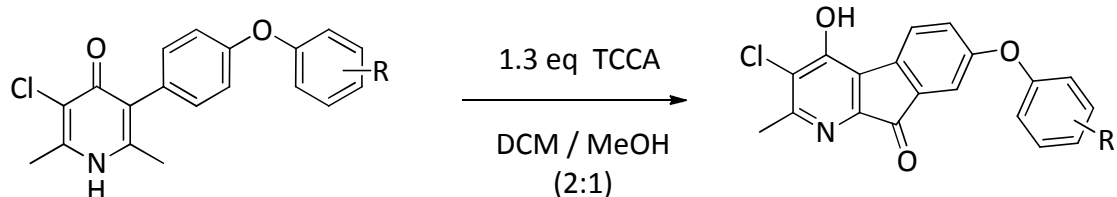
A solution of Intermediate **22** (165 mg) in MeOH (3 mL) was added over a solution of acetyl chloride (Aldrich, 450  $\mu$ l, 30 eq.) at 0 °C under N<sub>2</sub> conditions. After stirring at room temperature during the night, solvent was removed under vacuum. Crude was dissolved in DCM (3ml) and added over TBME (10 ml) dropwise to give a precipitate which was filtered under N<sub>2</sub> conditions to obtain the desired compound as a pale yellow solid. Yield 72 %. <sup>1</sup>H NMR (300 MHz, DMSO-d<sub>6</sub>)  $\delta$  10.98 (br. s., 1H), 8.89 (br. s., 2H), 7.92-7.81 (m, 4H), 7.79-7.72 (m, 2H), 7.40-7.28 (m, *J*=2.60 Hz, 6H), 4.36 (d, *J*=4.83 Hz, 2H), 3.45-3.34 (m, 4H), 3.06 (s, 3H), 2.86-2.75 (m, 5H), 2.61 (s, 3H), 2.43-2.34 (m, 4H), 2.31 (s, 3H), 2.13-2.06 (m, 1H), 1.99 (br. s., 2H). **ESIMS** *m/z*: 681 [M+H]<sup>+</sup>. Purity was determined as >95 % by HPLC ( $\lambda$  269 nm), Rt: 1.81 min (Sunfire 3.5  $\mu$  C18 4.6 x 50 mm; formic acid 0.1 % pH 2.4 / Acetonitrile).

**Preparation of dibenzyl(3-chloro-2,6-dimethyl-5-(4'-((4-(4-(trifluoromethoxy)phenyl)piperidin-1-yl)methyl)-[1,1'-biphenyl]-4-yl)pyridin-4-yl) phosphate (24).**

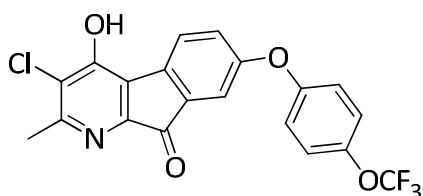


To a suspension of GSK1146191B (2 g) in Tetrahydrofuran (THF) (100 mL, 20 mL/mmol) stirred under nitrogen at rt was added neat sodium hydride oil suspension 60 % (0.928 g, 7 eq.) in one charge. The reaction mixture was stirred at rt for 30 min to obtain a suspension of the corresponding sodium salt. The crude was cooled down until 0 °C and a solution of (BnO)<sub>2</sub>P(O)Cl (3.93 g, 4 eq.) in acetonitrile (40ml, 3 mL/mmol) was added through a nylon filter. A few minutes later the crude was completely dissolved. The reaction mixture was checked 1 h later by HPLC and two compounds were detected in a proportion of 25:75 (SM : Product). Two hours later no progression was observed. The reaction mixture was diluted with ethyl acetate washed with sat NH<sub>4</sub>Cl aq. and brine. The solid suspension was filtrated (starting material) and the organic layer was dried over Na<sub>2</sub>SO<sub>4</sub>, filtered and concentrated under vacuum. Purification was carried out by column chromatography on silica (Si) 25 g, using a 0-15 % methanol-dichloromethane gradient over 20 min. Title compound was isolated as a colorless solid. Yield: 23 %. **<sup>1</sup>H NMR** (300 MHz, CDCl<sub>3</sub>) δ 7.63 (d, *J*=8.35 Hz, 2H), 7.48 (d, *J*=8.06 Hz, 2H), 7.42-7.36 (m, 6H), 7.25-7.20 (m, 6H), 7.16-7.07 (m, 6H), 4.69 (ddd, *J*=7.03, 13.18, 33.83 Hz, 4H), 3.61 (s, 2H), 3.06 (d, *J*=11.28 Hz, 2H), 2.67 (s, 3H), 2.55 (d, *J*=5.71 Hz, 1H), 2.32 (s, 3H), 2.20-2.07 (m, 2H), 1.83 (d, *J*=5.57 Hz, 4H). **ESIMS** *m/z*: 828 [M+H]<sup>+</sup>. Purity was determined as >95 % by HPLC (λ 254 nm), Rt: 4.83 min (X-Terra 5μ 6mm. Gradient 10 % ACN to 100 % ACN-0.1 % TFA).

- **General method for the synthesis of the azafluorenone scaffold:**

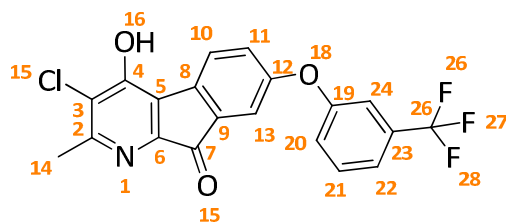


**Preparation of 3-chloro-4-hydroxy-2-methyl-7-(4-(trifluoromethoxy)phenoxy)-9H-indeno[2,1-b]pyridin-9-one (27)**



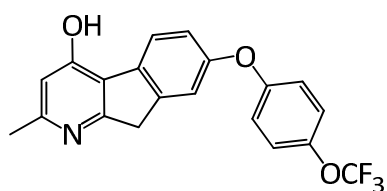
In a 2 L, 3-necks, round-bottom flash, GW844520 (10 g) was dissolved in 900 mL of a mixture DCM/MeOH (2:1). The solution was cooled down to 0 °C and trichloroisocyanuric acid (Aldrich, 4.56 g, 1.3 eq.) was added. The mixture was stirred at rt and air was bubbled for 2 days. Reaction was then heated at 60 °C (for 4 days) until the total conversion to the desired tricyclic structure. The mixture was cooled down to rt and the solid was filtered (isocyanuric acid) and washed with DCM/MeOH (2:1). The red mother liquors obtained were concentrated under vacuum and then triturated in a mixture AcOEt/Hexane (6:4) (100 mL) during the night. The brown-red solid obtained was filtered and washed with a mixture AcOEt/Hexane (6:4) three times and then triturated with 10% NaHCO<sub>3</sub> for 1.5 h. The solid (sodium salt) was filtered, washed with water three times, dried under vacuum, poured in a 250 mL bottom flash and triturated in 1 N HCl to obtain the neutral compound. The red solid obtained was filtered, washed with water (x3) and dried in the vacuum-oven at 50 °C during the night, to obtain the desired compound as a red solid 2.42 g (Yield 23 %). <sup>1</sup>H NMR (300 MHz, DMSO-d<sub>6</sub>) δ 13.00 (br. s., 1H), 7.83 (d, *J*=7.76 Hz, 1H), 7.41 (d, *J*=9.23 Hz, 2H), 7.24-7.11 (m, 4H), 2.43 (s, 3H). **ESIMS** *m/z*: 422 [M+H]<sup>+</sup>. Purity was determined as >95 % by HPLC (λ 247 nm), Rt: 2.97 min (Ace C18 3 μ; 30 x 4.6 mm; formic acid 0.1 % pH 2.4 / Acetonitrile).

**Preparation of 3-chloro-4-hydroxy-2-methyl-7-(3-(trifluoromethyl)phenoxy)-9H-indeno[2,1-b]pyridin-9-one (26).**



This compound was synthesized following the same procedure described for **27** and using GW308678 as starting material. Yield: 12 %. <sup>1</sup>H NMR (400 MHz, DMSO-d<sub>6</sub>) δ 13.05 (br. s., 1H, OH or NH), 7.86 (d, *J*=7.58 Hz, 1H, CH-10), 7.66 (t, *J*=7.58 Hz, 1H, CH-21), 7.54 (d, *J*=7.58 Hz, 1H, CH-11), 7.43-7.34 (m, 2H, CH-20 And CH-24), 7.27-7.18 (m, 2H, CH-13 and CH-22), 2.44 (br. s., 3H, CH<sub>3</sub>-14). <sup>13</sup>C NMR (101 MHz, DMSO-d<sub>6</sub>) δ 157.4 (C-19), 156.2 (C-12), 132.0 (C-21), 131.5, 131.2 (C-23), 130.8, 128.2 (C-5), 127.8 (C-3), 125.7 (C-8), 125.5 (C-22), 124.6 (C-10), 123.0 (C-20), 122.8, 120.9, 120.8, 120.0 (C-11), 116.3 (C-13), 115.5 (C-24), 25.95 (-OCF<sub>3</sub> not visible in the spectrum). ESIMS *m/z*: 406 [M+H]<sup>+</sup>. Purity was determined 94 % by HPLC (λ 207 nm), Rt: 1.11 min (Acquity UPLC BEH C18 1.7 μ 3 x 50 mm; ammonium acetate 25 μM + 10 % Acetonitrile at pH 6.6 / Acetonitrile). Proton and carbon assignment for compound **26** was based on HMQC and HMBC spectra analysis (see Appendix I).

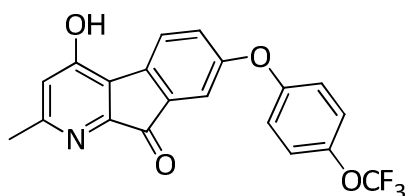
**Preparation of 2-methyl-7-(4-(trifluoromethoxy)phenoxy)-9H-indeno[2,1-b]pyridin-4-ol (28).**



Azafluorenone **27** (500 mg) was suspended in 40 mL of a mixture DCM/MeOH (1:1) and under Nitrogen atmosphere the catalyst Pd(C) (100 mg) was added. Reaction was stirred under Hydrogen pressure of 35 psi for 66 h. Pd was filtered and concentrated under vacuum to lead 433 mg of the desired compound as a white solid. Yield: 98 %. <sup>1</sup>H NMR (300 MHz, DMSO-d<sub>6</sub>) δ 7.99 (d, *J*=8.35 Hz, 1H), 7.46-7.34 (m, 3H), 7.10-7.21 (m, 4H), 4.26 (s, 2H), 2.62 (s, 3H) (-OH not visible in the spectrum). <sup>13</sup>C NMR (101 MHz, DMSO-d<sub>6</sub>) δ 165.7, 158.9, 156.5, 156.0, 150.9, 144.3,

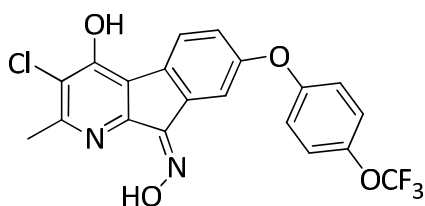
141.7, 132.4, 124.8, 123.5, 123.4, 121.9, 120.5 (2C), 119.3, 118.9, 116.5, 111.9, 36.6, 19.3. **ESIMS**  $m/z$ : 374  $[M+H]^+$ . Purity was determined as >95 % by HPLC ( $\lambda$  282 nm), Rt: 2.47 min (Ace C18; 3  $\mu$ ; 30 x 2.0 mm; formic acid 0.1 % pH 2.4 / Acetonitrile ).

**Preparation of 4-hydroxy-2-methyl-7-(4-(trifluoromethoxy)phenoxy)-9H-indeno[2,1-b]pyridin-9-one (29).**



Compound **28** (417 mg) was suspended in 23 mL of anh. Acetone and under Nitrogen atmosphere  $KMnO_4$  (212 mg, 1.2 eq.) was added. 30 min later reaction was finished. The mixture was concentrated under vacuum and the crude obtained was purified by column chromatography ( $SiO_2$  25 g, DCM-DCM/MeOH 20 %) to lead 247 mg of the title compound as an orange-red solid. Yield: 57 %  **$^1H$  NMR** (300 MHz,  $DMSO-d_6$ )  $\delta$  12.5-12.35 (m, 0.2H), 11.52 (s, 0.8H), 7.68 (d,  $J=8.20$  Hz, 1H), 7.41 (d,  $J=8.93$  Hz, 2H), 7.28-7.23 (m, 1H), 7.14-7.21 (m, 3H), 6.77 (s, 1H), 2.40 (s, 3H).  **$^{13}C$  NMR** (101 MHz,  $DMSO-d_6$ )  $\delta$  156.8, 155.6, 144.5(2C), 130.6, 125.6, 125.1, 124.4, 123.6(2C), 121.8(2C), 120.9, 120.6(2C), 119.3, 115.57, 115.2, 25.08 (- $OCF_3$  not visible in the spectrum). **ESIMS**  $m/z$ : 388  $[M+H]^+$ . Purity was determined as >95 % by HPLC ( $\lambda$  270 nm), Rt: 3.27 min (Ace C18; 3  $\mu$ ; 30 x 4.6 mm; formic acid 0.1 % pH 2.4 / Acetonitrile).

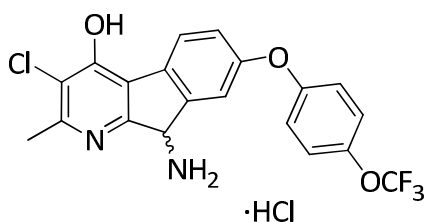
**Preparation of 3-chloro-4-hydroxy-2-methyl-7-(4-(trifluoromethoxy)phenoxy)-9H-indeno[2,1-b]pyridin-9-one oxime (30).**



Over a solution of  $KOH$  (285 mg) in 20 mL of a mixture EtOH/ $H_2O$  (3:1), hydroxylamine hydrochloride (111 mg, 2.7 eq.) was added. The mixture was stirred for a few minutes and azafluorenone **27** was added (250 mg) leading a red suspension. Reaction mixture was heated under reflux. After 30 min a yellow solution was obtained and 15 min later reaction was cooled down and the solvent removed under vacuum. 1 N  $HCl$  solution was added and a solid precipitate. This solid was filtered and washed with water to obtain the title compound (210 mg) as a yellow solid. Yield: 81 %  **$^1H$  NMR** (300 MHz,  $CDCl_3$ )  $\delta$

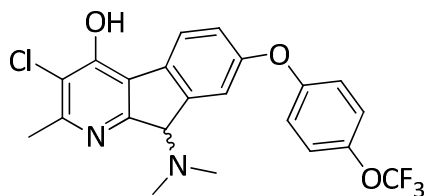
7.70 (d,  $J=7.91$  Hz, 1H), 7.46 (d,  $J=8.05$  Hz, 1H), 7.38-7.27 (m, 2H), 7.24-7.12 (m, 3H), 7.12-7.00 (m, 2H), 2.63 (s, 3H).  **$^1\text{H NMR}$**  (300 MHz, DMSO- $d_6$ )  $\delta$  13.60-13.32 (m, 1H), 12.86-12.55 (m, 1H), 8.04 (d,  $J=8.35$  Hz, 1H), 7.82 (d,  $J=2.34$  Hz, 1H), 7.39 (d,  $J=9.08$  Hz, 2H), 7.19-7.08 (m, 3H), 2.47 (s, 3H). **ESIMS**  $m/z$ : 437  $[\text{M}+\text{H}]^+$ . Purity was determined as >85 % by HPLC ( $\lambda$  254 nm), Rt: 3.22 min (Ace C18; 3  $\mu$ ; 30 x 4.6 mm; formic acid 0.1 % pH 2.4 / Acetonitrile).

**Preparation of 9-amino-3-chloro-2-methyl-7-(4-(trifluoromethoxy)phenoxy)-9H-indeno[2,1-b]pyridin-4-ol hydrochloride (31).**



Compound **30** (120mg) was dissolved EtOH and under  $\text{N}_2$  atmosphere, activated Ni-Raney was added. The mixture was stirred under Hydrogen condition at 1.5 bar for 5.5 h. Under  $\text{N}_2$  atmosphere the catalyst was carefully filtered to lead a green solution. This solution was acidulated with 2 N HCl and then concentrated under reduce pressure to give an orange solid. The solid was triturated in ACN, filtered and washed with more ACN to lead the desired compound (45 mg) as a beige solid. Yield: 40 % (part of the compound was lost with the ACN washes).  **$^1\text{H NMR}$**  (300 MHz, DMSO- $d_6$ )  $\delta$  9.30 (br. s., 3H), 8.02 (s, 1H), 7.58 (s, 1H), 7.41 (br. s., 2H), 7.25-7.09 (m, 3H), 5.52 (br. s., 1H) 2.49 (s, 3H). **ESIMS**  $m/z$ : 423  $[\text{M}+\text{H}]^+$ . Purity was determined as > 80% by HPLC ( $\lambda$  254 nm), Rt: 2.09 min (Ace C18; 3  $\mu$ ; 30 x 4.6 mm; formic acid 0.1 % pH 2.4 / Acetonitrile).

**Preparation of 3-chloro-9-(dimethylamino)-2-methyl-7-(4-(trifluoromethoxy)phenoxy)-9H-indeno[2,1-b]pyridin-4-ol (32).**



A suspension of the Intermediate **31** (50 mg, 0.109 mmol) in THF (5 mL/mmol) was slowly added to a stirred mixture of 37 % aq formaldehyde (0.82 mL, 10 eq.) and 4 M  $\text{H}_2\text{SO}_4$  (23 mL, 4 eq.). Temperature was cooled to 0  $^\circ\text{C}$  and  $\text{NaBH}_4$  (41.23 mg, 10 eq.) was added at such a rate that the temperature did not exceed 30  $^\circ\text{C}$  (Note: the reaction is strongly exothermic).



After the addition was complete, the mixture was stirred for 20 min at rt and then was basify with 2 N NaOH. The resultant mixture was extracted with EtOAc (x3). The combined EtOAc extracts were washed with brine, dried over Na<sub>2</sub>SO<sub>4</sub>, filtered and the solvent was removed on the rotary evaporator. The oily residue was purified by column chromatography in a 2 g cartridge NH<sub>2</sub>-SiO<sub>2</sub>, DCM-DCM/MeOH 20 % to give the desired compound (10 mg) as a white solid. Yield: 19 %. <sup>1</sup>H NMR (300 MHz, CDCl<sub>3</sub>) δ 8.25 (br. s., 1H), 7.25-7.14 (m, 3H), 7.10-6.94 (m, 3H), 4.70 (s, 1H), 2.58 (s, 3H), 2.36 (s, 6H). **ESIMS** m/z: 451 [M+H]<sup>+</sup>. Purity was determined as >95 % by HPLC (λ 196 nm), Rt: 2.47 min (Ace C18; 3 μ; 30 x 4.6 mm; formic acid 0.1 % pH 2.4 / Acetonitrile).

### 5.3 Assay details

The stability, permeability and pharmacokinetic studies presented in this thesis were performed by the Pharmacology Department at DDW-GSK Tres Cantos.

#### **In vitro Assay Protocols.**

##### **Solubility by CLND assay**

The aqueous solubility of compounds was determined using chemiluminescent nitrogen detection (CLND) as a quantification method. Stock solutions of 10 mM compounds in DMSO were serially diluted in phosphate buffered saline (pH7.4) and analysed by HPLC (Agilent 1100 HPLC system; mobile phase 90% methanol, 10% water; flow rate 0.2 ml/min) using CLND (Antek 8060C chemiluminescent nitrogen detector).<sup>146</sup>

##### **FaSSIF Solubility Assay**

This assay was designed as a high-throughput method to measure the solubility of compounds, from solid, in fasted state simulated intestinal fluid (FaSSIF). FaSSIF solution (2.24 mg/ml, pH 6.5) was prepared by the addition of 2.24 mg SIF powder to 0.5 ml assay buffer (3.437 g sodium dihydrogen phosphate, 6.186 g sodium chloride and 0.42 g sodium hydroxide pellets in 500 ml distilled water) and 0.5 ml distilled water. This solution was added to a vial containing compound (1 mg), which was capped, inverted three times, and shaken at 900 rpm for 4 hours. 175 μl was transferred to a filter plate

(0.4  $\mu$  pore size), which was centrifuged for 5 min at 2000 rpm to capture the filtrated. The filtrate was analyzed by HPLC, and the solubility generated by comparison with HPLC data generated by analyzing the compound when fully dissolved in DMSO.

#### ***P. falciparum* in vitro whole cell drug susceptibility.**

Sensitivity of *P. falciparum* infected erythrocytes to the drugs was determined using a modification of the *in vitro*  $^3\text{H}$ -hypoxanthine incorporation method.<sup>147</sup> This assay relies on the parasite incorporation of labeled hypoxanthine that is proportional to *P. falciparum* growth. A culture of parasitized red blood cells (RBC) of strain 3D7A, FCR3 or Tm90c2B with a 0.5 % parasitemia and 2 % haematocrit in RPMI-1640, albumax or serum and 5  $\mu\text{M}$  hypoxanthine is exposed to serial dilutions of the compounds. Plates are incubated 48 h at 37 °C, 5 %  $\text{CO}_2$ , 5 %  $\text{O}_2$ , 90 %  $\text{N}_2$ . After 24 h of incubation,  $^3\text{H}$ -hypoxanthine is added and plates are incubated for an additional 24 h. After that period, plates are harvested on glass fiber filters using a TOMTEC Cell harvester 96. Filters are dried and melt-on scintillator sheets are used to determine the incorporation of  $^3\text{H}$ -hypoxanthine. Radioactivity is measured using a microbeta counter. Data are normalized using the incorporation of the positive control, (parasitized red blood cells without drug).  $\text{IC}_{50}$ 's (50 % inhibitory concentrations) values were determined using Excel and Grafit software.

#### **Cytotoxicity assays.**

Cytotoxic effects were determined as previously described (PLoS ONE (2012), 7, e35019). HepG cells were grown and maintained in EMEM (Sigma-ALDRICH) supplemented with 2 mM L-glutamine (Sigma-ALDRICH) and 10 % fetal calf serum (Perbio). Cultures were maintained at 37 °C in a humidified incubator containing 5 %  $\text{CO}_2$ , 95 % air and passages were routinely made upon reaching 80 % to 90 % confluence. For cytotoxicity experiments, cells were seeded onto 96-well clear bottom black plates coated with type I collagen (Biocoat, Becton Dickinson) at a cell density of 10000 cells/well. To determine cytotoxic effects, represented by the  $\text{IC}_{50}$  value (the concentration of drug that reduces cell viability by 50 %), cells were exposed to serial

dilutions of test compounds for 48 h at 37 °C. The culture medium was as described above, but supplemented with 5 % fetal calf serum. Following the 48 h exposure period, a 0.004 % resazurin solution was prepared by adding 60 mL of Dulbecco's PBS to each resazurin tablet (VWR International). The tablet was allowed to dissolve by placing the container in a bath maintained at 37 °C, protected from light, for approximately 30 min. Medium was removed and 200 µL of fresh culture medium and 50 µL of resazurin solution were added to each well. Plates were incubated for a further 1.5 h. Cytotoxicity is indicated by decreased reduction of resazurin to its fluorescent product resorufin. The fluorescence was stabilized at room temperature for 15 min protected from light. Fluorescence was measured using a fluorescence plate reader (Victor V, Perkin Elmer) at an excitation wavelength of 515 nm and an emission wavelength of 590 nm. Percentages of inhibition were calculated relative to the control wells.

### **In vivo Assay Protocols.**

Authors declare that all animal studies were ethically reviewed and approved by the DDW Ethical Committee on Animal Research, performed at the DDW Laboratory Animal Science facilities accredited by AAALAC and carried out in accordance with European Directive 2010/63/EU and the GSK Policy on the Care, Welfare and Treatment of Animals.

### **Pharmacokinetic studies in mice.**

For pharmacokinetic (PK) studies in mice, two different groups of animals were dosed by intravenous bolus (IV) or post-oral gavage (PO). For IV administration, the dosing volume was 10 mL/kg for a total dose of 1 mg/kg, and for PO administration, the dosing volume was 20 mL/kg for a total dose of 10 mg/kg. Dosing solution for intravenous administration was prepared in 20 % encapsine 5 % DMSO in saline solution (0.1 mg/mL) and for PO administration a suspension in 1 % methylcellulose (w:v) was formulated (0.5 mg/mL). Following IV or PO dosing, 25 µL whole blood samples were collected from lateral tail vein at 5, 15 and 30 min, 1, 2, 4, 6, 8 and 24 h (IV) and at 15, 30 and 45 min, 1, 2, 4, 6, 8 and 24 h (PO). These 25 µL of fresh blood were mixed with 25 µL of saponine solution (0.1 % in water) and immediately stored frozen at -80 °C until analysis.

Diluted blood samples were processed under standard liquid-liquid extraction procedures using acetonitrile and analyzed by LC-MS/MS in positive ion mode with electrospray. Samples were assayed for parent compound using a Sciex API 4000 Triple Quadrupole Mass Spectrometer (Sciex, Division of MDS Inc., Toronto, Canada), against a series of matrix matched calibration curve standards, using multiple reaction monitoring (MRM) at the specific transitions for the compound. Non-compartmental analysis was performed using Phoenix, version 6.3. (Phoenix™ WinNonlin® Copyright ©1998-2012, Certara L.P.) and the main pharmacokinetic parameters were estimated. Additional statistical analysis of the data was performed with GraphPad Prism® Version 5.01 (GraphPad Software Inc., San Diego CA).

#### ***In vivo* Antimalarial Activity against *P. yoelii*.**

The blood schizontocidal activity of test compounds was determined using a modified 4-day suppressive assay. Mice (CD1) were infected intraperitoneally with about  $3 \times 10^6$  *P. yoelii* (YM strain) parasitized erythrocytes. Drugs were formulated by ball milling overnight in 0.25 % Celacol to form a fine suspension, which was kept at 4 °C. The test compounds were administered orally in seven doses over 4 days. On day 5 blood films were prepared and the extent of parasitemia was determined by microscopy; the degree of inhibition of parasitemia relative to control animals was calculated, and analysis of the dose–response curve yielded an ED50 (mg/kg) value.

#### ***In Silico* Modelling Details**

##### **Calculated ChromlogD at pH7.4 Model.**

This model predicts the chromatographic logD, which is a measure of the ionised form of the compound and is therefore dependent on pH. The model was initially generated using all the current results (as of 8 August 2008) of the measured ChromlogD assay. It was regularly updated as new data became available to improve its predictive capability. Using SIMCA-P v11.5 software, an orthogonal partial least squares model of ChromlogD was developed.

### Passive permeability in MDCK2 cells model

In order to build *in silico* models for passive permeability through MDCK2 cells at pH 6.5 and pH7.4, the physicochemical properties of 1362 compounds were calculated. These properties included the calculated ACD logP and logD, total polar surface area, molecular weight, the Abraham descriptors Alpha, Beta, Vx, R2 and Pi, CMR, number of hydrogen bond acceptors, number of hydrogen bond donors, acid and base classes (an in-house scale based on the pK<sub>a</sub> of the compounds) and numbers of positive ionisable centres, negative ionisable centres, aromatic rings, non aromatic rings and rotatable bonds. In addition, an additional set of descriptors based on a PCA analysis of the three-dimensional structure of the compounds was also included. Compounds were classified as 'high permeability' (> 200 nm/s), 'medium permeability' (from 50 nm/s to 200 nm/s) and 'low permeability' (<50nm/s) and split up randomly in a training and validation set. The training set consisted of 600 compounds, while the remaining compounds made up the validation set. The number of high permeability compounds in the validation set was bigger at pH7.4, and the number of low permeability compounds almost negligible

---

## **6 REFERENCES**

---

1. World malaria report 2017.
2. Wells, T. N. C., Alonso, P. L. & Gutteridge, W. E. New medicines to improve control and contribute to the eradication of malaria. *Nat. Rev. Drug Discov.* **8**, 879–891 (2009).
3. Wilairatana, P., Krudsood, S., Treeprasertsuk, S., Chalermrut, K. & Looareesuwan, S. The Future Outlook of Antimalarial Drugs and Recent Work on the Treatment of Malaria. *Arch. Med. Res.* **33**, 416–421 (2002).
4. Pasvol, G. The treatment of complicated and severe malaria. *Br. Med. Bull.* **75–76**, 29–47 (2005).
5. Parasite lifecycle. Available at: <http://www.mmv.org/malaria-medicines/parasite-lifecycle>. (Accessed: 20th April 2009)
6. Schlitzer, M. Malaria chemotherapeutics part I: History of antimalarial drug development, currently used therapeutics, and drugs in clinical development. *ChemMedChem* **2**, 944–986 (2007).
7. Alonso, P. L. *et al.* A Research Agenda to Underpin Malaria Eradication. *PLoS Med.* **8**, e1000406 (2011).
8. Curtis, C. F., Jana-Kara, B. & Maxwell, C. a. Insecticide treated nets: Impact on vector populations and relevance of initial intensity of transmission and pyrethroid resistance. *J. Vector Borne Dis.* **40**, 1–8 (2003).
9. Ballou, W. R. The development of the RTS,S malaria vaccine candidate: Challenges and lessons. *Parasite Immunol.* **31**, 492–500 (2009).
10. When-is-enough-enough-the-need-for-a-robust-pipeline-of-high-quality-antimalarials. Available at: <http://www.discoverymedicine.com/Timothy-N-Wells/2010/05/01/when-is-enough-enough-the-need-for-a-robust-pipeline-of-high-quality-antimalarials/>. (Accessed: 10th September 2015)
11. Talisuna, A. O., Bloland, P., Alessandro, D. & Alessandro, U. D. Resistance History , Dynamics , and Public Health Importance of Malaria Parasite Resistance. *Clin. Microbiol. Rev.* **17**, 235–254 (2004).
12. Olliaro, P. & Wells, T. N. C. The global portfolio of new antimalarial medicines under development. *Clin. Pharmacol. Ther.* **85**, 584–595 (2009).
13. Dondorp, A. M. *et al.* Artemisinin resistance: current status and scenarios for containment. *Nat. Rev. Microbiol.* **8**, 272–280 (2010).
14. Das, D. *et al.* Artemisinin Resistance in. *N. Engl. J. Med.* **361**, 455–467 (2009).
15. Calderón, F., Wilson, D. M. & Gamo, F.-J. *Antimalarial Drug Discovery.* **52**, (2013).
16. Achan, J. *et al.* Quinine, an old anti-malarial drug in a modern world: role in the treatment of malaria. *Malar. J.* **10**, 144 (2011).
17. Yeka, A., Achan, J., D’Alessandro, U. & Talisuna, A. O. Quinine monotherapy for treating uncomplicated malaria in the era of artemisinin-based combination therapy: an appropriate public health policy? *Lancet Infect. Dis.* **9**, 448–452 (2009).
18. Coatney, G. R. Pitfalls in a Discovery: The Chronicle of Chloroquine. *Am J Trop Med Hyg* **12**, 121–128 (1943).
19. Krafts, K., Hempelmann, E. & Skórska-Stania, A. From methylene blue to chloroquine: A brief review of the development of an antimalarial therapy. *Parasitol. Res.* **111**, 1–6 (2012).

20. Tempera, C. *et al.* Characterization and optimization of the haemozoin-like crystal (HLC) assay to determine Hz inhibiting effects of anti-malarial compounds. *Malar. J.* **14**, 403 (2015).
21. Baird, J. K. & Hoffman, S. L. Primaquine Therapy for Malaria. *Clin. Infect. Dis.* **39**, 1336–1345 (2004).
22. Jean, P. L. S. *et al.* Tafenoquine treatment of Plasmodium vivax malaria : suggestive evidence that CYP2D6 reduced metabolism is not associated with relapse in the Phase 2b DETECTIVE trial. *Malar. J.* 1–9 (2016). doi:10.1186/s12936-016-1145-5
23. Llanos-cuentas, A. *et al.* Tafenoquine plus chloroquine for the treatment and relapse prevention of Plasmodium vivax malaria ( DETECTIVE ): a multicentre , double-blind , randomised , phase 2b dose-selection study. *Lancet Infect. Dis.* **383**, 1049–1058 (2014).
24. GSK and MMV announce positive headline phase III results showing single-dose tafenoquine reduces risk of relapse in patients with Plasmodium vivax malaria. (2017). Available at: <http://us.gsk.com/en-us/media/press-releases/2017/gsk-and-mmv-announce-positive-headline-phase-iii-results-showing-single-dose-tafenoquine-reduces-risk-of-relapse-in-patients-with-plasmodium-vivax-malaria>.
25. US FDA approves Krintafel (tafenoquine) for the radical cure of P. vivax malaria. Available at: <https://www.mmv.org/newsroom/press-releases/us-fda-approves-krintafel-tafenoquine-radical-cure-p-vivax-malaria>.
26. Trenholme, C. *et al.* Mefloquine (WR 142,490) in the treatment of human malaria. *Science (80- )*. **190**, 792–794 (1975).
27. G. D. Shanks. The rise and fall of mefloquine as an antimalarial drug in Southeast Asia. *Mil.Med.* 275–281
28. D.J. Abraham. Antimalarial Agents. in *Medicinal Chemistry and Drug Discovery* 920–999 (2003).
29. P. J. Rosenthal. *Anti- malarial Chemotherapy: Mechanisms of Action, Resistance, and New Directions in Drug Discovery*. *Journal of Chemical Information and Modeling* **53**, (2001).
30. Hyde, J. E. Exploring the folate pathway in Plasmodium falciparum. *Acta Trop.* **94**, 191–206 (2005).
31. Christopher V. Plowe. Folate Antagonists and Mechanisms of Resistance. in *Anti-malarial Chemotherapy: Mechanisms of Action, Resistance, and New Directions in Drug Discovery* 173–190 (2001).
32. Gregson, A. & Plowe, C. V. Mechanisms of Resistance of Malaria Parasites to Antifolates. *Pharmacol Rev* **57**, 117–145 (2005).
33. Chan, D. C. M. & Anderson, A. C. Towards Species-specific Antifolates. **13**, 377–398 (2006).
34. Nzila, A. The past, present and future of antifolates in the treatment of Plasmodium falciparum infection. *J. Antimicrob. Chemother.* **57**, 1043–54 (2006).
35. Olliaro, P. Mode of action and mechanisms of resistance for antimalarial drugs. *Pharmacol. Ther.* **89**, 207–219 (2001).
36. Chulay, J. D., Atkins, W. M. & Sixsmith, D. G. Synergistic antimalarial activity of pyrimethamine and sulfadoxine against Plasmodium falciparum in vitro. *Am. J. Trop. Med. Hyg.* **33**, 325–330 (1984).
37. Spencer, H. C., Watkins, W. M., Sixsmith, D. G., Koech, D. K. & Chulay, J. D. A new



- in vitro test for pyrimethamine/sulfadoxine susceptibility of *Plasmodium falciparum* and its correlation with in vivo resistance in Kenya. *Bull. World Health Organ.* **62**, 615–621 (1984).
38. Haynes, R. K. & Vonwiller, S. C. From Qinghao, Marvelous Herb of Antiquity, to the Antimalarial Trioxane Qinghaosu and Some Remarkable New Chemistry. *Acc. Chem. Res.* **30**, 73–79 (1997).
  39. Medical Discoveries: Quinine. (2012). Available at: <http://www.discoveriesinmedicine.com/Ni-Ra/Quinine.html>.
  40. Klayman DL. Qinghaosu (artemisinin): an antimalarial drug from China. *Science (80-. )*. **228**, 1049–1055 (1985).
  41. Luo, X. D. & Shen, C. C. The chemistry, pharmacology, and clinical applications of qinghaosu (artemisinin) and its derivatives. *Med. Res. Rev.* **7**, 29–52 (1987).
  42. Golenser, J., Waknine, J. H., Krugliak, M., Hunt, N. H. & Grau, G. E. Current perspectives on the mechanism of action of artemisinins. *Int. J. Parasitol.* **36**, 1427–1441 (2006).
  43. Olliaro, P. L., Haynes, R. K., Meunier, B. & Yuthavong, Y. Possible modes of action of the artemisinin-type compounds. *Trends Parasitol.* **17**, 122–126 (2001).
  44. Falade, C. *et al.* Efficacy and safety of artemether-lumefantrine (Coartem) tablets (six-dose regimen) in African infants and children with acute, uncomplicated *falciparum* malaria. *Trans. R. Soc. Trop. Med. Hyg.* **99**, 459–67 (2005).
  45. Slack, R. D., Jacobine, A. M. & Posner, G. H. Antimalarial peroxides: advances in drug discovery and design. *Medchemcomm* **3**, 281–297 (2012).
  46. Activity, A. *et al.* Synthesis and Antimalarial Activity of 3,3-Spiroanellated 5,6-Disubstituted 1,2,4-Trioxanes. *Med. Chem. Lett.* **4**, 165–169 (2013).
  47. O'Neill, P. M. The therapeutic potential of semi-synthetic artemisinin and synthetic endoperoxide antimalarial agents. *Expert Opin. Investig. Drugs* **14**, 1117–28 (2005).
  48. G. H. Posner, M. Kra-savin, M. McCutchen, P. Ploypradith, J. P. Maxwell, J. S. Elias, M. H. P. New Antimalarial Trioxanes and Endoperoxides. in *Antimalarial Chemotherapy: Mechanisms of Action, Resistance, and New Directions in Drug Discovery* 255–265 (2001).
  49. Haynes, R. K. *et al.* Convenient access both to highly antimalaria-active 10-aryl aminoartemisinins, and to 10-alkyl ethers including artemether, arteether, and artelinate. *Chembiochem* **6**, 659–67 (2005).
  50. Ploypradith, P. Development of artemisinin and its structurally simplified trioxane derivatives as antimalarial drugs. *Acta Trop.* **89**, 329–342 (2004).
  51. Borstnik, K., Paik, I. H., Shapiro, T. a. & Posner, G. H. Antimalarial chemotherapeutic peroxides: Artemisinin, yingzhaosu A and related compounds. *Int. J. Parasitol.* **32**, 1661–1667 (2002).
  52. Tang, Y., Dong, Y. & Vennerstrom, J. L. Synthetic peroxides as antimalarials. *Med. Res. Rev.* **24**, 425–448 (2004).
  53. Valecha, N. *et al.* Arterolane Maleate Plus Piperaquine Phosphate for Treatment of Uncomplicated *Plasmodium falciparum* Malaria: A Comparative, Multicenter, Randomized Clinical Trial. *Clin. Infect. Dis.* **55**, 663–671 (2012).
  54. Gautam, A. *et al.* Pharmacokinetics and pharmacodynamics of arterolane maleate following multiple oral doses in adult patients with *P. falciparum* malaria. *J. Clin. Pharmacol.* **51**, 1519–28 (2011).

55. Vennerstrom, J. L. *et al.* Identification of an antimalarial synthetic trioxolane drug development candidate. *Nature* **430**, 900–904 (2004).
56. Phase IIb Study to Investigate the Efficacy of OZ439 & Piperaquine Phosphate Co-administered to Adults & Children With Uncomplicated Plasmodium Falciparum. (2014). Available at: <https://clinicaltrials.gov/ct2/show/NCT02083380?term=oz439&rank=8>.
57. Valecha, N. *et al.* Arterolane, a New Synthetic Trioxolane for Treatment of Uncomplicated *Plasmodium falciparum* Malaria: A Phase II, Multicenter, Randomized, Dose-Finding Clinical Trial. *Clin. Infect. Dis.* **51**, 684–691 (2010).
58. Phyto, A. P. *et al.* Antimalarial activity of artefenomel (OZ439), a novel synthetic antimalarial endoperoxide, in patients with Plasmodium falciparum and Plasmodium vivax malaria: an open-label phase 2 trial. *Lancet Infect. Dis.* 61–69 (2015). doi:10.1016/S1473-3099(15)00320-5
59. Fry, M. Site of Action of the Antimalarial Hydroxynaphthquinone. *Biochem. Pharmacol.* **43**, 1545–1553 (1992).
60. Srivastava, I. K., Morrillsey, J. M., Darrouzet, E., Daldal, F. & Vaidya, A. B. Resistance mutations reveal the atovaquone-binding domain of cytochrome b in malaria parasites. *Mol. Microbiol.* **33**, 704–711 (1999).
61. Baggish, A. L. & Hill, D. R. Antiparasitic Agent Atovaquone. *Antimicrob. Agents Chemother* **46**, 1163–1173 (2002).
62. Nakato, H., Vivancos, R. & Hunter, P. R. A systematic review and meta-analysis of the effectiveness and safety of atovaquone - Proguanil (Malarone) for chemoprophylaxis against malaria. *J. Antimicrob. Chemother.* **60**, 929–936 (2007).
63. Krudsood, S. *et al.* Efficacy of atovaquone-proguanil for treatment of acute multidrug-resistant Plasmodium falciparum malaria in Thailand. *Am. J. Trop. Med. Hyg.* **76**, 655–658 (2007).
64. Looasreesuwon, S., Canfield, J. & Hutchinson, C. Malarone®(atovaquone and proguanil (HCL): a review of its clinical development for treatment of malaria. *Am. J. Trop. Med. Hyg* **60**, 533–541 (1999).
65. Kessl, J. J. *et al.* Molecular basis for atovaquone binding to the cytochrome bc1 complex. *J. Biol. Chem.* **278**, 31312–8 (2003).
66. Srivastava, I. K., Morrillsey, J. M., Darrouzet, E., Daldal, F. & Vaidya, a B. Resistance mutations reveal the atovaquone-binding domain of cytochrome b in malaria parasites. *Mol. Microbiol.* **33**, 704–11 (1999).
67. Färnert, A. *et al.* Evidence of Plasmodium falciparum malaria resistant to atovaquone and proguanil hydrochloride: case reports Media criticism of doctors: review of UK junior doctors' concerns raised in surveys. *Brit.Med.J.* **326**, 628–629 (2003).
68. Schwartz, E., Bujanover, S. & Kain, K. C. Genetic confirmation of atovaquone-proguanil-resistant Plasmodium falciparum malaria acquired by a nonimmune traveler to East Africa. *Clin. Infect. Dis.* **37**, 450–1 (2003).
69. Pradines, B. *et al.* In vitro potentiation of antibiotic activities by a catecholate iron chelator against chloroquine-resistant Plasmodium falciparum. *Antimicrob. Agents Chemother.* **46**, 225–228 (2002).
70. Bell, C. A. *et al.* Structure-activity relationships of analogs of pentamidine against Plasmodium falciparum and Leishmania mexicana amazonensis. *Antimicrob Agents Chemother* **34**, 1381–1386 (1990).

71. Newton, P. N. *et al.* Pharmacokinetics of Oral Doxycycline during Combination Treatment of Severe *Falciparum* Malaria. *Antimicrob. Agents Chemother.* **49**, 1622–1625 (2005).
72. Manuscript, A. & Medicines, N. Antimalarial Drug Discovery: Approaches and Progress towards New Medicines. *Nat. Rev. Microbiol.* **11**, 849–862 (2014).
73. Coteron, J. M. *et al.* Structure-guided lead optimization of triazolopyrimidine-ring substituents identifies potent *Plasmodium falciparum* dihydroorotate dehydrogenase inhibitors with clinical candidate potential. *J. Med. Chem.* **54**, 5540–5561 (2011).
74. Payne, D. J., Gwynn, M. N., Holmes, D. J. & Pompliano, D. L. Drugs for bad bugs: confronting the challenges of antibacterial discovery. *Nat. Rev. Drug Discov.* **6**, 29–40 (2007).
75. Plouffe, D. *et al.* In silico activity profiling reveals the mechanism of action of antimalarials discovered in a high-throughput screen. *Proc. Natl. Acad. Sci. U. S. A.* **105**, 9059–64 (2008).
76. Guiguemde, W. A. *et al.* Chemical genetics of *Plasmodium falciparum*. *Nature* **465**, 311–315 (2010).
77. Gamo, F.-J. *et al.* Thousands of chemical starting points for antimalarial lead identification. *Nature* **465**, 305–310 (2010).
78. Calderón, F. *et al.* An invitation to open innovation in malaria drug discovery: 47 quality starting points from the TCAMS. *ACS Med. Chem. Lett.* **2**, 741–746 (2011).
79. Burrows, J. N. *et al.* Antimalarial drug discovery - the path towards eradication. *Parasitology* **141**, 128–39 (2014).
80. ChEMBL - Neglected Tropical Disease. Available at: <https://www.ebi.ac.uk/chemblntd>.
81. Rueda, L. *et al.* Cyclopropyl Carboxamides : A New Oral Antimalarial Series Derived. 840–844 (2011).
82. Calderón, F. *et al.* A Divergent SAR Study Allows Optimization of a Potent 5-HT. *Med. Chem. Lett.* 373–377 (2012).
83. Bueno, J. M. *et al.* Case Study of Small Molecules As Antimalarials: 2 - Amino-1-phenylethanol (APE) Derivatives. 1–5 (2014).
84. Sandoval, E.; Lafuente-Monasterio, M.J.; Almela, M.J.; Castañeda, P.; Jiménez Díaz, M.B.; Martínez-Martínez, M.S.; Vidal, J.; Angulo-Barturen, I.; Bamborough, P.; Burrows, J.; Cammack, N.; Chaparro, M.J.; Coteron, J.M.; Puente, M.; Calderón, C. The Discovery of Novel Antimalarial Aminoxadiazoles as a Promising Nonendoperoxide Scaffold. *J. Med. Chem.* **60**, 6880–6896 (2017).
85. Fernández, E. *et al.* Quinazolindione series identified from TCAMS: a new anti-malarial series with potential for blocking transmission of the disease. in *18th SCI-RSC MedChem Symposium* (2015).
86. Jane, N. & Kirk, K. The malaria parasite cation ATPase PfATP4 and its role in the mechanism of action of a new arsenal of antimalarial drugs. *Int. J. Parasitol.* **5**, 149–162 (2015).
87. Bennett, T. N. *et al.* Novel , Rapid , and Inexpensive Cell-Based Quantification of Antimalarial Drug Efficacy Novel , Rapid , and Inexpensive Cell-Based Quantification of Antimalarial Drug Efficacy. *Antimicrob. Agents Chemother.* **48**, 1807–1810 (2004).
88. Yeung, B. K. S. *et al.* Spirotetrahydro  $\beta$ -carbolines (spiroindolones): A new class of

- potent and orally efficacious compounds for the treatment of malaria. *J. Med. Chem.* **53**, 5155–5164 (2010).
89. NITD609: a novel and potent drug candidate for the treatment of uncomplicated malaria. Available at: [http://www.mmv.org/sites/default/files/uploads/docs/events/2012/Stakeholder\\_meeting\\_presentations/Diagana\\_NITD609.pdf](http://www.mmv.org/sites/default/files/uploads/docs/events/2012/Stakeholder_meeting_presentations/Diagana_NITD609.pdf).
  90. Zhou, Y., Fomovska, A., Muench, S., Lai, B. & Mui, E. Spiroindolone That Inhibits PfATPase4 Is a Potent, Cidal Inhibitor of *Toxoplasma gondii* Tachyzoites In Vitro and In Vivo. *Antimicrob. Agents Chemother.* **58**, 1789–1792 (2014).
  91. Leong, F. J. *et al.* A First-in-Human Randomized, Double-Blind, Placebo-Controlled, Single- and Multiple-Ascending Oral Dose Study of Novel Antimalarial Spiroindolone KAE609 (Cipargamin) To Assess Its Safety, Tolerability, and Pharmacokinetics in Healthy Adult Volunteers. *Antimicrob. Agents Chemother.* **58**, 6209–6214 (2014).
  92. White, N. J. *et al.* Spiroindolone KAE609 for Falciparum and Vivax Malaria. *N. Engl. J. Med.* **371**, 403–410 (2014).
  93. Smilkstein, M., Sriwilaijaroen, N., Kelly, J. X., Wilairat, P. & Riscoe, M. Simple and Inexpensive Fluorescence-Based Technique for High-Throughput Antimalarial Drug Screening Simple and Inexpensive Fluorescence-Based Technique for High-Throughput Antimalarial Drug Screening. *Antimicrob. Agents Chemother.* **48**, 1803–1806 (2004).
  94. Wu, T. *et al.* Imidazolopiperazines: Hit to lead optimization of new antimalarial agents. *J. Med. Chem.* **54**, 5116–5130 (2011).
  95. Nagle, A. *et al.* Imidazolopiperazines: lead optimization of the second-generation antimalarial agents. *J. Med. Chem.* **55**, 4244–73 (2012).
  96. Efficacy, Safety, Tolerability and Pharmacokinetics of KAF156 in Adult Patients With Acute, Uncomplicated Plasmodium Falciparum or Vivax Malaria Mono-infection. (2015). Available at: <https://clinicaltrials.gov/ct2/show/NCT01753323?term=NCT01753323&rank=1>.
  97. Meister, S. *et al.* Imaging of Plasmodium liver stages to drive next-generation antimalarial drug discovery. *Science (80-. )*. **334**, 1372–1377 (2012).
  98. Magistrado, P. A. *et al.* Plasmodium falciparum Cyclic Amine Resistance Locus (PfCARL), a Resistance Mechanism for Two Distinct Compound Classes. *ACS Infect. Dis.* **2**, 816–826 (2016).
  99. Harris, C. J., Hill, R. D., Sheppard, D. W., Slater, M. J. & Stouten, P. F. W. The design and application of target-focused compound libraries. *Comb. Chem. High Throughput Screen.* **14**, 521–531 (2011).
  100. Younis, Y. *et al.* 3,5-Diaryl-2-aminopyridines as a novel class of orally active antimalarials demonstrating single dose cure in mice and clinical candidate potential. *J. Med. Chem.* **55**, 3479–3487 (2012).
  101. Phase I Study of Ascending Doses of MMV390048 in Healthy Adult Volunteers. (2015). Available at: <https://clinicaltrials.gov/ct2/show/NCT02230579?term=MMV390048&rank=3>.
  102. Ghidelli-disse, S. *et al.* Identification of Plasmodium PI4 kinase as target of MMV390048 by chemoproteomics. *Malar. J.* **13**, P38 (2014).
  103. Barnett, D. S. & Guy, R. K. Antimalarials in Development in 2014. (2014).
  104. About RBM.

105. Global Technical Strategy for Malaria 2016–2030.
106. Action and Investment to defeat Malaria 2016–2030 (AIM).
107. Schlitzer, M. & Ortmann, R. Feeding the antimalarial pipeline. *ChemMedChem* **5**, 1837–1840 (2010).
108. Burrows, J. N., Hooft van Huijsduijnen, R., Möhrle, J. J., Oeuvray, C. & Wells, T. N. Designing the next generation of medicines for malaria control and eradication. *Malar. J.* **12**, 187 (2013).
109. Katsuno, K. *et al.* Hit and lead criteria in drug discovery for infectious diseases of the developing world. *Nat. Rev. Drug Discov.* 1–8 (2015). doi:10.1038/nrd4683
110. Mather, M. W. & Vaidya, A. B. Mitochondria in malaria and related parasites: Ancient, diverse and streamlined. *J. Bioenerg. Biomembr.* **40**, 425–433 (2008).
111. Basselin, M., Hunt, S. M., Abdala-Valencia, H. & Kaneshiro, E. S. Ubiquinone synthesis in mitochondrial and microsomal subcellular fractions of *Pneumocystis* spp.: differential sensitivities to atovaquone. *Eukaryot. Cell* **4**, 1483–92 (2005).
112. Gardner, M. *et al.* Genome sequence of the human malaria parasite *Plasmodium falciparum*. *Nature* **419**, 498–511 (2002).
113. Srivastava, I. K., Rottenberg, H. & Vaidya, A. B. Atovaquone, a broad spectrum antiparasitic drug, collapses mitochondrial membrane potential in a malarial parasite. *J. Biol. Chem.* **272**, 3961–3966 (1997).
114. Painter, H. J., Morrisey, J. M., Mather, M. W. & Vaidya, A. B. Specific role of mitochondrial electron transport in blood-stage *Plasmodium falciparum*. *Nature* **446**, 88–91 (2007).
115. Mather, M. W., Henry, K. W. & Vaidya, A. B. Mitochondrial drug targets in apicomplexan parasites. *Curr. Drug Targets* **8**, 49–60 (2007).
116. Hunte, C., Palsdottir, H. & Trumppower, B. L. Protonmotive pathways and mechanisms in the cytochrome bc<sub>1</sub> complex. *FEBS Lett.* **545**, 39–46 (2003).
117. Eschemann, A., Galkin, A., Oettmeier, W., Brandt, U. & Kerscher, S. HDQ (1-Hydroxy-2-dodecyl-4(1H)quinolone), a High Affinity Inhibitor for Mitochondrial Alternative NADH Dehydrogenase: EVIDENCE FOR A PING-PONG MECHANISM. *J. Biol. Chem.* **280**, 3138–3142 (2005).
118. Suraveratum, N., Krungkrai, S. R., Leangaramgul, P., Prapunwattana, P. & Krungkrai, J. Purification and characterization of *Plasmodium falciparum* succinate dehydrogenase. *Mol. Biochem. Parasitol.* **105**, 215–222 (2000).
119. Christopherson, R. I., Lyons, S. D. & Wilson, P. K. Inhibitors of de novo nucleotide biosynthesis as drugs. *Acc. Chem. Res.* **35**, 961–971 (2002).
120. Baldwin, J., Farajallah, A. M., Malmquist, N. A., Rathod, P. K. & Phillips, M. A. Malarial Dihydroorotate Dehydrogenase: SUBSTRATE AND INHIBITOR SPECIFICITY. *J. Biol. Chem.* **277**, 41827–41834 (2002).
121. Rodrigues, T., Lopes, F. & Moreira, R. Inhibitors of the mitochondrial electron transport chain and de novo pyrimidine biosynthesis as antimalarials: The present status. *Curr. Med. Chem.* **17**, 929–956 (2010).
122. Schütz, M. *et al.* Early evolution of cytochrome bc complexes. *J. Mol. Biol.* **300**, 663–75 (2000).
123. Lemsle-Meunier, D. *et al.* Cytochrome b-deficient mutants of the ubiquinol-cytochrome c oxidoreductase in *Saccharomyces cerevisiae*. *J. Biol. Chem.* **268**, 15626–15632 (1993).
124. Gao, X. *et al.* The crystal structure of mitochondrial cytochrome bc<sub>1</sub> in complex

- with famoxadone: The role of aromatic-aromatic interaction in inhibition. *Biochemistry* **41**, 11692–11702 (2002).
125. Darrouzet, E., Valkova-Valchanova, M., Moser, C. C., Dutton, P. L. & Daldal, F. Uncovering the [2Fe2S] domain movement in cytochrome bc1 and its implications for energy conversion. *Proc. Natl. Acad. Sci. U. S. A.* **97**, 4567–72 (2000).
  126. Fisher, N., Bourges, I., Hill, P., Brasseur, G. & Meunier, B. Disruption of the interaction between the Rieske iron-sulfur protein and cytochrome b in the yeast bc1 complex owing to a human disease-associated mutation within cytochrome b. *Eur. J. Biochem.* **271**, 1292–1298 (2004).
  127. Brandt, U., Haase, U., Schägger, H. & von Jagow, G. Significance of the 'Rieske' iron-sulfur protein for formation and function of the ubiquinol-oxidation pocket of mitochondrial cytochrome c reductase (bc1 complex). *J. Biol. Chem.* **266**, 19958–19964 (1991).
  128. Kim, H. *et al.* Inhibitor binding changes domain mobility in the iron-sulfur protein of the mitochondrial bc1 complex from bovine heart. *Proc. Natl. Acad. Sci. U. S. A.* **95**, 8026–8033 (1998).
  129. O'Neill, P. M. Research Highlights from the O' Neill Group. *Expert Opin. Invest. Drugs* (2008).
  130. Markley, L. D., Heertum, J. C. Van & Doorenbos, H. E. Antimalarial Activity of Clopidol 3,5-Dichloro-2,6-dimethyl-4-pyridinol, and its Esters, Carbonates and Sulfonates. *J. Med. Chem.* **15**, 1188–1189 (1972).
  131. Fry, M. & Williams, R. B. Effects of Decoquinat and Clopidol on Electron-Transport in Mitochondria of *Eimeria-Tenella* (Apicomplexa, Coccidia). *Biochem. Pharmacol.* **33**, 229–240 (1984).
  132. Victoria S. Latter; Alan T. Hudson, both of Kent; William H. G.' Richards, Herts; Anthony W. Randall, K. ANTIPROTOZOAL AGENTS. **1**, (1991).
  133. Markley, Lowell D.; Eckman, M. K. Synthesis and Anticoccidial Activity of 3-Fluoro-5-chloro- and -bromo-2, 6-dimethyl-4-pyridinol. *J. Med. Chem. Chem.* **6**, 297–298 (1973).
  134. Yeates, C. L. *et al.* Synthesis and Structure – Activity Relationships of 4-Pyridones as Potential Antimalarials Synthesis and Structure – Activity Relationships of 4-Pyridones as Potential Antimalarials. *J. Med. Chem.* **51**, 2845–2852 (2008).
  135. Valko, K., Du, C. M., Bevan, C., Reynolds, D. P. & Abraham, M. H. Rapid Method for the Estimation of Octanol / Water Partition Coefficient ( Log P oct ) from Gradient RP-HPLC Retention and a Hydrogen Bond Acidity Term. 1137–1146 (2001).
  136. Dressman, J. B. & Reppas, C. In vitro–in vivo correlations for lipophilic, poorly water-soluble drugs. *Eur. J. Pharm. Sci.* **11**, S73–S80 (2000).
  137. Xiang, H. *et al.* Preclinical drug metabolism and pharmacokinetic evaluation of GW844520, a novel anti-malarial mitochondrial electron transport inhibitor. *J. Pharm. Sci.* **95**, 2657–2672 (2006).
  138. Bueno, J. M. *et al.* Exploration of 4(1H)-pyridones as a novel family of potent antimalarial inhibitors of the plasmodial cytochrome bc1. *Future Med. Chem.* **4**, 2311–23 (2012).
  139. Bueno, J. M. *et al.* Potent antimalarial 4-pyridones with improved physico-chemical properties. *Bioorganic Med. Chem. Lett.* **21**, 5214–5218 (2011).
  140. Lovell, S., Subramony, P., Kahr, B. & February, R. V. Poppy Acid : Synthesis and

- Crystal Chemistry. *J. Am. Chem. Soc* 7020–7025 (1999).
141. Sakagami, K.; Ill'amatsu, K; Atsumi, K.; Shibahara, K. CEPHALOSPORIN COMPOUNDS AND ANTIBACTERIAL AGENTS. (1992).
  142. Bueno, J. M.; Chicharro, J.; Lorenzo, M.; Manzano, M. P. Novel heterocyclic compounds. (2007).
  143. Tilstam, U. & Weinmann, H. Trichloroisocyanuric acid: A safe and efficient oxidant. *Org. Process Res. Dev.* **6**, 384–393 (2002).
  144. GSK Criteria: ChromLogD\_ good < 4; bad > 6. LE\_ good > 0.3; bad < 0.2. SOLUBILIT\_ good >100 mg/mL; bad <5 mg/mL (FaSSIF)\_ good > 200 mg/mL; bad < 30 mg/mL (CLND).
  145. Young, R. J., Green, D. V. S., Luscombe, C. N. & Hill, A. P. Getting physical in drug discovery II : the impact of chromatographic hydrophobicity measurements and aromaticity. *Drug Discov. Today* **16**, 822–830 (2011).
  146. Kestranek, A.; Chervenak, A.; Longenberger, J.; Placko, S. Chemiluminescent Nitrogen Detection (CLND) to Measure Kinetic Aqueous Solubility. *Curr. Protoc. Chem. Biol.* **5**, 269–280 (2013).
  147. Desjardins, R. E., Canfield, C. J., Haynes, J. D. & Chulay, J. D. Quantitative Assessment of Antimalarial Activity In Vitro by a Semiautomated Microdilution Technique. *Antimicrob. Agents Chemother.* **16**, 710–718 (1979).
  148. Hopkins, A. L., Keserü, G. M., Leeson, P. D., Rees, D. C. & Reynolds, C. H. The role of ligand efficiency metrics in drug discovery. *Nat. Rev. Drug Discov.* **13**, 105–121 (2014).
  149. Capper, M. J. *et al.* Antimalarial 4(1H)-pyridones bind to the Q<sub>i</sub> site of cytochrome bc 1. *Proc. Natl. Acad. Sci.* **112**, 755–760 (2015).
  150. Gao, X. *et al.* Structural Basis for the Quinone Reduction in the bc 1 Complex : A Comparative Analysis of Crystal Structures of Mitochondrial Cytochrome bc 1 with Bound Substrate and Inhibitors at the Q<sub>i</sub> Site †,‡. 9067–9080 (2003).
  151. Li, H., Zhu, X. & Yang, W. Comparative Kinetics of Q<sub>i</sub> Site Inhibitors of Cytochrome bc 1 Complex : Picomolar Antimycin and Micromolar Cyazofamid. *Chem. Biol. Drug Des.* **83**, 71–80 (2014).
  152. Berry, E. A. *et al.* Ascochlorin is a novel , speci fi c inhibitor of the mitochondrial cytochrome bc 1 complex. *Biochim. Biophys. Acta* **1797**, 360–370 (2010).
  153. Cytochrome bc1 bound to the 4(1H)-pyridone GSK932121. Available at: <http://www.rcsb.org/pdb/explore/explore.do?structureId=4D6U>.
  154. Esser, L. *et al.* Crystallographic studies of quinol oxidation site inhibitors: A modified classification of inhibitors for the cytochrome bc1 complex. *J. Mol. Biol.* **341**, 281–302 (2004).
  155. Bueno, J. M.; Fernandez-Molina, J.; Leon, M.L.; Mallo, A.; Manzano, M. P. 4(1H)-pyridones derivatives and their use as antimalaria agents.
  156. Brewster, M. E. & Loftsson, T. Cyclodextrins as pharmaceutical solubilizers. *Adv. Drug Deliv. Rev.* **59**, 645–666 (2007).
  157. Müller, R. H., Jacobs, C. & Kayser, O. Nanosuspensions as particulate drug formulations in therapy: Rationale for development and what we can expect for the future. *Adv. Drug Deliv. Rev.* **47**, 3–19 (2001).
  158. Man, C. C. *et al.* Prodrugs for the treatment of neglected diseases. *Molecules* **13**, 616–677 (2008).
  159. Albert, A. No TitleChemical aspects of selective toxicity. *Nature* **182**, 421–2

- (1958).
160. Karaman, R. Using prodrugs to optimize drug candidates. 1405–1419 (2014).
  161. Sonsoles Velazquez, Sonia de Castro, Alberto Diez-Torrubia, Jan Balzarini, M.-J. C. Dipeptidyl-Peptidase IV (DPP IV/CD26)-Activated Prodrugs: A Successful Strategy for Improving Water Solubility and Oral Bioavailability. *Curr. Med. Chem.* **22**, 1041–54 (2015).
  162. BUTLER, J. M. & DRESSMAN, J. B. The Developability Classification System: Application of Biopharmaceutics Concepts to Formulation Development. *J. Pharm. Sci.* **99**, 4940–4954 (2010).
  163. Rautio, J. *et al.* Prodrugs: design and clinical applications. *Nat. Rev. Drug Discov.* **7**, 255–270 (2008).
  164. Wu, K. M. A new classification of prodrugs: Regulatory perspectives. *Pharmaceuticals* **2**, 77–81 (2009).
  165. Hejazi, S. A., Osman, O. I., Alyoubi, A. O. & Aziz, S. G. The Thermodynamic and Kinetic Properties of 2-Hydroxypyridine/2-Pyridone Tautomerization: A Theoretical and Computational Revisit. *Int. J. Mol. Sci.* **17**, 1893 (2016).
  166. Manetsch, A. Monastyrskyi, K. D. E. 4(1H)-Pyridone and 4(1H)-Quinolone Derivatives as Antimalarials with Erythrocytic, Exoerythrocytic, and Transmission Blocking Activities *Andrii.* **14**, 1693–1705 (2015).
  167. Alan R. Katritzky,\* Mati Karelson, and P. A. H. Prototropic Tautomerism of Heteroaromatic Compounds. *Heterocycles* **32**, 329–369 (1991).
  168. Elsadek, B. *et al.* Development of a novel prodrug of paclitaxel that is cleaved by prostate-specific antigen : An in vitro and in vivo evaluation study. *Eur. J. Cancer* **46**, 34 34 –34 44 (2010).
  169. Furfine, E. S. *et al.* Preclinical pharmacology and pharmacokinetics of GW433908, a water-soluble prodrug of the human immunodeficiency virus protease inhibitor amprenavir. *Antimicrob. Agents Chemother.* **48**, 791–8 (2004).
  170. Heimbach T, Fleisher D, K. A. overcoming poor aqueous solubility of drugs by oral delivery. In: Prodrugs: Challenges and Rewards, Part 1. in *Prodrugs: Challenges and Rewards, Part 1* (2007).
  171. Kim, E. E. & Wyckoff, H. W. Reaction Mechanism of Alkaline Phosphatase Based on Crystal Structures. *J. Mol. Biol.* **218**, 449–464 (1991).
  172. Goldstein, D. J., Rogers, C. E. & Harris, H. Expression of alkaline phosphatase loci in mammalian tissues. *Proc. Natl. Acad. Sci. U. S. A.* **77**, 2857–2860 (1980).
  173. Gomes, P., Vale, N. & Moreira, R. Cyclization-activated prodrugs. *Molecules* 2484–2506 (2007). doi:10.3390/12112484
  174. Beaumont, K., Webster, R., Gardner, I. & Dack, K. Design of ester prodrugs to enhance oral absorption of poorly permeable compounds: challenges to the discovery scientist. *Curr. Drug Metab.* **4**, 461–485 (2003).
  175. Yang, Y., Aloysius, H., Inoyama, D., Chen, Y. & Hu, L. Enzyme-mediated hydrolytic activation of prodrugs. *Acta Pharm. Sin. B* **1**, 143–159 (2011).
  176. Saari, W. S., Schwering, J. E., Lyle, P. a, Smith, S. J. & Engelhardt, E. L. Cyclization-activated prodrugs. Basic esters of 5-bromo-2'-deoxyuridine. *J. Med. Chem.* **33**, 2590–2595 (1990).
  177. Aitken, R. A., Collett, C. J. & Mesher, S. T. E. Convenient preparation of long-chain dialkyl phosphates: Synthesis of dialkyl phosphates. *Synth.* **44**, 2515–2518 (2012).
  178. Connors, K. A. & Pandit, N. K. N-Methylimidazole as a catalyst for analytical



- acetylations of hydroxy compounds. *Anal. Chem.* **50**, 1542–1545 (1978).
179. Bueno, J. M.; Fiandor, J. M.; Puente-Felipe, M.; Chicharro-Gonzalo, Jesus, Kusalakumari sukumar, S. K.; Maleki, M. Phosphate Ester of a 4-Pyridone derivative. (2012).
  180. Yamashita, S. *et al.* Optimized conditions for prediction of intestinal drug permeability using Caco-2 cells. *Eur. J. Pharm. Sci.* **10**, 195–204 (2000).
  181. Artursson, P., Palm, K. & Luthman, K. Caco-2 monolayers in experimental and theoretical drug transport predictions of drug transport. *Adv. Drug Deliv. Rev.* **46**, 27–43 (1996).
  182. Clark, M. ANTICANDIDAL ACTIVITY OF EUPOLAUROIDINE AND ONYCHINE, ALKALOIDS FROM CLEISTOPHOLIS PATENS. *J. Nat. Prod.* **5**, 3–6 (1987).
  183. Yang-Chang Wu. Azafluorene and Aporphine Alkaloids words: from Polyalthia Longifolia. *Heterocycles* **29**, 463–475 (1989).
  184. Koyama, J. *et al.* Structure-activity relations of azafluorenone and azaanthraquinone as antimicrobial compounds. *Bioorganic Med. Chem. Lett.* **15**, 1079–1082 (2005).
  185. Prachayasittikul, S. *et al.* Bioactive azafluorenone alkaloids from Polyalthia debilis (pierre) finet & Gagnep. *Molecules* **14**, 4414–4424 (2009).
  186. Kraus, G. a. & Kempema, A. Synthesis of azafluorenone antimicrobial agents. *J. Nat. Prod.* **73**, 1967–1968 (2010).
  187. Addla, D., Bhima, Sridhar, B., Devi, A. & Kantevari, S. Design, synthesis and antimicrobial evaluation of novel 1-benzyl 2-butyl-4-chloroimidazole embodied 4-azafluorenones via molecular hybridization approach. *Bioorg. Med. Chem. Lett.* **22**, 7475–80 (2012).
  188. Mueller, D. *et al.* Antimalarial activity of azafluorenone alkaloids from the Australian tree Mitrephora diversifolia. *J. Nat. Prod.* **72**, 1538–1540 (2009).
  189. Manpadi, M. *et al.* Three-component synthesis and anticancer evaluation of polycyclic indenopyridines lead to the discovery of a novel indenoheterocycle with potent apoptosis inducing properties. *Org. Biomol. Chem.* **5**, 3865–72 (2007).
  190. Banjerdpongchai, R., Khaw-on, P., Ristee, C. & Pompimon, W. 6,8-Dihydroxy-7-methoxy-1-methyl-azafluorenone Induces Caspase-8- and -9-mediated Apoptosis in Human Cancer Cells. *Asian Pacific J. Cancer Prev.* **14**, 2637–2641 (2013).
  191. Shook, B. C. *et al.* In vivo characterization of a dual adenosine A2A/A1 receptor antagonist in animal models of Parkinson's disease. *J. Med. Chem.* **53**, 8104–8115 (2010).
  192. Kyba, E. P., Liu, S. T., Chockalingam, K. & Reddy, B. R. A general synthesis of substituted fluorenones and azafluorenones. *J. Org. Chem.* **53**, 3513–3521 (1988).
  193. Marquise, N. *et al.* Synthesis of azafluorenones and related compounds using deprotection-arylation followed by intramolecular direct arylation. *Tetrahedron* **69**, 10123–10133 (2013).
  194. Marquise, N., Dorcet, V., Chevallier, F. & Mongin, F. Synthesis of substituted azafluorenones from dihalogeno diaryl ketones by palladium-catalyzed auto-tandem processes. *Org. Biomol. Chem.* **12**, 8138–41 (2014).
  195. Ting, P. C. *et al.* The synthesis of substituted fluorenes as novel non-imidazole histamine H3 inhibitors. *Bioorganic Med. Chem. Lett.* **12**, 2643–2646 (2002).
  196. Hrobárik, P., Sigmundová, I. & Zahradník, P. Preparation of novel push-pull benzothiazole derivatives with reverse polarity: Compounds with potential non-

## References

- linear optic application. *Synthesis (Stuttg)*. 600–604 (2005). doi:10.1055/s-2004-837309
197. Cannon, J. G., Perez, J. A., Bhatnagar, R. K., Long, P. & Sharabit, F. M. Conformationally Restricted Congeners of Dopamine Derived from 2-Aminoindan. *J. Med. Chem.* **25**, 1442–1446 (1982).
  198. Petrovskaia, O., Taylor, B. M., Hauze, D. B., Carroll, P. J. & Joullie, M. M. Investigations of the Reaction Mechanisms of 1, 2-Indanediones with Amino Acids. *J. Org. Chem.* **66**, 7666–7675 (2001).
  199. GlaxoSmithKline Laboratories, unpublished work.